TEXTE
115/2026

Final report

Historical nutrient emissions and loads in German river basins of the North Sea and Baltic Sea

1880 scenario modelled with MoRE

by:

Karoline Morling, Stephan Fuchs
Karlsruhe Institute of Technology (KIT), Karlsruhe

Georges Bruns, Julia Krumm, Ingo Haag
HYDRON Ingenieurgesellschaft für Umwelt und Wasserwirtschaft mbH, Karlsruhe

Micha Gebel

VisDat geodatentechnologie GmbH, Dresden

publisher:
German Environment Agency

TEXTE 115/2026

REFOPLAN of the Federal Ministry for the Environment, Nature
Conservation, Nuclear Safety and Consumer Protection

Project No. (FKZ) 3723 25 202 2

Final report

Historical nutrient emissions and loads in German river basins of the North Sea and Baltic Sea

1880 scenario modelled with MoRE

by

Karoline Morling, Stephan Fuchs
Karlsruhe Institute of Technology (KIT), Karlsruhe

Georges Bruns, Julia Krumm, Ingo Haag
HYDRON Ingenieurgesellschaft für Umwelt und Wasserwirtschaft
mbH, Karlsruhe

Micha Gebel
VisDat geodatentechnologie GmbH, Dresden

On behalf of the German Environment Agency

Imprint

Publisher
Umweltbundesamt
Wörlitzer Platz 1
06844 Dessau-Roßlau
Tel: +49 340-2103-0
Fax: +49 340-2103-2285
buergerservice@uba.de
Internet: www.umweltbundesamt.de

Report performed by:
Institute for Water and Environment - Water Quality Management, Karlsruhe Institute of Technology
Gotthard-Franz-Straße 3
76131 Karlsruhe
Germany

HYDRON – Ingenieurgesellschaft für Umwelt und Wasserwirtschaft mbH
Ritterstraße 9
76137 Karlsruhe

VisDat geodatentechnology GmbH
Berggartenstraße 11
01277 Dresden

Report completed in:
August 2025

Edited by:
Section II 2.3 Protection of the Seas and Polar Regions
Andreas Gericke / Wera Leujak

DOI:
https://doi.org/10.60810/openumwelt-8174

ISSN 1862-4804

Dessau-Roßlau, July 2026

Abstract: Historical nutrient emissions and loads in German river basins of the North Sea and Baltic Sea

Historical nutrient emissions from inland waters into the sea are often considered as marine reference conditions. However, the application of different models resulted in significant uncertainties of these reference conditions and resulting reduction requirements in marine environments. Thus, the MoRE model was used for a more consistent revised historical nutrient emission scenario for 1880 for all river basins of the German North Sea and Baltic Sea. The approach is further improved by using e.g. the water balance model LARSIM-ME, which provided the necessary runoff components of the 1880 period as model input for MoRE in a consistent way.

Recently published datasets for historical conditions as well as historical literature were used to derive suitable input data for modelling. Currently implemented model approaches in MoRE were adapted and partly simplified to reflect 1880 conditions.

Nitrogen and phosphorus emissions into surface waters as well as transported riverine loads and surface water concentrations were modelled. Model results represent an early-industrial state with distinct anthropogenic impact before intensification of agricultural production. Comparison of results to reported concentrations from historical literature showed an overall good agreement of magnitude. Comparison of results to further historical modelling studies revealed more similarities with previous MONERIS modelling than with regional and global estimations, although, e.g., the importance of individual emission pathways differed.

The results from this study can contribute to revise target values for nutrients at the limnic-marine transition points as well as for coastal and marine waters of Germany.

Kurzbeschreibung: Modellierung historischer Nährstoffeinträge und -frachten in deutsche Nord- und Ostseeeinzugsgebiete

Historische Nährstoffeinträge aus Binnengewässern ins Meer werden häufig als marine Referenzbedingungen angesehen. Die Anwendung unterschiedlicher Modelle führte jedoch zu erheblichen Unsicherheiten hinsichtlich dieser Referenzbedingungen und der sich daraus ergebenden Minderungsanforderungen für die Meeresumwelt. Deshalb wurde das Modell MoRE genutzt, um ein konsistenteres, überarbeitetes historisches Nährstoffeintragsszenario für das Jahr 1880 darzustellen, das alle Flussgebiete der deutschen Nord- und Ostsee abdeckt. Die für die Modellierung notwendigen Abflusskomponenten für den Zeitraum um 1880 wurden in konsistenter Weise mit dem Wasserhaushaltsmodell LARSIM-ME ermittelt.

Kürzlich veröffentlichte Datensätze zu historischen Bedingungen sowie historische Literatur wurden genutzt, um Eingangsdaten für die Modellierung abzuleiten. Die derzeit in MoRE implementierten Modellansätze wurden angepasst und teilweise vereinfacht um die Bedingungen um 1880 darzustellen.

Die Stickstoff- und Phosphor-Einträge in Oberflächengewässer sowie die transportierten Frachten und resultierenden Konzentrationen wurden modelliert. Die Ergebnisse repräsentieren einen frühindustriellen Zustand mit deutlich anthropogenen Einflüssen vor der Intensivierung der landwirtschaftlichen Produktion. Vergleiche der Ergebnisse mit Konzentrationen aus historischen Literaturquellen zeigten eine insgesamt gute Übereinstimmung der Größenordnung. Vergleiche der Ergebnisse mit weiteren historischen Modellszenarien ergaben mehr Übereinstimmungen mit früheren MONERIS-Modellierungen als mit regionalen und globalen Abschätzungen. Trotz der Ähnlichkeit zu früheren Gesamtergebnissen aus MONERIS unterschieden sich die mit MoRE ermittelten Teilergebnisse wie der Anteil einzelner Eintragspfade.

Die Ergebnisse dieser Studie können dazu beitragen, die Zielwerte für Nährstoffe an den limnisch-marinen Übergangspunkten und in den Küsten- und Meeresgewässern Deutschlands zu überprüfen.

Table of content

List of figures

List of tables

List of abbreviations

Abbreviation	Explanation
ABAG	Universal soil loss equation (Allgemeine Bodenabtragsgleichung)
AU	Analytical unit (spatial modelling unit of the MoRE model)
BfG	Federal Institute of Hydrology (Bundesanstalt für Gewässerkunde)
BFI	Base flow index
ccv	Climate change vector(s)
CLC	Corine Land Cover
DWD	German Meteorological Service (Deutscher Wetterdienst)
ECMWF	European Centre for Medium-Range Weather Forecasts
E	Inhabitants (Einwohner)
E-HYPE	Pan-European Hydrological Predictions for the Environment
EU	European Union
GRDC	Global Runoff Data Centre
HELCOM	Baltic Marine Environment Protection Commission (Helsinki Commission)
HL	Hydraulic load
HRU	Hydrological response unit
HYDE	History Database of the Global Environment
inh	inhabitants
IWU-WG	Institute for Water and Environment – Water Quality Management (Institut für Wasser und Umwelt – Wassergütewirtschaft)
LARSIM-ME	water balance model (Large Area Runoff SImulation Model – Middle Europe)
MONERIS	Substance emission model (MOdelling Nutrient Emissions in RIver Systems)
MoRE	Substance emission model (Modeling of Regionalized Emissions)
MSFD	Marine Strategy Framework Directive
MWWTP	Municipal wastewater treatment plant
N	Nitrogen
NOAA	National Oceanic and Atmospheric Administration
OSPAR	Oslo-Paris Commission, Convention for the Protection of the Marine Environment of the North-East Atlantic
OGewV	German Surface Water Ordinance (Oberflächengewässerverordnung)
P	Phosphorus
Par	Parameter
SDR	Sediment delivery ratio

Abbreviation	Explanation
T	Temperature
Ta	Air temperature
TN	Total nitrogen
TP	Total phosphorus
UBA	German Environment Agency (Umweltbundesamt)
USLE	Universal soil loss equation
WFD	Water Framework Directive

Summary

Despite decreasing nutrient emissions since the 1990s, marine waters fail to achieve the good status with regard to eutrophication according to the Water Framework Directive (WFD) and Marine Strategy Framework Directive (MSFD). Most nutrient emissions originate from terrestrial sources and enter the sea via rivers.

Target values are a legal prerequisite to achieve the good environmental status and are fundamental for river basin management. For Germany, target annual average riverine concentrations have been derived in the past to achieve the good environmental status according to WFD and MSFD with respect to nutrients and chlorophyll-a concentrations in coastal and marine water bodies of the North Sea and Baltic Sea (BLANO 2015; BLMP 2011; Schernewski et al. 2015). For total nitrogen, annual average target concentrations of 2.8 mg N/L and 2.6 mg N/L were derived for North Sea and Baltic Sea tributaries, respectively. These targets have been laid down in the German Surface Water Ordinance (OGewV). The target for North Sea tributaries was originally derived for the Rhine River at the German-Dutch border from a Dutch threshold value for dissolved inorganic nitrogen (ICPR 2010) and was later transferred to other German North Sea tributaries (BLMP 2011). The target value for Baltic Sea tributaries was based on modelling historical nutrient emissions in 1880 and a permitted deviation of 50 % (Schernewski et al. 2015). There are no corresponding target concentrations for total phosphorus. Instead, riverine type-specific orientation values according to the OGewV (Annex 7) currently apply.

Historical nutrient emissions for 1880 were derived using the MONERIS model for German Baltic Sea (Hirt et al. 2014) and North Sea basins (Gadegast & Venohr 2015). Additional assumptions and extended input data were used for modelling of the North Sea basins, leading to inconsistent approaches between North and Baltic Sea basins. For instance, mean nitrogen surplus was estimated without considering nitrogen fixation for Baltic Sea basins (Hirt et al. 2014), while it was included for the modelling of North Sea basins (Gadegast & Venohr 2015). A harmonized modelling for 1900 conditions of North Sea basins was pursued using the model E-HYPE (Blauw et al. 2019). Historical total phosphorus loads obtained by E-HYPE are five times larger than the ones estimated by MONERIS. Differing results of both models led to significant uncertainties for ecosystem modelling and reduction requirements in marine environments (Stegert et al. 2021). These uncertainties raise the question how reliable the estimated reference conditions for Germany are in comparison to that of neighboring countries, but also how robust the former model assumptions have been.

The **objective** of this study was to model a historical nutrient emission scenario representing 1880 conditions for all river basins of the North Sea and Baltic Sea, which Germany shares with its neighbours. Further, the modelling should foster the consistency between North Sea and Baltic Sea basins as well as enable a plausibility assessment of previous historical modelling results. The new results for 1880 may also allow for a critical revision of currently implemented target values for nutrients at the limnic-marine transition points as well as for coastal and marine waters of Germany.

Modelling tools

The substance emission model **MoRE** (Modelling of Regionalized Emissions) was used to calculate nitrogen and phosphorus emissions via different pathways into surface waters and their resulting transported riverine loads. MoRE was derived in 2009 from the MONERIS model (Behrendt et al. 2000; Venohr et al. 2011) and has been continuously developed since then e.g. on behalf of the German Environment Agency (UBA). The UBA application of the MoRE model covers all river basins in Germany and their foreign parts.

In contrast to the previous historical modelling, MoRE considers a historical water balance which was provided by the hydrological model **LARSIM-ME** (Large Area Runoff SImulation Model – Middle Europe). Runoff components were derived by applying climate change vectors as well as considering historical land

use and imperviousness. Yearly precipitation and land use specific runoff components from LARSIM-ME were transferred to the MoRE analytical units following Morling et al. (2024).

Input data and adaptation of modelling approaches

Basic input data on **land use**, imperviousness and population in 1880 were obtained from a dataset covering Europe (Paprotny & Mengel 2023). Most land was dedicated to agricultural activities. Arable land and pastures made up 65 % and 66 % of land use in the basins of the North Sea and Baltic Sea, respectively. Naturally covered areas accounted for 29 %.

For river basins of the North Sea, the **total population** accounted to 44.1 million inhabitants. Approximately 9.8 million inhabitants were obtained for the Baltic Sea basins, which cover less densely populated areas.

The 20CRv3 re-analysis data of the US National Oceanic and Atmospheric Administration (NOAA) cover the time span 1836 – 2015 and contain all parameters needed for meteorological forcing of the **water balance** model LARSIM-ME. These re-analysis data were used to derive **climate change vectors** (ccv) based on the differences between the historic period 1873 – 1887 (representing average conditions in 1880) and the present period 2001 – 2015. For sake of simplicity, for each parameter one single ccv was derived for the whole study area. The most pronounced change was observed for air temperature, which was almost 1.5 K lower in 1880 compared to present.

Model runs were performed with LARSIM-ME with measured meteorological data of the present and with ccv applied to these measured input data to represent the historic climatic conditions of 1880. The impacts of 1880 land use and imperviousness were taken into account in the post-processing of the model results. According to the model results, mean yearly runoff would on average have been approximately 50 mm/a higher under 1880 climate conditions than nowadays for unsealed areas. Since precipitation has hardly changed, this is mainly owing to the lower air temperatures in 1880, thus leading to lower evapotranspiration and an increase of runoff. In contrast, for areas having a much higher degree of imperviousness today than in 1880, runoff used to be much lower in 1880 than it is today.

For modelling nutrient emissions via the pathway of **urban systems**, population density was used as a proxy for estimating the amount of population connected to sewers, since cities were growing tremendously in the late 19th century and massive construction of sewers started. For North Sea basins, covering more large cities and industrial centres, 14 % of the total population was connected to sewers. In Baltic Sea basins, only 8 % of the population was connected to sewers. Water consumption was set to 97 L/(inh·d) for urban population and to 55 L/(inh·d) for the population in rural areas (Franzius et al. 1893). Daily nutrient excretion rates currently implemented in MoRE [12 g N/(inh·d) and 1.9 g P/(inh·d)] were not adapted as they fall into the range of values reported in historical literature. Local wastewater treatment in form of sewage farms could only be considered for the Berlin area, assuming 65 % and 90 % retention in soils for nitrogen and phosphorus, respectively.

For modelling **atmospheric deposition** onto water surfaces, a global dataset covering historical conditions (Hegglin et al. 2016) was used for nitrogen. For phosphorus, a deposition rate of 75 g/(ha·a) was used following the estimation of Ruoho-Airola et al. (2012).

The dataset on nitrogen deposition was also used for modelling emissions via **surface runoff.** For phosphorus, concentration in surface runoff from all vegetated areas were set to 0.0125 mg P/L, based on average phosphorus leaching from unproductive vegetation (Prasuhn et al. 1996).

For modelling **erosion**, different approaches were used for present Germany and foreign territories of the river basins. For present Germany, the input data based on the universal soil loss equation (USLE) were adapted from results of a recent erosion modelling covering only Germany (Fuchs et al. 2022). The crop factor (C factor) on arable land was increased by around 41 %, assuming no conservation tillage took place in the past. The rainfall erosivity factor (R factor) was recalculated using the mean annual precipitation of the derived historical water balance according to DIN 19708 (2017), assuming that the relationship between annual rainfall and rainfall erosivity in the late 19th century matches the one in the late 20th century. The remaining USLE factors were not adapted. As adjustments of watercourse distance and connection probability involves too much uncertainty, the sediment delivery ratios were kept as obtained by Fuchs et al. (2022). For foreign territories, a dataset on historical soil loss in Europe (Fendrich et al. 2022) was used and sediment inputs calculated following the original MONERIS approach of Venohr et al. (2011).

For both present Germany and foreign territories, the currently implemented nitrogen topsoil contents (Morling et al. 2024) were used for modelling 1880 emissions via erosion. The currently implemented phosphorus contents of naturally covered areas (Fuchs et al. 2022) were used as P contents for agriculturally used land (arable land, fruits, vineyards, pasture), assuming that soils were not over-fertilized in 1880.

For modelling **interflow** and **base flow** emissions, currently implemented nitrogen concentrations were adapted according to an upper limit of 2.257 mg N/L (10 mg/L of nitrate), representing unaffected groundwater conditions. For phosphorus, the currently implemented input data by Fuchs et al. (2022) were kept for modelling 1880, assuming that P concentrations in groundwater are predominantly depending on geological properties instead of agricultural practices.

Due to the lack of reliable data, currently used percentages of drained agricultural land (arable land and pasture) were reduced to meet a total drained area of the entire MoRE model area of 6 % for the year 1880, following the approach of Gadegast & Venohr (2015). A constant nitrate concentration of 10 mg/L (2.257 mg N/L) was assumed for modelling emissions via **tile drainage**. Fuchs et al. (2022) derived P concentrations in groundwater from recent phosphate measurements, averaging to 0.022 mg P/L for Germany. These were also used for modelling tile drainage P emissions in 1880.

For modelling **retention** in river basins, the THL approach by Venohr (2006) is used for nitrogen in MoRE, which considers water temperature (T) and hydraulic load (HL). Currently implemented average water temperatures were reduced by 1 K to reflect generally cooler climate conditions of the past. For phosphorus, retention is modelled as a function of hydraulic load following Venohr et al. (2011).

Results of historical emission modelling

Total emission for nitrogen amounted to roughly 257 kt N/a and 36 kt N/a for North Sea and Baltic Sea basins in 1880, respectively (Table 1). Interflow and base flow were the most important pathways for nitrogen (Figure 1), contributing 77 % – 82 % of total emissions. Total phosphorus emissions amounted to 8.2 kt P/a and 1 kt P/a for North Sea and Baltic Sea basins in 1880, respectively (Table 1). Erosion was the most important emission pathway for phosphorus (Figure 1), making up 49 % and 38 % of the modelled emissions for the North Sea and Baltic Sea basins, respectively. Urban systems were the second largest emission pathway for phosphorus (23 % – 25 %).

Rivers transported nutrient loads of around 180 kt N/a and 4.2 kt P/a into the North Sea (Table 1, Figure 1). This corresponds to a retention of total emissions of 30 % and 49 % for nitrogen and phosphorus, respectively. The Baltic Sea received around 22 kt N/a and 0.46 kt P/a of riverine loads, which equals an in-stream retention of 38 % and 58 % for nitrogen and phosphorus, respectively (Table 1, Figure 1).

Nutrient concentrations in water bodies were calculated by dividing transported loads by total runoff. For both nitrogen and phosphorus, **modelled concentrations** followed partly the spatial pattern of emissions. The highest nutrient concentrations were modelled in densely populated urban areas. Also, mountainous areas showed higher concentrations for phosphorus due to higher emissions via erosion.

Table 1: Summarized modelling results for North Sea and Baltic Sea basins in 1880.

Nutrient parameter	unit	North Sea basins	Baltic Sea basins
Total nitrogen emission	[kt/a]	257	36
Total nitrogen load	[kt/a]	180	22
Nitrogen retention	[%]	30	38
Average nitrogen concentration	[mg/L]	1.37	1.11
Total phosphorus emission	[t/a]	8 208	1 065
Total phosphorus load	[t/a]	4 204	446
Phosphorus retention	[%]	49	58
Average phosphorus concentration	[mg/L]	0.032	0.022

Figure 1: Nitrogen (top, green) and phosphorus (blue, bottom) flows within the river basins to the North Sea (left) and Baltic Sea (right) in 1880.

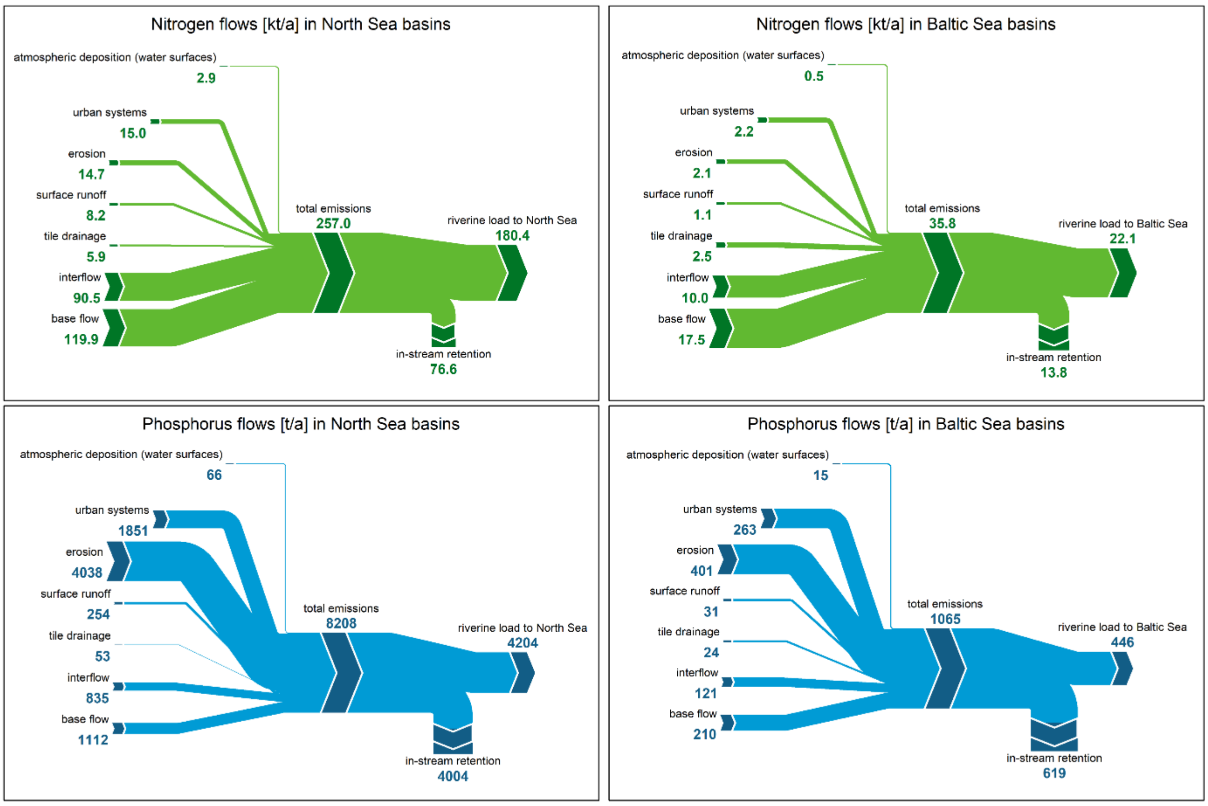

Source: Gericke et al. (2025)

Model validation

Discharge measurements at river gauges in the study area are available for only a few locations since 1873 at the Global Runoff Data Centre (BfG 2024). These were used for an evaluation of the modelled water balance. Average annual runoff was calculated from original measurements for 11 gauging stations. This observed runoff was compared to the modelled total runoff of the MoRE analytical units covering the location of the corresponding gauging stations. Even though the limited number of observations hampers a thorough validation, the comparison revealed a good agreement with historical records.

The validation of modelled concentrations is hampered by a lack of suitable data as only a few measurements are reported in historical literature. A comparison was conducted mainly to assure modelled concentrations are in the same order of magnitude rather than fitting individual data. Nutrient concentrations showed an overall good agreement to historical literature data. Modelled concentrations are also on average in good agreement with results of further historical modelling studies (Gadegast & Venohr 2015; Hirt et al. 2014; Jensen 2017).

Comparison to further historical modelling scenarios

Results of MoRE and MONERIS modelling were more alike compared to results from regional E-HYPE and global modelling (Beusen et al. 2016) for all parameters considered (emissions, loads as well as retention and surface water concentrations). Differences between MoRE and MONERIS modelling still exist in the importance of individual emission pathways. For instance, surface runoff and tile drainage are proportionally less important, while the sum of interflow and base flow is more important for nitrogen emissions in the MoRE modelling. For phosphorus, the sum of interflow and base flow is less important; while the pathways of erosion and urban systems are proportionally more important in this study compared to previous MONERIS results.

In comparison to the limited measurements of nutrient concentrations reported in literature, concentrations predicted by MoRE and MONERIS models fit historical conditions best for all models considered. The 1880 scenario in MoRE provided generally the lowest nutrient concentrations in this model comparison, implying also the highest reduction needs for marine and coastal environments.

Limitations and uncertainties in historical modelling

Modelling is generally subject to many uncertainties. Reproducing past conditions is additionally challenged by availability of historical data, necessary model assumptions and simplifications as well as very limited validation options. The choice of input data highly influences model results and might lead to over- or underestimation of emissions and loads. Each emission pathway depends on specific input data and variables. Thus, the contributions of individual emission pathways to the total emissions differs and their relative importance varies spatially as well. Therefore, a full assessment of the uncertainty in the great number of input data and adjustments of modelling approaches is not feasible. Instead, we point out some important aspects.

A simple approach was used and currently implemented **groundwater concentrations** adapted according to an upper limit of 2.257 mg N/L (10 mg/L of nitrate) based on a drinking water analysis in 1915 reported in literature (UBA 1994). This assumption is associated with a high degree of uncertainty as the exact distribution and representativeness of the samples is unknown. Groundwater concentrations are unknown for 1880 and thus could be over- or underestimated in the modelling scenario in different regions of the study area.

Topsoil content is one main variable affecting the resulting emissions via erosion. The real situation of **topsoil contents** of arable land and pastures in 1880 for the whole study area remains unknown. We assumed that current topsoil P contents of naturally covered areas are representative for agricultural soils as these were not over-fertilized in 1880. Phosphorus emissions via erosion were 2.5-fold higher for the Rhine basin compared to previous MONERIS results. This deviation is due to differing model assumptions on **soil loss and delivery** for alpine areas, for which we assumed that all eroded material is entering surface waters. This example highlights the importance of land use specific assumptions for river basin modeling.

Emissions from urban sources are likely underestimated, as no **commercial and industrial wastewaters** potentially delivering nutrients to surface waters were included in the modelling. The composition of these wastewaters is only roughly known from single observations reported in historical literature. Wastewaters from different production stages and processes were typically discharged together and therefore its exact composition remained mostly unknown (Büschenfeld 1997). This hampers the derivation of reliable substance concentrations besides the quantification of emitted volumes. Further, it can be expected that industrial emissions were much more decentralized compared to today.

Retention in surface water bodies was modelled with currently implemented approaches in this study, neglecting changes due to the many hydraulic engineering measures carried out since 1880. Nutrient retention might have been higher in the past due to less flow regulations by hydraulic measures and historically presence of more wetlands (Jensen 2017). A reconstruction of the water network and coastal morphology around 1880 was not possible and would have required extensive adaptations and calibrations in both MoRE and LARSIM-ME models.

Conclusions

In comparison to previous works, the historical scenario developed here comprises modelling nutrient emissions and loads more consistently for all river basins of the German North Sea and Baltic Sea tributaries. Further, a consistent albeit simplified historical water balance was developed with the hydrological model LARSIM-ME for the study area using climate change vectors and accounting for historical land use and imperviousness.

The comparison to other historical modelling studies revealed that the 1880 results of the MoRE model are more similar to that of previous MONERIS (Gadegast et al. 2012; Gadegast & Venohr 2015; Hirt et al. 2014) than regional (Blauw et al. 2019) and global applications (Beusen et al. 2016). Despite all the differences in input data and modelling approaches between MoRE and MONERIS, the total nutrient emissions and loads changed hardly – at least on the level of river basins. However, individual pathways differed in their importance between the two models.

Despite the overall similarities of MoRE and MONERIS results, average nutrient concentrations at the outlet of the river basins modelled with MoRE are on average lower. In fact, lower nutrient concentrations imply stronger requirements for reduction needs to protect marine and coastal waters. In this sense, our work supports the need for a critical revision (Gericke et al. 2025) of currently implemented annual average target values for total nitrogen and total phosphorus for North Sea and Baltic Sea tributaries of Germany concerning their validity.

The results of this project are visualized for the area of present Germany in the **MoRE toolbox**, which allows to interactively explore selected input data and results in more detail: https://stoffeintraege-more.de/

The model results of the 1880 scenario presented here as well as the geometry of the modeling units can be downloaded from the **ZENODO repository**: https://doi.org/10.5281/zenodo.15227585.

Zusammenfassung

Trotz rückläufiger Nährstoffeinträge seit den 1990er Jahren erreichen die Meeresgewässer nicht den guten Zustand in Bezug auf Eutrophierung gemäß der Wasserrahmenrichtlinie (WRRL) und der Meeresstrategie-Rahmenrichtlinie (MSRL). Die meisten Nährstoffemissionen stammen aus terrestrischen Quellen und gelangen über Flüsse in die Meere.

Zielwerte sind eine rechtliche Voraussetzung für das Erreichen des guten Umweltzustands und eine wichtige Grundlage für das Flussgebietsmanagement. Für Deutschland wurden in der Vergangenheit zur Erreichung des guten Umweltzustands gemäß MSRL Zielwerte für die Jahresmittelkonzentrationen von Nährstoffen und Chlorophyll-a in den Küsten- und Meereswasserkörpern von Nord- und Ostsee abgeleitet (BLANO 2015; BLMP 2011; Schernewski et al. 2015). Für Gesamtstickstoff wurden jährliche durchschnittliche Zielkonzentrationen von 2,8 mg N/L bzw. 2,6 mg N/L für die Zuflüsse der Nord- und Ostsee abgeleitet. Diese sind in der deutschen Oberflächengewässerverordnung (OGewV) festgeschrieben. Der Zielwert für die Nordseezuflüsse wurde ursprünglich für den Rhein an der deutsch-niederländischen Grenze aus einem niederländischen Grenzwert für gelösten anorganischen Stickstoff abgeleitet (IKSR 2010) und später auf andere deutsche Nordseezuflüsse übertragen (BLMP 2011). Der Zielwert für die Ostseezuflüsse basiert auf der Modellierung historischer Nährstoffemissionen im Jahr 1880 und einer zulässigen Abweichung von 50 % (Schernewski et al. 2015). Für Gesamtphosphor gibt es keine entsprechenden Zielkonzentrationen. Stattdessen gelten derzeit flusstypspezifische Orientierungswerte gemäß OGewV (Anhang 7).

Historische Nährstoffeinträge für 1880 wurden mit dem MONERIS-Modell für die deutschen Ostsee- (Hirt et al. 2014) und Nordseezuflüsse (Gadegast & Venohr 2015) abgebildet. Für die Modellierung der Nordseegebiete wurden zusätzliche Modellannahmen und erweiterte Eingangsdaten verwendet, wodurch inkonsistente Ansätze für Nord- und Ostseegebiete vorliegen. So wurden beispielsweise mittlere Stickstoffüberschüsse für die Ostseegebiete ohne Berücksichtigung der Stickstofffixierung abgeschätzt (Hirt et al. 2014), während diese bei der Modellierung der Nordseegebiete einbezogen wurde (Gadegast & Venohr 2015). Mit dem Modell E-HYPE (Blauw et al. 2019) wurde eine einheitliche Modellierung für die Bedingungen in 1900 für die Einzugsgebiete der Nordsee vorgenommen. Die mit E-HYPE ermittelten historischen Gesamtphosphorfrachten sind fünfmal höher als die mit MONERIS modellierten. Die unterschiedlichen Ergebnisse der beiden Modelle führten zu erheblichen Unsicherheiten bei der Ökosystem-Modellierung und den Reduktionsanforderungen (Stegert et al. 2021). Diese Unsicherheiten werfen die Frage auf, wie verlässlich die geschätzten Referenzbedingungen für Deutschland im Vergleich zu denen der Nachbarländer sind, aber auch, wie robust die bisherigen Modellannahmen waren.

Ziel dieser Studie war die Modellierung eines historischen Szenarios für Nährstoffeinträge, das die Bedingungen von 1880 für alle Flusseinzugsgebiete der Nord- und Ostsee, die Deutschland mit seinen Nachbarn teilt, widerspiegelt. Dies ermöglichte eine konsistente Darstellung der Einzugsgebiete von Nord- und Ostsee und eine Plausibilitätsbewertung der bisherigen historischen Modellierungsergebnisse. Die neuen Modellergebnisse für 1880 ermöglichen ebenfalls eine kritische Überprüfung der derzeit geltenden Zielwerte für Gesamtstickstoff und Gesamtphosphor an den limnisch-marinen Übergangspunkten Deutschlands hinsichtlich ihrer Gültigkeit.

Modellwerkzeuge

Das Stoffeintragsmodell **MoRE** (Modelling of Regionalized Emissions) wurde verwendet, um die Stickstoff- und Phosphoreinträge über verschiedene Pfade in die Oberflächengewässer und die daraus resultierenden transportierten Frachten zu berechnen. MoRE wurde 2009 auf Basis des Modells MONERIS (Behrendt et al. 2000; Venohr et al. 2011) erweitert und wird seither u.a. im Auftrag des Umweltbundesamtes (UBA) kontinuierlich weiterentwickelt. Die UBA-Anwendung des MoRE-Modells deckt alle Einzugsgebiete in Deutschland und deren ausländische Teile ab.

Im Gegensatz zu früheren historischen Modellierungen wurde in MoRE eine historische Wasserbilanz berücksichtigt, die durch das hydrologische Modell **LARSIM-ME** (Large Area Runoff SImulation Model - Middle Europe) bereitgestellt wurde. Die Abflusskomponenten wurden unter Berücksichtigung von Klimaänderungsvektoren sowie der historischen Landnutzung und Versiegelung abgeleitet. Die jährlichen Niederschlags- und landnutzungsspezifischen Abflusskomponenten aus LARSIM-ME wurden auf die Analysegebiete von MoRE übertragen (Morling et al. 2024).

Eingangsdaten und Modellansätze

Die grundlegenden Eingangsdaten zur **Landnutzung**, Versiegelung und Bevölkerung in 1880 wurden aus einem europäischen Datensatz (Paprotny & Mengel 2023) entnommen. Die meisten Flächen wurden landwirtschaftlich genutzt. Acker- und Weideflächen machten 65 % bzw. 66 % der Landnutzung in den Einzugsgebieten der Nord- und Ostsee aus. Der Anteil der natürlich bedeckten Flächen lag bei 29 %.

Für die Nordseeeinzugsgebiete wurde eine **Gesamtbevölkerung** von 44,1 Millionen Einwohnern ermittelt. Für die Einzugsgebiete der Ostsee, die weniger dicht besiedelt sind, wurden rund 9,8 Millionen Einwohner ermittelt.

Die 20CRv3 Re-Analyse-Daten der US National Oceanic and Atmospheric Administration (NOAA) decken die Zeitspanne 1836 – 2015 ab und enthalten alle meteorologischen Parameter, die als Eingangsdaten für die Simulation der **Wasserbilanz** mit LARSIM-ME benötigt wurden. Aus diesen Re-Analysedaten wurden **Klimaänderungsvektoren** abgeleitet, die auf der Differenz des historischen Zeitraums 1873 – 1887 (repräsentiert durchschnittliche Bedingungen im Jahr 1880) und des gegenwärtigen Zeitraums 2001 – 2015 basieren. Zur Vereinfachung wurde für jeden Parameter ein einheitlicher Klimaänderungsvektor für das gesamte Modellgebiet abgeleitet. Die stärkste Änderung zeigte sich bei der Lufttemperatur, die 1880 um fast 1,5 K niedriger war als heute.

Mit LARSIM-ME wurden Modellläufe mit den gemessenen meteorologischen Eingangsdaten der Gegenwart und für die historischen klimatischen Bedingungen von 1880 (unter Verwendung der Klimaänderungsvektoren) durchgeführt. Die Einflüsse von veränderter Landnutzung und verändertem Versiegelungsgrad im Jahr 1880 wurden im Post-Processing der simulierten Abflusshöhen mit einbezogen. Nach den Modellergebnissen war der mittlere jährliche Abfluss in Bereichen mit heute weiterhin unversiegelten Böden um 1880 bis zu 50 mm/a höher als heute. Da sich die Niederschläge kaum verändert haben, ist dies hauptsächlich auf die niedrigeren Lufttemperaturen im Zeitraum um 1880 zurückzuführen, die eine geringere Evapotranspiration und damit verbunden einen höheren Abfluss bedingen. In Bereichen, die heute wesentlich stärker versiegelt sind als in der Vergangenheit, traten um 1880 hingegen erwartungsgemäß deutlich geringere Abflüsse auf als heute.

Für die Modellierung der Nährstoffeinträge über **Kanalisationssysteme** wurde die Bevölkerungsdichte verwendet um die an die Kanalisation angeschlossenen Bevölkerung abzuschätzen, da die Städte im späten 19. Jahrhundert enorm wuchsen und der massive Bau von Abwasserkanälen begann. In den Nordseeeinzugsgebieten, die mehr Großstädte und Industriezentren umfassen, waren 14 % der Gesamtbevölkerung an die Kanalisation angeschlossen. In den Ostseegebieten waren nur 8 % der Bevölkerung an die Kanalisation angeschlossen. Der Wasserverbrauch wurde für die Stadtbevölkerung auf 97 l/(E·d) und für die Bevölkerung in ländlichen Gebieten auf 55 l/(E·d) festgelegt (Franzius et al. 1893). Die derzeit in MoRE angewandten täglichen Nährstoffabgaben [12 g N/(E·d) und 1,9 g P/(E·d)] wurden nicht angepasst, da sie im Wertebereich historischer Literaturquellen liegen. Eine lokale Abwasserbehandlung in Form von Rieselfeldern wurde nur für Berlin berücksichtigt, wobei für Stickstoff und Phosphor ein Rückhalt von 65 % bzw. 90 % in den Böden angenommen wurde.

Für die Modellierung der **atmosphärischen Deposition** auf Wasserflächen wurde für Stickstoff ein globaler Datensatz zu historischen Bedingungen (Hegglin et al. 2016) verwendet. Für Phosphor wurde eine Depositionsrate von 75 g/(ha·a) nach der Schätzung von Ruoho-Airola et al. (2012) verwendet.

Der Datensatz zur Stickstoffdeposition wurde auch für die Modellierung der Einträge über **Oberflächenabfluss** verwendet. Für Phosphor wurde die Konzentration im Oberflächenabfluss von allen bewachsenen Flächen auf 0,0125 mg P/L festgelegt, basierend auf der Phosphorauswaschung von unproduktiver Vegetation (Prasuhn et al. 1996).

Für die Modellierung der **Erosion** wurden unterschiedliche Ansätze für das heutige Deutschland und die ausländischen Gebiete der Flusseinzugsgebiete verwendet. Für das heutige Deutschland wurden die Eingangsdaten auf Grundlage der allgemeinen Bodenabtragsgleichung (ABAG) angepasst, die aus einer kürzlich vorgenommene Erosionsmodellierung für Deutschland stammen (Fuchs et al. 2022). Der Bodenbedeckungs- und -bearbeitungsfaktor (C-Faktor) auf Ackerland wurde um etwa 41 % erhöht, um zu berücksichtigen, dass in der Vergangenheit keine konservierende Bodenbearbeitung stattgefunden hat. Der Niederschlagserosivitätsfaktor (R-Faktor) wurde anhand des mittleren Jahresniederschlags aus der historischen Wasserbilanz nach DIN 19708 (2017) neu berechnet, wobei davon ausgegangen wurde, dass das Verhältnis zwischen Jahresniederschlag und Niederschlagserosivität im späten 20. Jahrhundert dem im späten 19. Jahrhundert entsprach. Die übrigen ABAG-Faktoren wurden nicht angepasst. Da Anpassungen der Gewässerdistanz und Anbindungswahrscheinlichkeit mit zu großen Unsicherheiten behaftet sind, wurde für die Berechnung der Sedimenteinträge die von Fuchs et al. (2022) ermittelten Sedimenteintragsverhältnisse beibehalten. Für die ausländischen Gebiete wurde ein Datensatz zu historischem Bodenabtrag in Europa (Fendrich et al. 2022) verwendet und die Sedimenteinträge nach dem originalen MONERIS-Ansatz von Venohr et al. (2011) berechnet.

Sowohl für das heutige Deutschland als auch für das Ausland wurden die aktuell implementierten Stickstoff-Oberbodengehalte (Morling et al. 2024) für die Modellierung der Einträge über Erosion im Jahr 1880 verwendet. Als Phosphorgehalte für landwirtschaftlich genutzte Flächen (Ackerland, Obstbau, Weinbau, Grünland) wurden die aktuell implementierten Gehalte natürlicher Flächen (Fuchs et al. 2022) verwendet, unter der Annahme, dass die Böden im Jahr 1880 nicht überdüngt waren.

Für die Modellierung der Einträge über **Zwischenabfluss** und **Basisabfluss** wurden die derzeit implementierten Stickstoffkonzentrationen entsprechend einer Obergrenze von 2,257 mg N/L (10 mg/L Nitrat) angepasst, die unbeeinflusste Grundwasserbedingungen darstellt. Für Phosphor wurden die derzeit implementierten Eingangsdaten von Fuchs et al. (2022) für die Modellierung von 1880 beibehalten. Dabei wird davon ausgegangen, dass die P-Konzentrationen im Grundwasser in erster Linie von geologischen Eigenschaften und nicht von landwirtschaftlicher Bewirtschaftung abhängen.

Da keine verlässlichen Daten vorliegen, wurden die derzeit verwendeten Anteile dränierter landwirtschaftlicher Flächen (Ackerland und Grünland) in Anlehnung an den Ansatz von Gadegast und Venohr (2015) soweit reduziert, dass die gesamte dränierte Fläche des MoRE-Modellgebietes 6 % für das Jahr 1880 entspricht. Für die Modellierung der Einträge über **Dränagen** wurde eine konstante Nitratkonzentration von 10 mg/L (2,257 mg N/L) angenommen. Fuchs et al. (2022) leiteten aus aktuellen Messungen P-Konzentrationen im Grundwasser ab, die im Mittel 0,022 mg P/L für Deutschland betragen. Diese wurden auch für die Modellierung der P-Einträge über Dränagen für 1880 verwendet.

Für die Modellierung der **Retention** in den Flusseinzugsgebieten wurde der THL-Ansatz von Venohr (2006) für Stickstoff in MoRE verwendet, der die Wassertemperatur (T) und die hydraulische Belastung (HL) berücksichtigt. Für das historische Szenario wurden die aktuell implementierten durchschnittlichen Wassertemperaturen um 1 K reduziert, um die allgemein kühleren Klimabedingungen der Vergangenheit widerzuspiegeln. Für Phosphor wird die Retention als Funktion der hydraulischen Belastung nach Venohr et al. (2011) modelliert.

Ergebnisse der historischen Eintragsmodellierung

Die **Gesamteinträge** für Stickstoff im Jahr 1880 belaufen sich auf rund 257 kt N/a und 36 kt N/a für die Nord- und Ostseeeinzugsgebiete (Table 2). Zwischenabfluss und Basisabfluss sind mit 77 % – 82 % der gesamten Einträge die wichtigsten Pfade für Stickstoff (Figure 2). Die gesamten Phosphor-Einträge belaufen sich auf 8,2 kt P/a bzw. 1 kt P/a für die Einzugsgebiete von Nord- und Ostsee (Tabelle 2). Die Erosion ist der wichtigste Eintragspfad für Phosphor (Figure 2) und macht 49 % bzw. 38 % der modellierten Einträge für die Einzugsgebiete der Nord- und Ostsee aus. Kanalisationssysteme sind der zweitwichtigste Eintragspfad für Phosphor (23 % – 25 %).

Table 2: Zusammengefasste Modellergebnisse für die Einzugsgebiete der Nord- und Ostsee im Jahr 1880.

Parameter	Einheit	Nordsee-Einzugsgebiete	Ostsee-Einzugsgebiete
Gesamtstickstoff-Eintrag	[kt/a]	257	36
Gesamtstickstoff-Fracht	[kt/a]	180	22
Stickstoffretention	[%]	30	38
Durchschnittliche Stickstoffkonzentration	[mg/L]	1,37	1,11
Gesamtphosphor-Eintrag	[t/a]	8 208	1 065
Gesamtphosphor-Fracht	[t/a]	4 204	446
Phosphorretention	[%]	49	58
Durchschnittliche Phosphorkonzentration	[mg/L]	0,032	0,022

Figure 2: Stickstoff- (obere Reihe) und Phosphorflüsse (untere Reihe) in den Flussgebieten zur Nordsee (links) und Ostsee (rechts) um 1880.

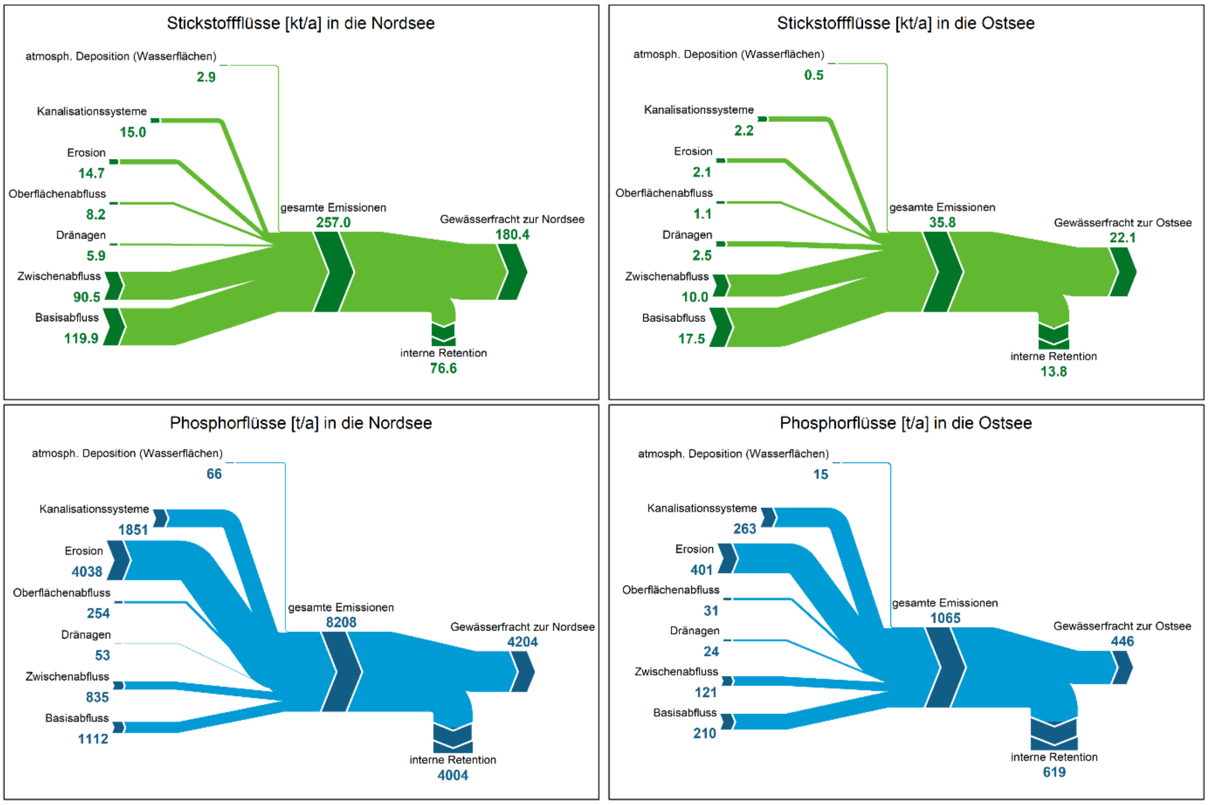

Quelle: Gericke et al. (2025)

Die Einzugsgebiete der Nordsee transportieren rund 180 kt N/a und 4,2 kt P/a an **Stofffrachten** ins Meer (Table 2, Figure 2). Das entspricht einer Retention der gesamten Einträge von 30 % für Stickstoff und 49 % für Phosphor. In die Ostsee wurden rund 22 kt N/a und 0,46 kt P/a an Frachten eingetragen, was einer Retention der Einträge von 38 % für Stickstoff und 58 % für Phosphor entspricht (Table 2, Figure 2).

Die Nährstoffkonzentrationen in den Gewässern wurden aus den transportierten Frachten und dem Gesamtabfluss berechnet. Sowohl für Stickstoff als auch für Phosphor folgten die **modellierten Konzentrationen** teilweise dem räumlichen Muster der Einträge. Die höchsten Nährstoffkonzentrationen wurden in dicht besiedelten städtischen Gebieten modelliert. Auch in Gebirgsregionen waren die Phosphorkonzentrationen höher, was auf die höheren Einträge durch Erosion zurückzuführen ist.

Modellvalidierung

Abflussmessungen an Pegeln im Modellgebiet sind für wenige Standorte seit 1873 beim Global Runoff Data Centre verfügbar (BfG 2024). Diese wurden für eine Bewertung der modellierten Wasserbilanz verwendet. Für 11 Pegelstationen wurde der durchschnittliche jährliche Abfluss aus Originalmessungen berechnet. Dieser beobachtete Abfluss wurde mit dem modellierten Gesamtabfluss der MoRE-Analysegebiete verglichen, in denen die Pegelstationen verortet sind. Obwohl die begrenzte Anzahl von verfügbaren Pegeln eine eingehende Validierung erschwert, ergab der Vergleich eine gute Übereinstimmung des simulierten Abflusses mit historischen Aufzeichnungen.

Die Validierung der modellierten Konzentrationen wird durch einen Mangel an geeigneten Daten erschwert, da in der historischen Literatur nur wenige Messungen verzeichnet sind. Ein Vergleich wurde hauptsächlich durchgeführt, um sicherzustellen, dass die modellierten Konzentrationen in der gleichen Größenordnung liegen. Dabei zeigte sich insgesamt eine gute Übereinstimmung der Nährstoffkonzentrationen mit den historischen Literaturdaten. Die modellierten Konzentrationen stimmen im Schnitt auch gut mit den Ergebnissen weiterer historischer Modellierungsstudien überein (Gadegast & Venohr 2015; Hirt et al. 2014; Jensen 2017).

Vergleich mit anderen historischen Modellszenarien

Die Ergebnisse der MoRE- und MONERIS-Modellierung sind im Vergleich zu den Ergebnissen der regionalen E-HYPE-Modellierung und den globalen Daten von Beusen et al. (2016) für alle betrachteten Parameter (Einträge, Frachten, Retention und Konzentrationen) sehr ähnlich. Unterschiede zwischen der MoRE- und der MONERIS-Modellierung bestehen vor allem in der Bedeutung einzelner Eintragspfade. So sind beispielsweise für die Stickstoff-Einträge in der MoRE-Modellierung Oberflächenabfluss und Dränagen verhältnismäßig geringer, während die Summe aus Zwischenabfluss und Basisabfluss größer ist. Für Phosphor ist die Summe aus Zwischenabfluss und Basisabfluss geringer, während die Pfade Erosion und Kanalisationssysteme im Vergleich zu früheren MONERIS-Ergebnissen verhältnismäßig wichtiger sind.

Für historische Nährstoffkonzentrationen in Oberflächengewässern gibt es nur wenige Messungen. Im Vergleich zu diesen stimmen die von den Modellen MoRE und MONERIS vorhergesagten Konzentrationen von allen betrachteten Modellierungen am besten mit den historischen Bedingungen überein. Das 1880-Szenario in MoRE lieferte in diesem Modellvergleich generell die niedrigsten Nährstoffkonzentrationen, was auch den höchsten Reduktionsbedarf für die Küsten- und Meeresumwelt impliziert.

Einschränkungen und Unsicherheiten in der historischen Modellierung

Modellierung ist im Allgemeinen mit vielen Unsicherheiten behaftet. Die Abbildung historischer Bedingungen wird zusätzlich durch die Verfügbarkeit historischer Daten, die notwendigen Modellannahmen und Vereinfachungen sowie die sehr begrenzten Validierungsmöglichkeiten erschwert. Die Wahl der Eingangsdaten hat großen Einfluss auf die Modellergebnisse und kann zu einer Über- oder Unterschätzung von Einträgen und Frachten führen. Jeder Eintragspfad hängt von spezifischen Eingangsdaten und Variablen ab. Daher ist der Beitrag einzelner Eintragspfade zu den Gesamteinträgen unterschiedlich und variiert auch räumlich. Eine vollständige Bewertung der Unsicherheit ist aufgrund der großen Zahl von Eingangsdaten und Anpassungen der Modellierungsansätze nicht möglich. Stattdessen wird auf einige wichtige Aspekte eingegangen.

Die derzeit angewandten **Grundwasserkonzentrationen** wurden entsprechend einer Obergrenze von 2,257 mg N/L (10 mg/L Nitrat) angepasst, die auf einer Analyse von Trinkwasserproben aus dem Jahr 1915 beruht (UBA 1994). Diese Annahme ist mit einer hohen Unsicherheit behaftet, da die Verteilung und Repräsentativität der Proben nicht bekannt sind. Die tatsächlichen Grundwasserkonzentrationen für das Jahr 1880 sind nicht bekannt, daher werden diese im Modellszenario in verschiedenen Regionen des Untersuchungsgebiets sicherlich über- oder unterschätzt.

Der **Oberbodengehalt** ist eine der Hauptvariablen, die die Einträge durch Erosion beeinflusst. Die Oberbodengehalte von Acker- und Weideland im Jahr 1880 sind für das gesamte Modellgebiet unbekannt. Es wurde davon ausgegangen, dass die heutigen Phosphor-Oberbodengehalte der natürlich bedeckten Flächen repräsentativ für die landwirtschaftlichen Böden sind, da diese 1880 nicht überdüngt waren. Die Phosphor-Einträge durch Erosion waren für das Rheineinzugsgebiet im Vergleich zu früheren MONERIS-Ergebnissen um das 2,5-fache höher. Dies ist auf abweichende Modellannahmen zum **Bodenabtrag** für alpine Gebiete zurückzuführen, bei denen davon ausgegangen wurde, dass das gesamte erodierte Material in die Oberflächengewässer gelangt. Dieses Beispiel unterstreicht die Bedeutung von landnutzungsspezifischen Annahmen für die Modellierung von Flusseinzugsgebieten.

Die Einträge der Kanalisationssysteme wurden in diesem Projekt wahrscheinlich unterschätzt, da keine **gewerblichen und industriellen Abwässer**, die ebenfalls Nährstoffe in Oberflächengewässer liefern können, in die Modellierung einbezogen wurden. Die Zusammensetzung dieser Abwässer ist nur grob aus Einzelbeobachtungen in der historischen Literatur bekannt. Abwässer aus verschiedenen Produktionsstufen und -prozessen wurden in der Regel gemeinsam eingeleitet, so dass ihre genaue Zusammensetzung weitgehend unbekannt blieb (Büschenfeld 1997). Dies erschwert die Ableitung von zuverlässigen Stoffkonzentrationen zusätzlich zur Quantifizierung der Abwasservolumina. Außerdem ist davon auszugehen, dass die industriellen Einträge im Vergleich zu heute sehr viel dezentraler erfolgten.

Die **Retention** in Oberflächengewässern wurde mit den derzeit in MoRE implementierten Ansätzen modelliert, wobei Veränderungen aufgrund der vielen wasserbaulichen Maßnahmen seit 1880 vernachlässigt wurden. Der Nährstoffrückhalt könnte in der Vergangenheit höher gewesen sein, da der Abfluss durch hydraulische Maßnahmen weniger reguliert wurde und es historisch mehr Feuchtgebiete gab (Jensen 2017). Eine Rekonstruktion des Gewässernetzes und der Küstenmorphologie um 1880 war nicht möglich und würde umfangreiche Anpassungen und Kalibrierungen in den beiden Modellen MoRE und LARSIM-ME erfordern.

Schlussfolgerung

Im Vergleich zu früheren Arbeiten umfasst das hier erstellte historische Szenario eine konsistente Modellierung der Nährstoffeinträge und -frachten für alle Flusseinzugsgebiete der deutschen Nord- und Ostseezuflüsse. Dafür wurde mit dem hydrologischen Modell LARSIM-ME eine konsistente, wenn auch vereinfachte historische Wasserbilanz für das Untersuchungsgebiet abgeleitet, die sowohl die klimatischen Bedingungen wie auch die Landnutzung und den Versiegelungsgrad um 1880 berücksichtigt.

Der Vergleich mit weiteren historischen Modellierungsstudien ergab, dass die 1880 Ergebnisse aus MoRE den früheren Ergebnissen von MONERIS (Gadegast et al. 2012; Gadegast & Venohr 2015; Hirt et al. 2014) ähnlicher sind als regionale (Blauw et al. 2019) und globale Modell-Anwendungen (Beusen et al. 2016). Unterschiede in den Eingabedaten und Modellierungsansätzen zwischen MoRE und MONERIS hatten nur geringe Auswirkungen auf die Ergebnisse der gesamten Nährstoffeinträge und -frachten auf der Ebene der Flusseinzugsgebiete. Allerdings unterscheiden sich die einzelnen Pfade in ihrer Bedeutung zwischen den beiden Modellen.

Obwohl sich die Ergebnisse von MoRE und MONERIS insgesamt ähneln, sind die mit MoRE modellierten Nährstoffkonzentrationen an den Auslässen der Flusseinzugsgebiete im Durchschnitt niedriger. Diese niedrigeren Nährstoffkonzentrationen implizieren einen stärkeren Reduktionsbedarf zum Schutz der Meeres- und Küstengewässer. Somit können die Modellergebnisse auch zu einer kritischen Überprüfung der derzeit geltenden durchschnittlichen jährlichen Zielwerte für Gesamtstickstoff und Gesamtphosphor für die deutschen Zuflüsse der Nord- und Ostsee hinsichtlich ihrer Gültigkeit beitragen.

Die Ergebnisse dieses Projekts werden für das Gebiet des heutigen Deutschlands in der **MoRE-Toolbox** visualisiert, die es erlaubt, ausgewählte Eingangsdaten und Ergebnisse interaktiv zu erkunden: https://stoffeintraege-more.de/

Die **Modellergebnisse des 1880-Szenarios** sowie die Geometrien der Analysegebiete können über ZENODO heruntergeladen werden: https://doi.org/10.5281/zenodo.15227585.

1 Introduction

Despite decreasing nutrient emissions since the 1990s, marine waters fail to achieve good status with regard to eutrophication according to the Water Framework Directive (WFD) and Marine Strategy Framework Directive (MSFD). Most nutrient emissions originate from terrestrial sources and enter the sea via rivers.

Target values are a legal prerequisite to achieve the good environmental status and are fundamental for river basin management. For Germany, target annual average concentrations have been derived in the past to achieve the good environmental status according to MSFD with respect to nutrient and chlorophyll-a concentrations in coastal and marine water bodies of the North Sea and Baltic Sea (BLANO 2015; BLMP 2011; Schernewski et al. 2015). For total nitrogen, annual average target concentrations of 2.8 mg N/L and 2.6 mg N/L were derived for North Sea and Baltic Sea tributaries, respectively. These targets have been laid down in the German Surface Water Ordinance (OGewV). The target for North Sea tributaries was originally derived for the Rhine River at the German-Dutch border from a Dutch threshold value for dissolved inorganic nitrogen (ICPR 2010) and was later transferred to other German North Sea tributaries (BLMP 2011). The target value for Baltic Sea tributaries was based on modelling historical nutrient emissions in 1880 and a permitted deviation of 50 % (Schernewski et al. 2015). There are no corresponding target concentrations for total phosphorus. Instead, riverine type-specific orientation values according to the OGewV (Annex 7) currently apply.

Historical nutrient emissions for 1880 were derived using the MONERIS model for German Baltic Sea (Hirt et al. 2014) and North Sea basins (Gadegast & Venohr 2015). Additional assumptions and extended input data were used for the North Sea basins, leading to inconsistent approaches between North Sea and Baltic Sea basins. For instance, mean nitrogen surplus was estimated without considering nitrogen fixation for Baltic Sea basins (Hirt et al. 2014), while it was included for the modelling of North Sea basins (Gadegast & Venohr 2015). A harmonized modelling for 1900 conditions of North Sea basins was pursued using the model E-HYPE (Blauw et al. 2019). Historical total phosphorus loads obtained by E-HYPE are five times larger than the ones estimated by MONERIS. Differing results of both models led to significant uncertainties for ecosystem modelling and reduction requirements in marine environments (Stegert et al. 2021). These uncertainties raise the question how reliable the estimated reference conditions for Germany are in comparison to that of neighboring countries, but also how robust the former model assumptions have been.

In recent years, new historical data sets were published or existing ones improved (Batool et al. 2022; Fendrich et al. 2022; Klein Goldewijk et al. 2017; Paprotny & Mengel 2023), differing in their spatial resolution and methodological approaches. The substance emission model MoRE (Modelling of Regionalized Emissions) is used as tool for national reporting and is subject to continuous model developments (Morling et al. 2024, Fuchs et al. 2022, Morling & Fuchs 2021). Thus, previous input data and results on historical nutrient emissions have to be revised using newly available datasets and improved modelling approaches.

The **objectives** of this study were the modelling of a historical nutrient emission scenario representing 1880 conditions for all river basins of the North Sea and Baltic Sea, which Germany shares with its neighbours. This fosters the consistency between North Sea and Baltic Sea basins as well as enables a plausibility assessment of previous historical modelling results. In this study, the national reporting tool MoRE was used to compute historical nutrient emissions into surface waters and transported loads. The hydrological model LARSIM-ME provided a revised historical water balance, which was incorporated into the MoRE model. This collaboration has been successfully demonstrated before (Morling et al. 2024). The use of a water balance model allowed consideration of past conditions of climate, land use and imperviousness for runoff simulation in contrast to previous historical emission modelling applications of

MONERIS and E-HYPE, which made use of average hydrological conditions of 1983 – 2005 (MONERIS) and 1979 – 2013 (E-HYPE).

The new modelling of historical nutrient emissions for 1880 could also enable a critical revision of currently implemented target values at the limnic-marine border for total nitrogen and total phosphorus in riverine waters of Germany for their validity.

The results of this project are visualized for the area of present Germany in the **MoRE toolbox**, which allows to interactively explore selected input data and results in more detail: https://stoffeintraege-more.de/

The model results of the 1880 scenario presented here as well as the geometry of the modeling units can be downloaded from the ZENODO repository: https://doi.org/10.5281/zenodo.15227585

2 Modelling tools

2.1 MoRE

The German Environment Agency (UBA) uses the substance emission model MoRE for the nationwide estimation of a wide range of substances emitted into surface waters (UBA 2024). The substance emissions into water bodies are modelled via various **emission pathways** (Figure 3). The MoRE model includes pathways linked to point sources (e.g. municipal wastewater treatment plants, industrial direct dischargers) and diffuse sources (e.g. erosion, groundwater, tile drainage). It was extended in 2009 based on the nutrient emission model MONERIS (Modelling Nutrient Emissions in River Systems; Behrendt et al. 2000; Venohr et al. 2011) to consider further inorganic and organic pollutants (metals, PAHs, pharmaceuticals, pesticides) and has been continuously developed since then on behalf of the UBA, among others (Fuchs et al. 2010; Fuchs et al. 2017a; Fuchs et al. 2017b; Fuchs et al. 2022; Morling & Fuchs 2021). Recent developments include a revised erosion modelling for Germany (Fuchs et al. 2022) and an improved water balance, for which runoff components obtained by the hydrological model LARSIM-ME (see next section) were integrated as input data in MoRE (Morling et al. 2024).

Figure 3: General scheme of emission pathways in the MoRE model.

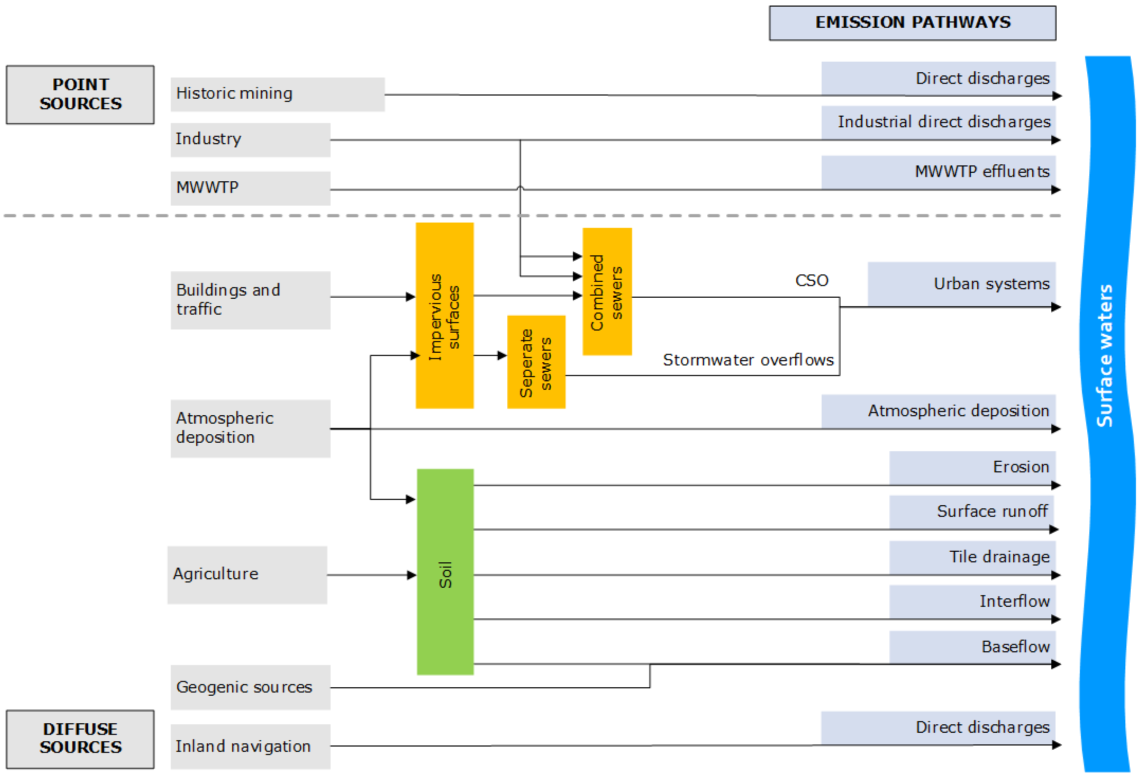

Source: own illustration, IWU-WG

The UBA application of the MoRE model covers all river basins in Germany and their foreign parts (Figure 4). In total, the area under consideration amounts to roughly 660,000 km². The smallest spatial modelling units in MoRE are referred to as **analytical units** (AU). They uniquely represent hydrological catchments as well as administrative units. Present Germany is represented by 2,759 analytical units with an average area of 130 km² (Figure 4). The foreign AU (n = 697) are generally larger in size with an average area of 433 km². The temporal resolution is currently one year. Thus, MoRE is providing annual average substance emissions and loads (Fuchs et al. 2017b), from which riverine average concentrations can be derived.

Figure 4: River basins and analytical units of the MoRE model.

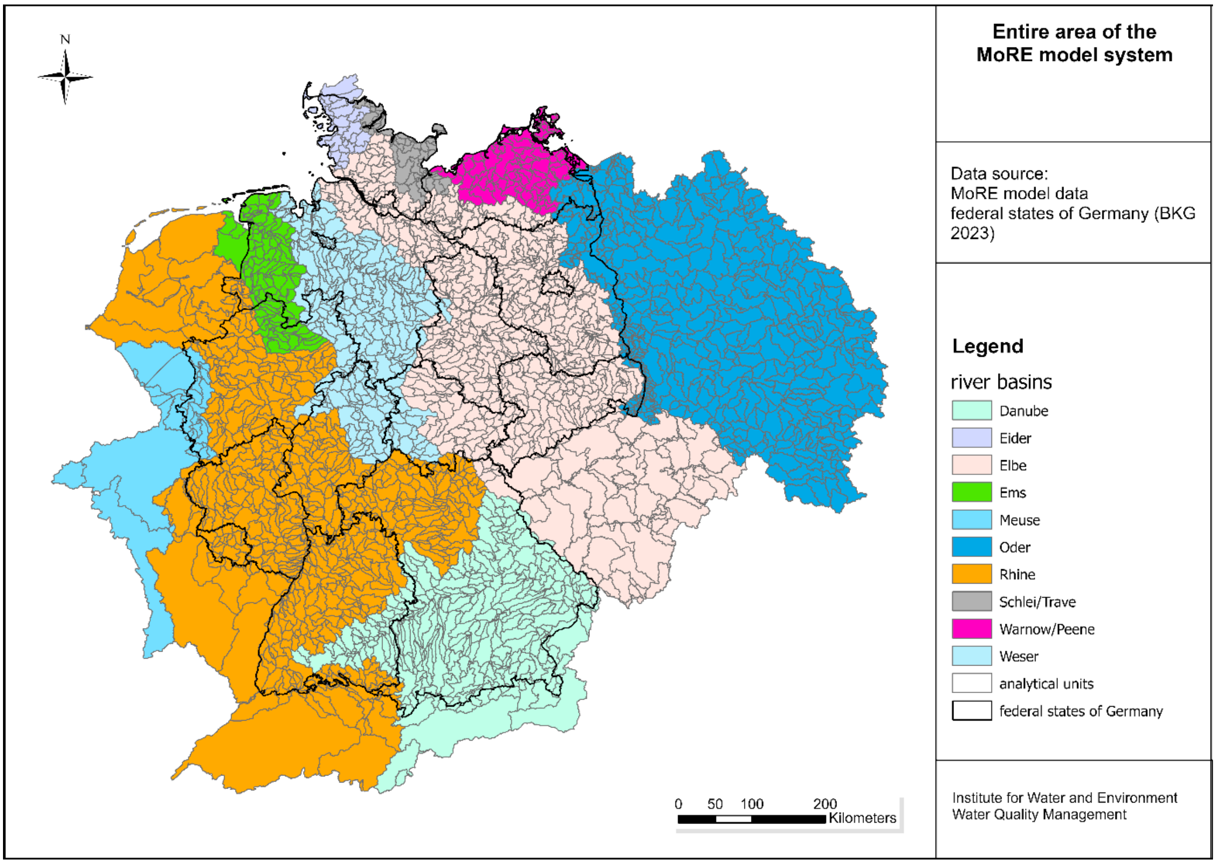

Source: own illustration, IWU-WG

For historical modelling, the point source pathways of municipal wastewater treatment plants (MWWTP) and industrial direct dischargers are not modelled. MWWTP were not relevant for the 1880 scenario (refer to chapter 5.3). Data on industrial emissions were unavailable (for uncertainties and limitations see chapter 8).

All river basins covered in MoRE were included in the 1880 scenario. This included the Upper Danube basin as well, even though it is not contributing to North Sea and Baltic Sea and is thus not in the focus of this study. For the Danube basin, the same input data sets were prepared as described in the main text and in Appendix A. The model results of the Upper Danube basin are shown in Appendix D.

2.2 LARSIM-ME

The process-oriented water balance model LARSIM (Large Area Runoff SImulation Model) was developed by Bremicker (2000) and has been continuously improved since then on behalf of the LARSIM Developer Group (LEG), which comprises the flood forecast centres of the German federal states of Baden-Württemberg, Bavaria, Hesse, North Rhine-Westphalia and Rhineland-Palatinate as well as the Swiss Federal Office for the Environment (e.g. Bremicker et al. 2004; Luce et al. 2006; Haag & Luce 2008; Haag et al. 2016; Haag et al. 2019; Haag et al. 2022; Haag et al. 2023; Krumm et al. in press; LEG 2024). LARSIM improvements also include developments to generate the hydrological input for the emission model MoRE in various applications in Germany, Luxembourg and Brazil (Fuchs et al. 2019; Morling et al. 2024). LARSIM is a well-established hydrological model, which is widely used in Germany, Switzerland, Luxembourg, Austria and parts of France for flood forecasting and various other hydrological tasks (e.g. Bremicker et al. 2013; LEG 2024).

LARSIM-ME (LARSIM - Middle Europe) is a specific LARSIM model set up on behalf of the Federal Institute of Hydrology (BfG; Meißner et al. 2017). With a total size of approx. 800,000 km², it covers all river basins that Germany shares with its neighbouring countries. LARSIM-ME consists of six separate models for distinct watersheds (Figure 5). The spatial resolution of LARSIM-ME is much coarser than the spatial resolution of the LARSIM models used by the federal states. The sub-basins are based on grid cells with a resolution of 5 km · 5 km (25 km²). The hydrological response units of LARSIM-ME are discriminated by land use only, whereas information on soil properties is averaged for each land use class within a grid cell. The original LARSIM-ME model was amended for improving the separation of total runoff into different runoff components for nutrient emission modelling (Morling et al. 2024).

Figure 5: Watershed models of LARSIM-ME model system.

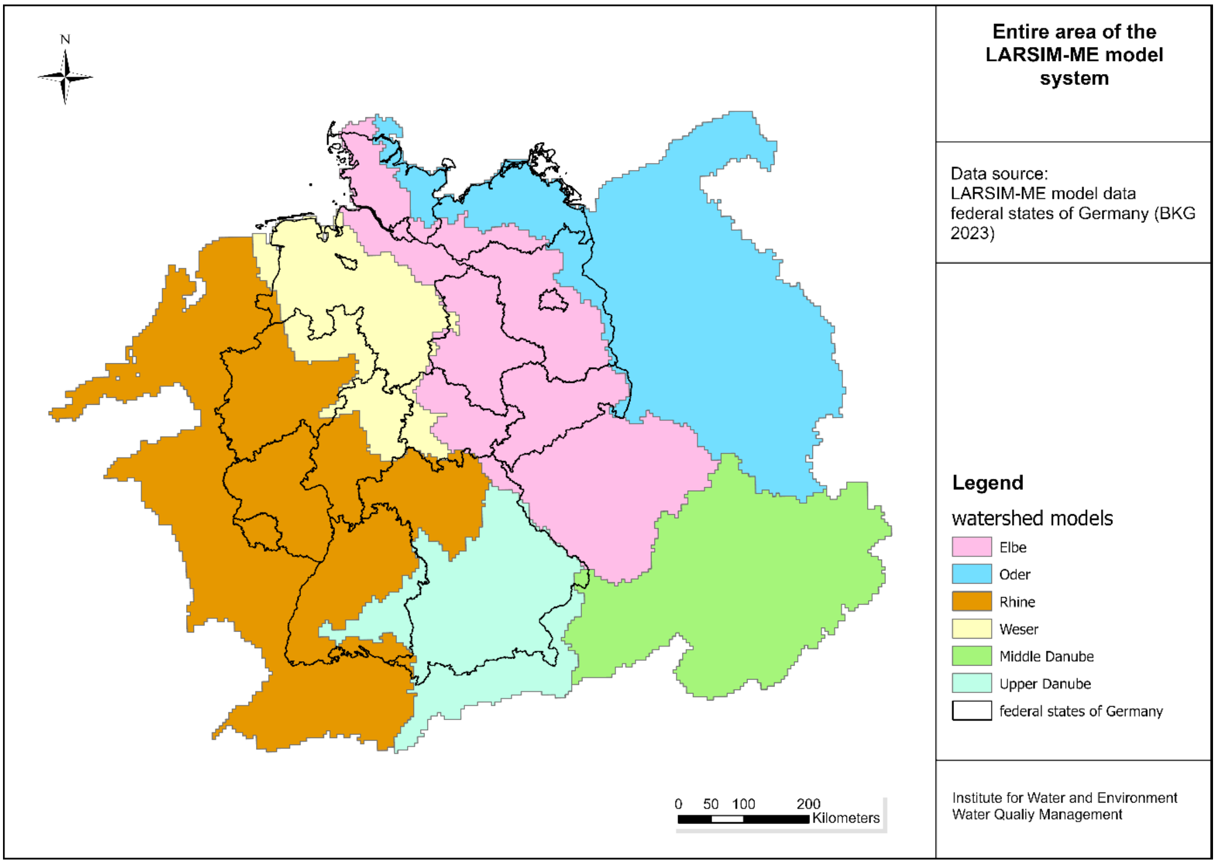

Source: own illustration, IWU-WG

3 Historical land use and population

3.1 Land use

For land use, the HANZE 2.0 dataset (Paprotny & Mengel 2023) was used. The dataset is freely available and contains land use information as well as information on imperviousness and population (refer to the next two chapters). The land use raster for the year 1880 was selected for further processing. The provided Corine land cover (CLC) classification of the HANZE 2.0 was used to assign the individual land use categories to the classes used in the MoRE model (see Appendix A.2 for classification details). The land use dataset was intersected with the MoRE analytical units to obtain the areas for each land use class in the sub-basins.

For the considered year 1880, most land was dedicated to agriculture as arable land and pastures made up 65 % and 66 % of land use in the North Sea and Baltic Sea basins, respectively (Table 3, Figure 6). Naturally covered areas (mostly forest) accounted for 29 %, while all other land use classes were represented with less than 6 % (Table 3, Figure 6).

Figure 6: Land use in 1880 aggregated to land use classes of the MoRE model.

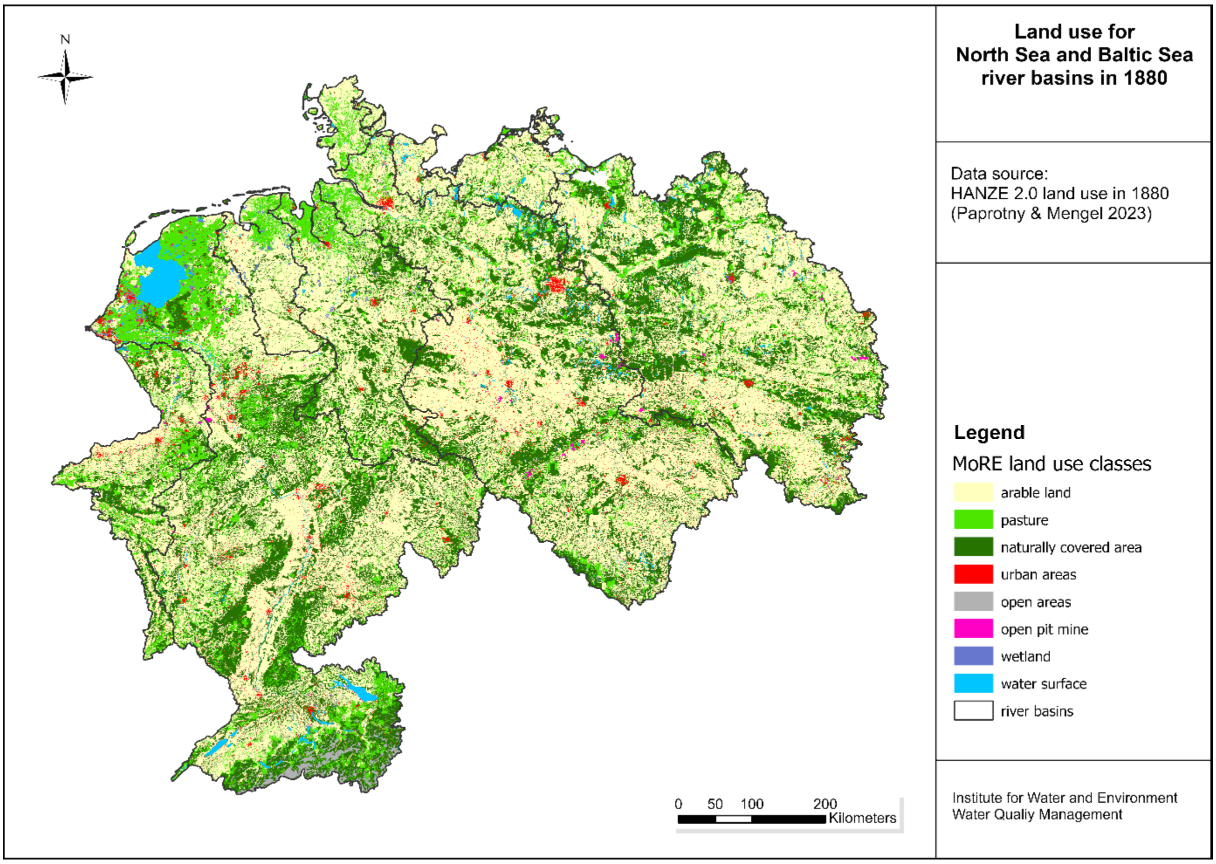

Source: own illustration, IWU-WG

Table 3: Land use in 1880 aggregated to MoRE land use classes for North Sea and Baltic Sea basins, values rounded.

	North Sea basins		Baltic Sea basins	
Land use category	**[km²]**	**[%]**	**[km²]**	**[%]**
Arable land	221 600	51	82 500	57
Pastures	59 600	14	13 700	9
Naturally covered areas	127 500	29	42 000	29
Urban areas	13 000	3	3 100	2
Open areas	3 300	1	100	< 1
Open pit mining	1 200	< 1	400	< 1
Wetlands	2 300	1	500	< 1
Water surfaces	8 800	2	2 000	1
Total	**437 300**	**100**	**144 300**	**100**

3.2 Imperviousness

Impervious (sealed) surfaces are a crucial part of the urban water cycle. To estimate their area, the imperviousness raster for the year 1880 from the HANZE 2.0 dataset by Paprotny & Mengel (2023) was used. Urban areas from the corresponding land use data of this dataset (see chapter 3.1) were used to select the impervious raster cells. Imperviousness, given in percent, was converted to impervious area per raster cell and subsequently aggregated to the analytical units of MoRE. On average, 40 % and 29 % of the urban areas were sealed in 1880 in the North Sea and Baltic Sea basins, respectively (Table 4).

Table 4: Imperviousness in 1880 aggregated to MoRE analytical units for North Sea and Baltic Sea basins, values rounded.

Land use parameter	Unit	North Sea basins	Baltic Sea basins
Urban areas[a]	[km²]	13 000	3 100
Impervious areas	[km²]	5 200	900
Sealing degree	[%]	40	29

[a] – see Table 3

3.3 Population

Population was taken from HANZE 2.0 dataset by Paprotny & Mengel (2023). The population raster for the year 1880 provides population in inhabitants per hectare. Total population was obtained for the analytical units of MoRE. For most of the study area, population density was low. However, analytical units covering larger cities such as Berlin or Hamburg showed clearly much higher population densities (Figure 7).

For North Sea basins, the total population accounts to 44.1 million inhabitants. In comparison, approximately 9.8 million inhabitants were obtained for the Baltic Sea basins, which cover less densely populated areas.

Figure 7: Population density per MoRE analytical unit in 1880.

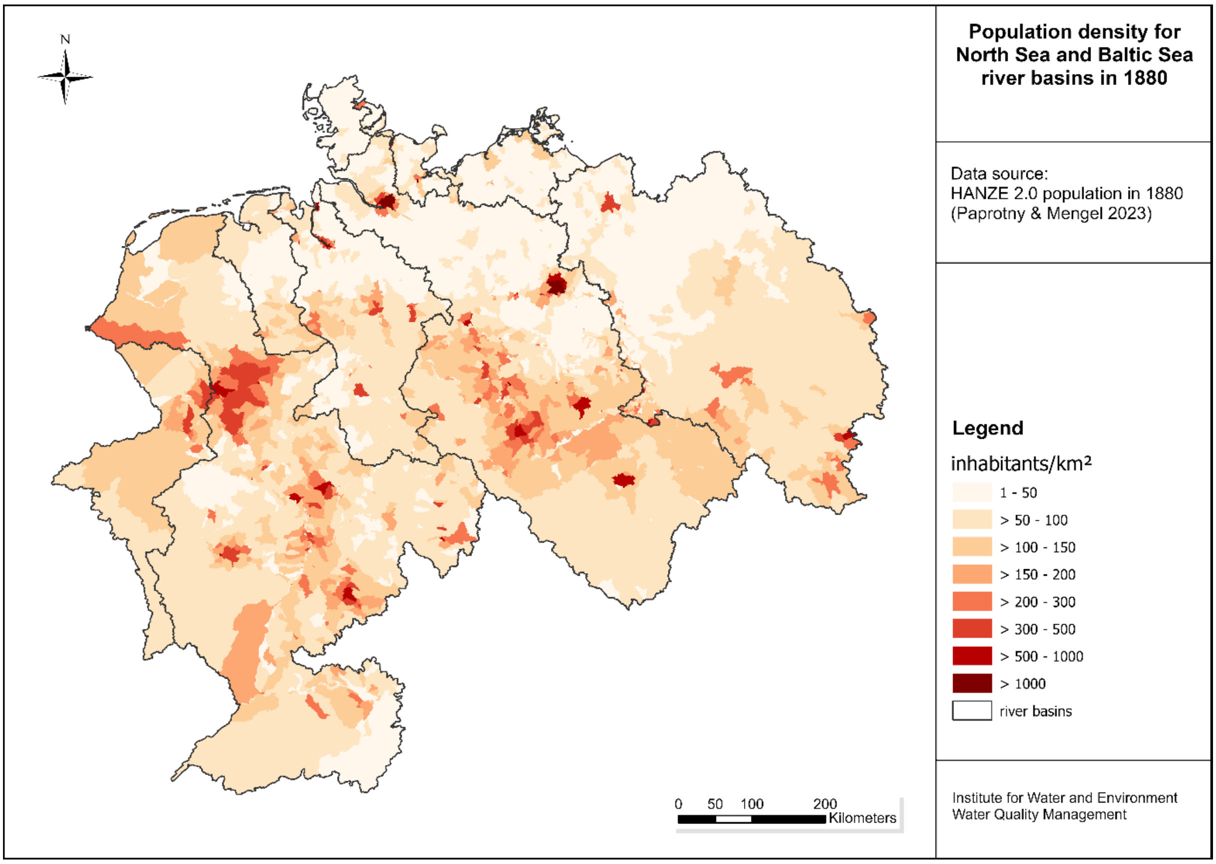

Source: own illustration, IWU-WG

4 Historical water balance

The hydrological model LARSIM-ME was used to derive natural runoff components for different land use categories for a 15-year period representing 1880 (chapter 4.1). To build a final water balance for emission modelling, mean values of the runoff components from LARSIM-ME were integrated in MoRE considering the wastewater from urban areas (chapter 4.2). Finally, results of the water balance of the 1880 scenario are presented and validated (chapter 4.3).

4.1 Deriving natural runoff components with LARSIM-ME

The hydrological model LARSIM-ME, including the improvements described in Morling et al. (2024), was used to simulate the natural runoff components for the historical water balance of 1880 (1880 scenario). This includes the following working steps:

- Deriving the climatological conditions of the period around 1880 as external meteorological forcing for the hydrological model using climate change vectors (chapter 4.1.1)
- Deriving the spatial distribution of land use and the degree of imperviousness for 1880 as internal forcing of the hydrological processes (chapter 4.1.2)
- Applying the model and deriving the spatial and land use specific distribution of the runoff components from the model results (post-processing) as input for MoRE (chapter 4.1.3)

4.1.1 Meteorological forcing using climate change vectors

4.1.1.1 Deriving climate change vectors for the 1880 scenario

LARSIM-ME needs the following meteorological parameters as input (external forcing):

- Precipitation [mm]
- Air temperature [°C]
- Relative humidity [%]
- Incoming short-wave radiation [W/m^2]
- Wind speed [m/s]
- Atmospheric pressure [hPa]

These parameters have to be provided as daily data in an adequate spatial resolution throughout the complete model domain, either as station data or as raster data.

Due to climate change, it is not adequate to simply use measurements of a recent time span to represent historical conditions. Thus, to account for the different climate in the water balance modelling, it is necessary to have consistent daily time series of the above-mentioned meteorological parameters for hundreds of stations or as spatially distributed raster data for the time span around 1880. For the time before 1900, no meteorological data sets are available meeting the requirements with respect to temporal and spatial resolution as well as quality and homogeneity (e.g. Lundstad et al. 2023). In addition, results of hydrological models partly depend on the spatial distribution of the meteorological input data. Using input data of different spatial resolution may therefore cause unintended artefacts. Given these circumstances, we decided to work with climate change vectors (ccv) instead of directly using measured meteorological data.

Climate change vectors (ccv) are defined as the difference between a parameters value (e.g. air temperature) under 1880 climatic conditions and the value under present climatic conditions. They can either be expressed in an additive way (for temperature) or a multiplicative way (for all other meteorological parameters):

For air temperature (Ta): $$Ta_{1880} = Ta_{present} + ccv_{Ta} \tag{1}$$

For all other parameters (Par): $$Par_{1880} = Par_{present} \times ccv_{Par} \tag{2}$$

Consequently, mean climatological conditions for the 1880 scenario are characterized by measurements from the present and the corresponding ccv for a parameter. However, because of climate fluctuations, ccv cannot be derived from a single year. It is rather necessary to use a longer time span, in order to capture mean climatological conditions. Therefore, a **15-year time span (1873 – 1887)** was chosen to represent mean conditions around 1880. Based on the evaluation of the sparse meteorological and discharge data from that time (BfG 2024; Lundstad et al. 2023; Slivinski et al. 2019), the selected period does not include extreme outliers and can thus be viewed as representative for mean meteorological and hydrological conditions for the 1880 scenario.

Hence, gaining ccv needs an internally consistent meteorological data set covering the whole model domain and the period around 1880 as well as the present. Since homogenous (internally consistent) measurements are not available for 1873 – 1887, the second-best choice to derive ccv is using re-analysis data. Fortunately, the 20CRv3 re-analysis data of the US National Oceanic and Atmospheric Administration (NOAA) cover the time span 1836 – 2015 and contain all meteorological parameters needed (Slivinski et al. 2019). 20CRv3 data were derived by combining historical weather data with modern data assimilation techniques using information from old weather maps and reports, as well as historical weather observations from various sources such as weather stations, ships and buoys. The data is available as a 0.703° · 0.702° grid in daily resolution (Slivinski et al. 2019). Slivinski et al. (2021) showed that these data compared well with various independent data (i.e. measurements, other re-analyses). In particular, they capture observed long-term trends well, fostering their applicability to derive ccv.

Since the 20CRv3 data end in 2015, the **15-year period 2001 – 2015** was defined as reference period for present conditions. Based on our analysis of the data (cf. section 4.1.1.2), we decided to use one single ccv for the complete year and the complete model region. The additive ccv for air temperature (Ta) is thus defined as follows:

$$ccv_{Ta} = \frac{1}{n} \cdot \sum_{01-01-1873}^{12-31-1887} Ta - \frac{1}{n} \cdot \sum_{01-01-2001}^{12-31-2015} Ta \tag{3}$$

Likewise, the multiplicative ccv for all other meteorological parameters (Par) are defined as follows:

$$ccv_{Par} = \frac{1}{n} \cdot \sum_{01-01-1873}^{12-31-1887} Par \Big/ \frac{1}{n} \cdot \sum_{01-01-2001}^{12-31-2015} Par \tag{4}$$

whereby

Ta	Air temperature
Par	All other meteorological parameters
n	Number of daily values available for the two 15-year periods (1873 – 1887 and 2001 – 2015)

Note, however, that historical climatic conditions derived with ccv do not reflect the actual meteorological time series for 1873 – 1887. Nevertheless, they represent the meteorological conditions of that period in a statistical way as required for the emission modelling of the 1880 scenario.

4.1.1.2 Evaluation and final definition of climate change vectors

Climate change vectors derived from 20CRv3 data were compared to ccv derived from an independent dataset of the German Meteorological Service (DWD) for evaluation. As a comparison, we used monthly gridded data for precipitation and air temperature starting in 1881 (DWD 2023). DWD data for that early period are also associated with errors, but valid for comparison (F. Imbery, personal comm.). From DWD data, ccv were derived for air temperature and precipitation considering the period 1881 – 1895 for historical conditions and 2001 – 2015 for present meteorological conditions and for the area of present Germany only. Note, that the historical 15-year period 1881 – 1895 used for this evaluation differs from the one used to derive the original ccv (1873 – 1887), because DWD data are not available before 1881.

Mean yearly precipitation derived from 20CRv3 data is consistently higher than precipitation from DWD data by 192 mm/a. Mean air temperature derived from 20CRv3 is 0.3 K higher than air temperature derived from DWD data. However, based on mean yearly values, the differences between the two data sources are almost constant throughout the whole period of investigation (Appendix A.4). Consequently, the ccv resulting from the two different data sources are similar, indicating minor changes for precipitation of -67.6 and -45.5 mm/a, but significant changes for air temperature of -1.61 and -1.54 K for DWD and 20CRv3, respectively. These small deviations imply that yearly, spatially constant ccv from 20CRv3 are in good accordance with ccv derived from DWD data. With higher temporal resolution of quarters or months, considerable differences emerge. Moreover, also the spatial distribution of ccv derived from DWD and 20CRv3 data differ. For the sake of simplicity and to avoid additional uncertainties, we chose constant (yearly) and spatially homogenous ccv.

The final ccv are based on the differences between 1873 – 1887 and 2001 – 2015 for the complete model domain, and therefore, differ from the ccv derived for evaluation. For atmospheric pressure and relative humidity, the ccv barely deviated from 1.0 and were thus set to 1.0. As expected, the most pronounced change emerges for air temperature, which was almost 1.5 K lower in 1880 compared to present. This temperature change equals a decrease in saturation vapour pressure of roughly 11 %. In comparison all other parameters considered showed relatively small changes (Table 5).

Table 5: Climate change vectors (ccv) used to model the water balance for 1873 – 1887.

Meteorological forcing parameter	unit	type of ccv	ccv
Air temperature	[K]	additive	-1.466
Precipitation	[mm/a]	multiplicative	0.9986
Relative humidity	[%]	multiplicative	1.0
Global radiation	[W/m²]	multiplicative	0.9669
Wind speed	[m/s]	multiplicative	0.9413
Atmospheric pressure	[hPa]	multiplicative	1.0

4.1.2 Land use and imperviousness

In line with MoRE, land use and imperviousness of the water balance are also based on the HANZE 2.0 dataset by Paprotny & Mengel (2023) as described in chapter 3. Accordingly, we used the data given for 1880 for the 1880 scenario. For reasons of consistency and comparability with the previous application (Morling et al. 2024), we used the data provided for 2018 to represent the present state. Note however, that land use and imperviousness were not directly implemented into LARSIM-ME, but they were rather used to post-process the model results as described in the next chapter.

4.1.3 Model application and deriving the input for MoRE (model runs and post-processing)

We used LARSIM-ME with the model settings described in Morling et al. (2024), without changing the calibration of the model, which was originally provided by BfG. To represent the climatic conditions of the present state we ran the model with measured meteorological data provided by BfG, for 2001 – 2015.

We applied the climate change vectors (ccv) from Table 5 to these measured input data of the period 2001 – 2015 and thereby adjusted the measurements to values representative for the climatic conditions of the period 1873 – 1887. We then re-ran LARSIM-ME with this adjusted meteorological forcing. This second model run represents the historic climatic conditions of the 1880 scenario. However, note that land use and imperviousness has not been adjusted to the 1880 conditions within LARSIM-ME. The impact of these changes is considered in the post-processing, as described below.

The land use and imperviousness considered in LARSIM-ME approximately represent the status of 2006 and do not originate from HANZE 2.0, but mainly from CORINE (cf. Morling et al. 2024 for details). Therefore, the modelling results for the 1880 scenario and the present-state-scenario both have to be modified in the post-processing in order to account for land use and imperviousness of the corresponding time. The post-processing consists of the following steps (cf. Morling et al 2024 for more details):

- LARSIM-ME results are converted to represent the runoff for each land use class within a 5 km · 5 km grid-cell in units of [mm/a]. The impervious areas within a grid-cell are thereby considered as a separate land use class.
- Runoff in [mm/a] is converted to water volume in [m^3/a] by multiplying runoff of each land use by its corresponding area.
- Changes in land use (including the land use class impervious area) were accounted for by adjusting the area of each land use class according to the respective scenario.

In a final step, we separated the land use-specific discharge volumes of each grid-cell into three different discharge components:

- Base flow, representing discharge that mainly originates from groundwater
- Interflow, representing subsurface runoff from the vadose zone
- Overland flow, representing surface runoff

The derivation of the runoff components and can be summarised as follows (cf. Morling et al. 2024 for more details):

- Within Germany, surface runoff from agricultural fields is a model result. The proportion of surface runoff from agricultural grassland and forest are reduced by factors of 0.82 and 0.42, respectively. Outside Germany, we used the original approach from MONERIS to determine overland flow.

- Within Germany, base flow is determined with the spatially distributed long-term base flow index (BFI), as defined in the Hydrological Atlas of Germany (BMU 2003; Jankiewicz et al. 2005). Outside Germany, base flow is directly taken from the model results.
- Interflow is the residual of the total discharge, neither classified as overland flow nor base flow.

4.2 Integrating LARSIM-ME runoff components in MoRE

Yearly precipitation and land use specific runoff components from LARSIM-ME were transferred to the MoRE analytical units following the pragmatic way of Morling et al. (2024).

Urban runoff components differ in both models. In MoRE, the runoff from impervious areas connected to sewer systems as well as the wastewater produced by inhabitants connected to the sewer systems are considered for the 1880 scenario (Figure 8). However, LARSIM-ME provides the runoff from impervious surfaces only, which is larger than the MoRE components for the 1880 scenario (Figure 8). The urban runoff from LARSIM-ME was transferred to MoRE analytical units as well and was then used for an internal correction of the water balance to maintain total runoff. The difference between the urban runoff components is added proportionally to the slow-flowing components (base flow, interflow and tile drainage flow) for each analytical unit (Morling et al. 2024).

Figure 8: Scheme comparing urban runoff components in both LARSIM-ME and MoRE model.

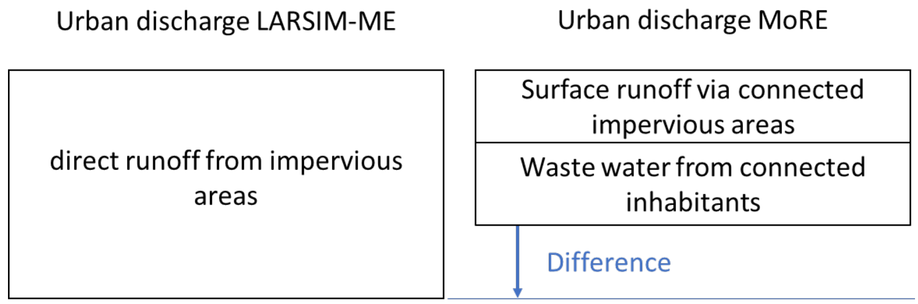

Source: own illustration, IWU-WG

Water usage by population

Water consumed by population and thus the amount of wastewater produced are essential parts of the urban water balance in MoRE (Figure 8). Thus, the amount of water used by population needs to be estimated for historical conditions.

Centralized (drinking) water supply was available in 52 % of the cities of the German Empire with > 10,000 inhabitants in 1876 (Büschenfeld 1997), the total number of people having a water connection being unknown.

Franzius et al. (1893) compiled daily water needs for different purposes such as households (cleaning, cooking, etc.), commercial and public use. They estimated the water consumption for urban population to 97 L/(inh·d) and for population in rural areas to 55 L/(inh·d). These values were used for modelling purposes and assigned to the population density raster of HANZE 2.0 dataset (Paprotny & Mengel 2023, chapter 3.3) as given in Table 6. For a population density of ≤ 9 inh/ha, no water consumption was assigned. The inhabitants of these rural areas were considered as not to be connected to sewers. Instead, wastewater is assumed to percolate into the ground and thus not contributing to urban runoff via sewer systems. Water consumption was transferred from the derived raster to the level of analytical units by averaging all raster cells located in an analytical unit.

Table 6: Daily per capita water consumption of population used for modelling 1880.

Population density[a] [inh/ha]	Water consumption [L/(inh·d)]
≤ 9	-
10 – 35	55
≥ 36	97

[a] – For choosing the population density classes, refer to Appendix A.3

A literature review on daily water consumption and wastewater volumes (Figure 9, see also Appendix A.5) revealed that these volumes differed in a wide range for German cities from less than 50 L/(inh·d) to a reported exceptional high consumption of more than 300 L/(inh·d) for the city of Freiburg (Dunbar 1998; Korn 1898). Even for individual cities, the range of reported values was high. For instance, the daily water consumption in the city of Brunswick dropped from approximately 161 L/(inh·d) to 73 L/(inh·d) after water meters were introduced in 1886/1887 (Lange 2002). The median water consumption of 99.6 L/(inh·d) for the collected literature data (Figure 9) agrees with the estimation of 97 L/(inh·d) by Franzius et al. (1893). The on average higher volumes of wastewater compared to water consumed (Figure 9) can be explained with additional private water suppliers discharging into sewers (Dunbar 1998, Mohajeri 2005) and higher estimations of wastewater volumes taking into account storm water runoff for dimensioning of the new sewer systems built in this period. The water volumes were found to be unrelated to the reported year and number of inhabitants (see Appendix A.5).

Figure 9: Historical daily per capita water usage for 36 German cities as taken from literature (see Appendix A.5 for details).

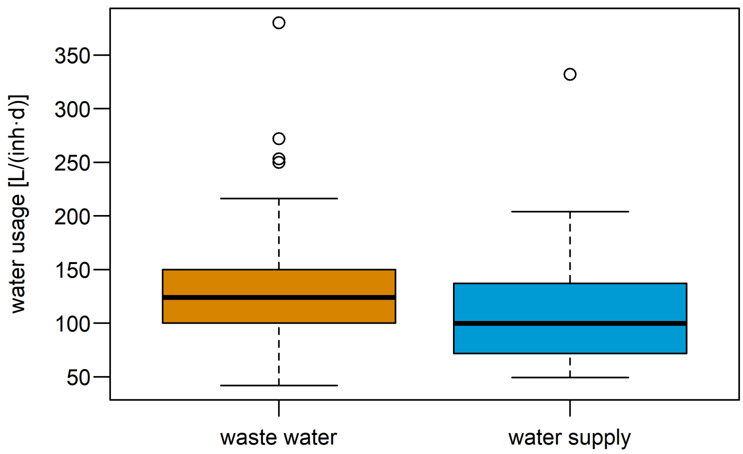

Source: own illustration, IWU-WG

4.3 Results of the water balance modelling

4.3.1 Impact of climate on total runoff

We performed model runs with measured meteorological data of 2001 – 2015 and with climatic conditions representing 1873 – 1887 with LARSIM-ME. Therefore, directly comparing the results of the two model runs (without post-processing them) indicates the impact of different climate conditions on runoff and discharge in 1880.

Figure 10 illustrates the differences of total mean yearly runoff under 1880 climate conditions as compared to today (neglecting the changes of land use and imperviousness). According to our results, mean yearly runoff would have been approximately 50 mm/a higher under 1880 climate conditions than nowadays in most regions. Since precipitation has barely changed, this is mainly owing to lower air temperatures in 1880, leading to a lower saturation vapour pressure and thus lower evapotranspiration, which resulted in an increase of runoff.

The exceptions in high altitude alpine regions are also due to the lower air temperatures. The lower temperatures led to larger amounts of snow in high altitudes, which were not melting during summer. Thus, the prevailing snow does not contribute to runoff generation in these high altitudes, but is rather transported to lower regions via glaciers, snowdrift and avalanches and contributes to increased runoff in the lower regions. Note, that these processes are simulated in a strongly simplified way in LARSIM-ME, since it does not include the glacier module of LARSIM (Haag et al. 2019).

Figure 10: Simulated differences of mean yearly runoff due to changes in climatic conditions only, neglecting changes of land use and imperviousness.

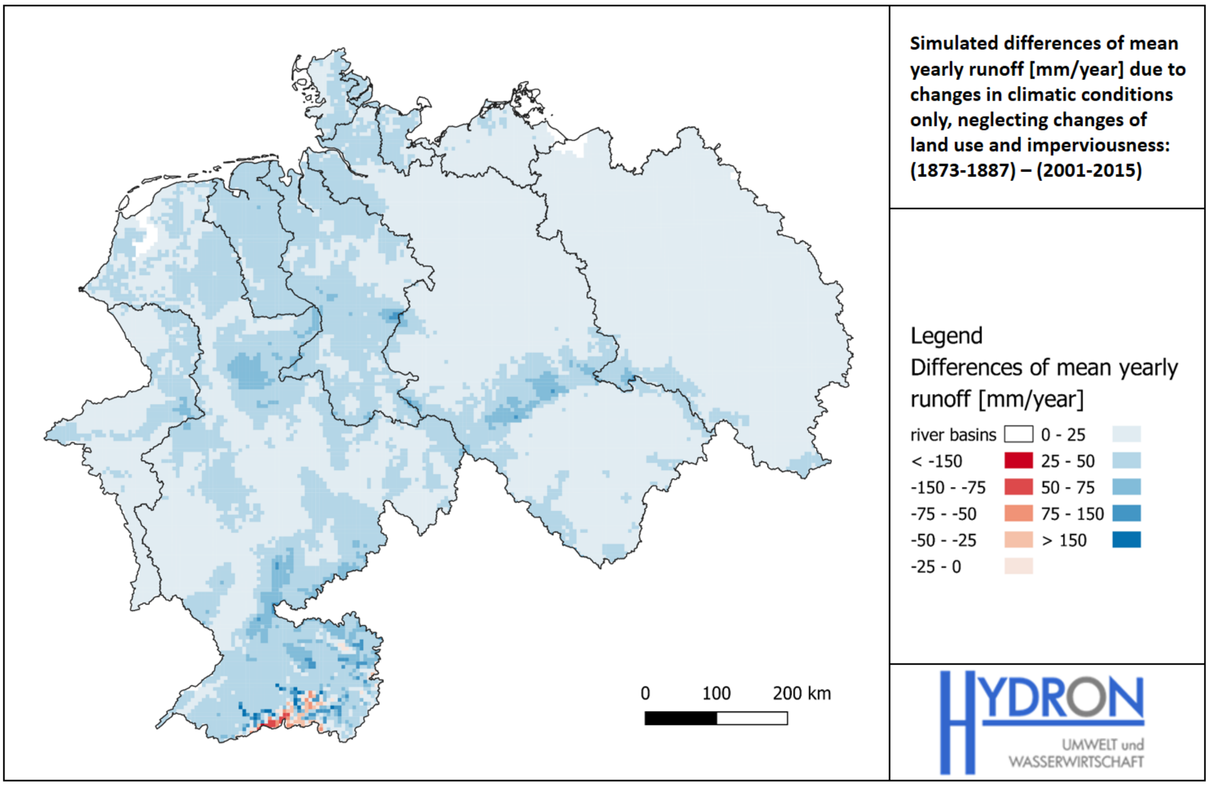

Source: own illustration, HYDRON

4.3.2 Overall impact of climate, imperviousness and land use on total runoff

The model results with climatic conditions of 1873 – 1887 were post-processed with the land use and imperviousness of 1880 and model results with climatic conditions of 2001 – 2015 were post-processed with the land use and imperviousness of 2018 (see chapter 4.1.3). This leads to hydrological results for the 1880 scenario and the present, including the influences of climate, land use and imperviousness.

The differences between the 1880 scenario and the present indicate the combined effect of changes in climate and land use (including imperviousness) on runoff (Figure 11). According to our results, the impact of imperviousness is inverse to that of climate. In today's urban agglomerations, the degree of imperviousness was much lower in 1880. Therefore, total runoff used to be much lower in these urban areas back in 1880. On the other hand, in rural areas, changes in runoff are dominated by the inverse influence of the cooler climate (Figure 11). All other changes of land use apart from urbanization, i.e. changes between forest and agricultural land, are much less significant.

Thus, the overall change of runoff between 1880 and the present seems to be dominated by the counteracting influences of less evapotranspiration (owing to lower temperatures) and a lower degree of imperviousness in 1880.

Figure 11: Simulated differences of mean yearly runoff due to changes in climatic conditions, land use and imperviousness.

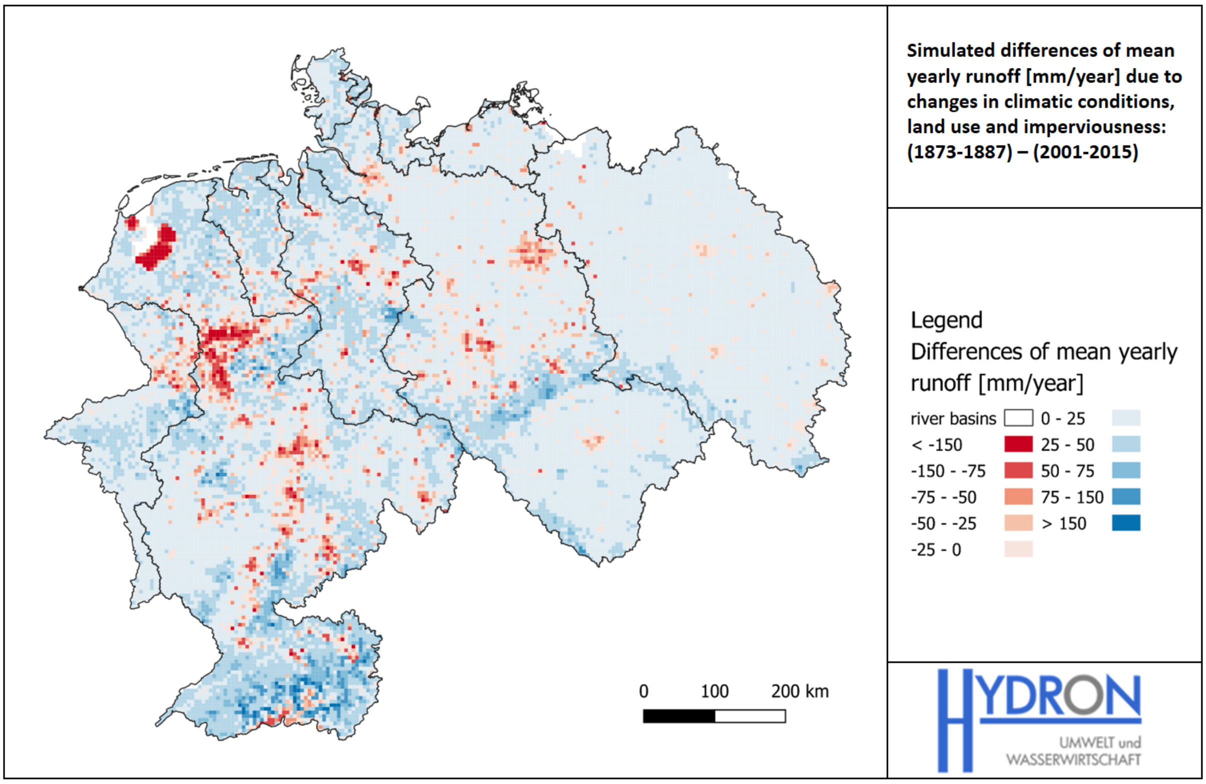

Source: own illustration, HYDRON

4.3.3 Mean annual runoff for the 1880 scenario

Figure 12 shows the simulated spatial distribution of the mean annual runoff for the 1880 scenario. This result reflects climatic conditions of 1873 – 1887 along with land use and degree of imperviousness of 1880. Simulated total runoff varies between less than 100 mm/a for the dry continental climate in the eastern part of the model domain and more than 1,500 mm/a in particularly wet regions of the Alps and the northern Black Forest. The overall values and the spatial distribution mainly reflect the large-scale climatology and orography, and were considered as plausible.

However, as discussed above, runoff is generally higher than today in rural areas, because of less evapotranspiration associated with lower air temperatures. In contrast, within nowadays highly urbanized areas, total runoff used to be lower in 1880, due to a lower degree of imperviousness.

Figure 12: Simulated mean yearly runoff of the 1880 scenario.

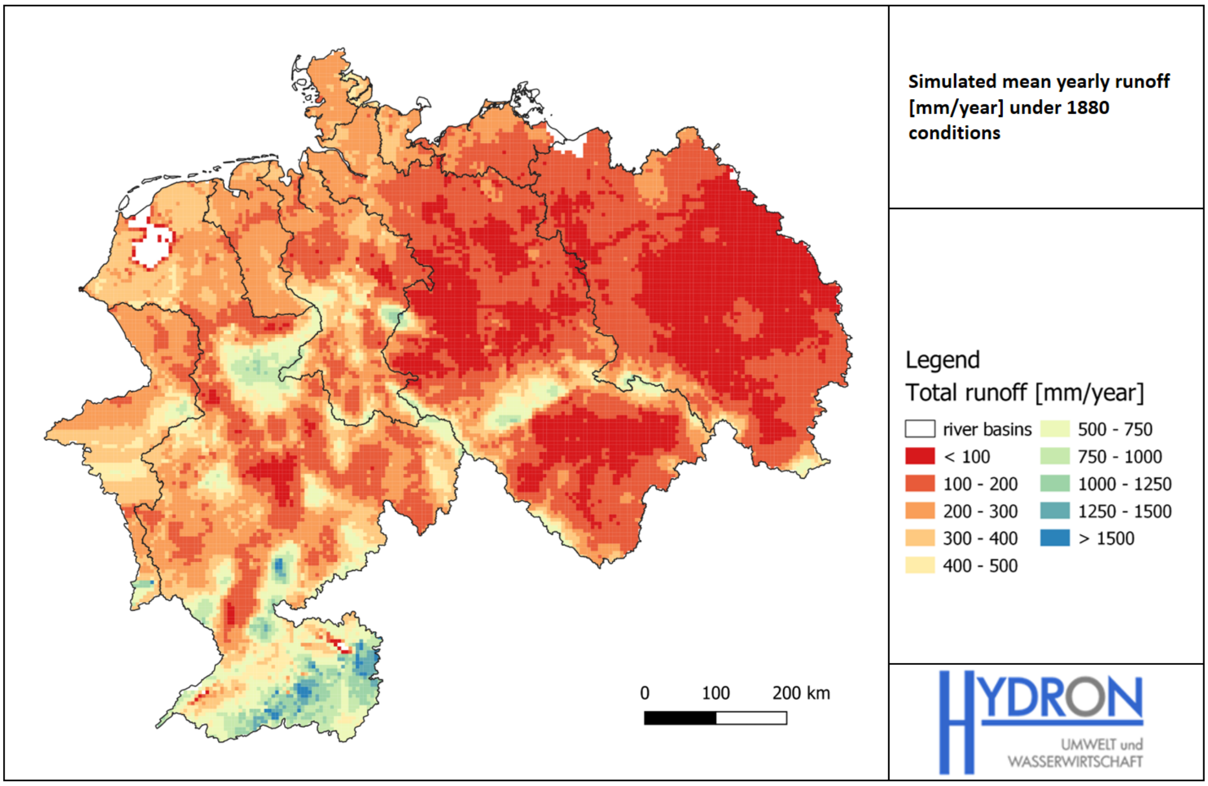

Source: own illustration, HYDRON

Table 7 summarises the modelled water volumes of the 1880 scenario in MoRE and its distribution into different runoff components. About 80 % of the total runoff is runoff via base flow and interflow. Since urban areas and tile drained areas are small, the corresponding runoff via these pathways make up only a small proportion.

Table 7: Runoff in 1880 from North Sea and Baltic Sea basins. Values are derived from LARSIM-ME results and are rounded.

	Runoff from North Sea basins		Runoff from Baltic Sea basins	
Runoff component	**[hm³/a]**	**[%]**	**[hm³/a]**	**[%]**
Surface runoff	20 470	15	2 480	12
Direct runoff onto water surfaces	4 360	3	580	3
Runoff via urban systems	560	< 1	60	< 1
Runoff via tile drainages	2 600	2	1 100	6
Interflow	43 840	33	5 720	29
Base flow	60 250	46	10 000	50
Total	**132 080**	**100**	**19 940**	**100**

4.3.4 Validation of the 1880 water balance

Discharge measurement at river gauges in the study area are only available for a few locations since 1873 at the GRDC (BfG 2024). These were used for a validation of the modelled water balance. Average annual runoff was calculated from original measurements for 11 gauging stations (refer also to Appendix A.6), covering at least 13 years of the considered 15 years span (1873 – 1887). This observed average annual runoff was compared to the modelled total runoff of the MoRE analytical units covering the location of the corresponding gauging stations (Figure 13). The average bias was 1.9 % with deviations ranging from -16 % to 12 %. Even though the limited number of observations hampers a thorough validation, the comparison revealed a good agreement with historical records.

We additionally used the differences of discharges reported for 1873 – 1887 and 2001 – 2015 to verify qualitatively our results: The mean runoff of the watershed of Intschede/Weser (37,370 km²) used to be 280 mm/a for the period 1873 – 1887 and reduced to 254 mm/a for 2001 – 2015. Thus, total runoff used to be 26 mm/a (10 %) higher around 1880 than it is today. Since, the influence of urbanization (less imperviousness in 1880) is only moderate within the Weser watershed, this corresponds well with our results (cf. Figure 11). Similarly, the mean annual runoff of the moderately urbanized watershed of Cologne/Rhine (144,232 km²) used to be 24 mm/a (5 %) higher in 1873 – 1887 than it was in 2001 – 2015. Note, that the gauge Cologne is just upstream of the nowadays heavily urbanized Ruhr agglomeration. In contrast, the mean runoff of the watershed of the gauge Rees/Rhine (159,300 km²), just downstream of the Ruhr agglomeration, was only 5 mm (1 %) higher in 1873 – 1887 than in 2001 – 2015. This shows that the counteracting influences of climate and imperviousness, derived from our results, can also be deduced from river gauge measurements.

In summary, our results for the water balance of the 1880 scenario are in good agreement with the scarce measurement data available for validation.

Figure 13: Comparison of observed and modelled runoff. Observed runoff was obtained from GRDC data (BfG 2024) and averaged for the period 1873 – 1887 (refer to Appendix A.6).

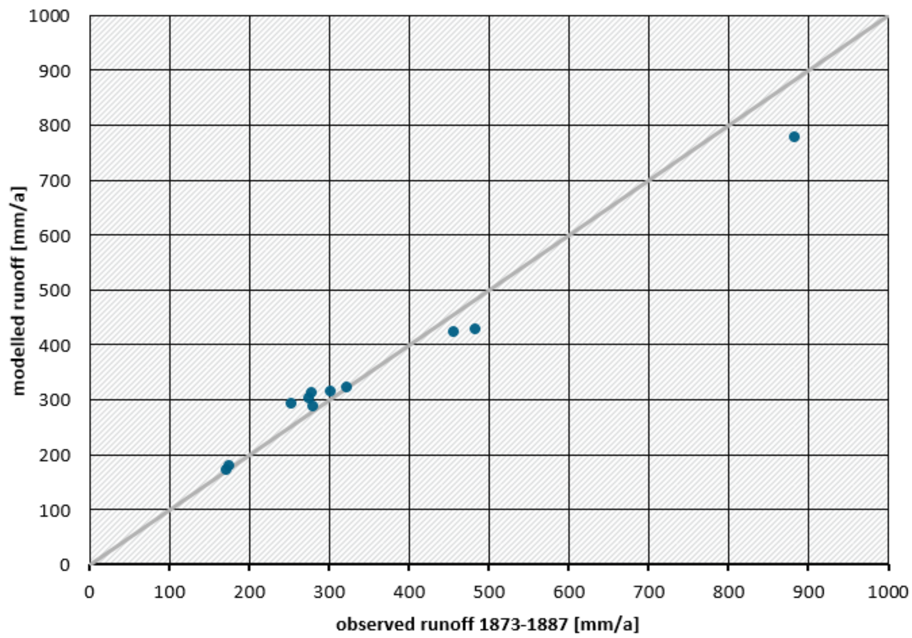

Source: own illustration, IWU-WG

5 Modelling of individual emission pathways

A wide spectrum of substance-specific input data is required for modelling historical conditions, which might differ significantly from present ones and thus cannot easily derived from current data. Since historical observation data are often scarce, other model results on historical conditions are an inevitable source next to the adaptation of modelling approaches.

Note, that the point sources pathways of municipal wastewater treatment plants (MWWTP) and industrial direct dischargers are not modelled in the 1880 scenario. While MWWTP were not relevant at that time (chapter 5.3.3), no data on industrial emissions were available (for uncertainties and limitations refer to chapter 8).

The following chapters are grouped according to the individual emission pathways modelled for the 1880 scenario in MoRE. Each chapter provides insight in the derivation of corresponding input data and model approaches for the individual nutrient-related emission pathways of MoRE followed by the in-stream retention.

5.1 Atmospheric deposition onto water surfaces

5.1.1 Nitrogen deposition rates

Spatial data on historical nitrogen deposition (CCMI v2.0 for input4MIPs, Hegglin et al. 2016) are freely available within the framework of the Coupled Model Intercomparison Project (CMIP6, v6.2.43). Nitrogen (N) deposition is available as wet and dry deposition rates for NH_x and NO_y for the years 1850 – 2014 in monthly resolution on a grid (2.5° · 1.9°) of global extent.

The period 1873 – 1887 (15 years) was extracted from the dataset to be in line with the considered historical water balance period. For each month, deposition rates were averaged over the selected period. Monthly averages were summed up to represent a yearly average over this period. As there is no distinction between dry and wet deposition in the MoRE model systems, these were summed up for both N species. These modified grid data were intersected with the analytical units of MoRE to obtain the relevant input data for modelling.

In general, low deposition rates can be found at coastal and mountainous areas, while slightly higher rates were obtained for parts of Central and Western Germany (Figure 14 and Figure 15). For the study area, the average NH_x and NO_y deposition rates accounted to 1.96 kg/(ha·a) and 1.50 kg/(ha·a), respectively. Thus, our NO_y deposition rates are on average 77 % to 88 % higher than the values of 0.8 and 0.85 kg/(ha·a) as reported for the previous historical modelling of the Oder basin (Gadegast et al. 2012) and the North Sea river basins (Gadegast & Venohr 2015), respectively. In contrast, the NH_x deposition rates are on average 57 % lower than the 4.5 kg/(ha·a) used for modelling the Oder river basin by Gadegast et al. (2012). Ruoho-Airola et al. (2012) reported deposition rates of nitrate-N below 2 kg/(ha·a) and ammonium-N ranging from 2 – 4 kg/(ha·a) based on a collection of observations in precipitation from Rothamsted Experimental Station in southern England for the period 1880 – 1920.

Jensen (2017) found N deposition in Denmark in 1900 was 26 – 30 % of that in 2000 while Ruoho-Airola et al. (2012) reported that N deposition in the Baltic Sea in 1880 was 35 % compared to 2000. This corresponds well to the N deposition rates obtained from CCMI v2.0 dataset, which are on average 25 % of the values for the year 2018 in MoRE (data not shown), considering that air pollution and thus deposition decreased generally in Europe since 2000 (Aas et al. 2024).

Figure 14: Yearly NH_x deposition rates per MoRE analytical unit as obtained from input4MIPs dataset, averaged for the period 1873 – 1887.

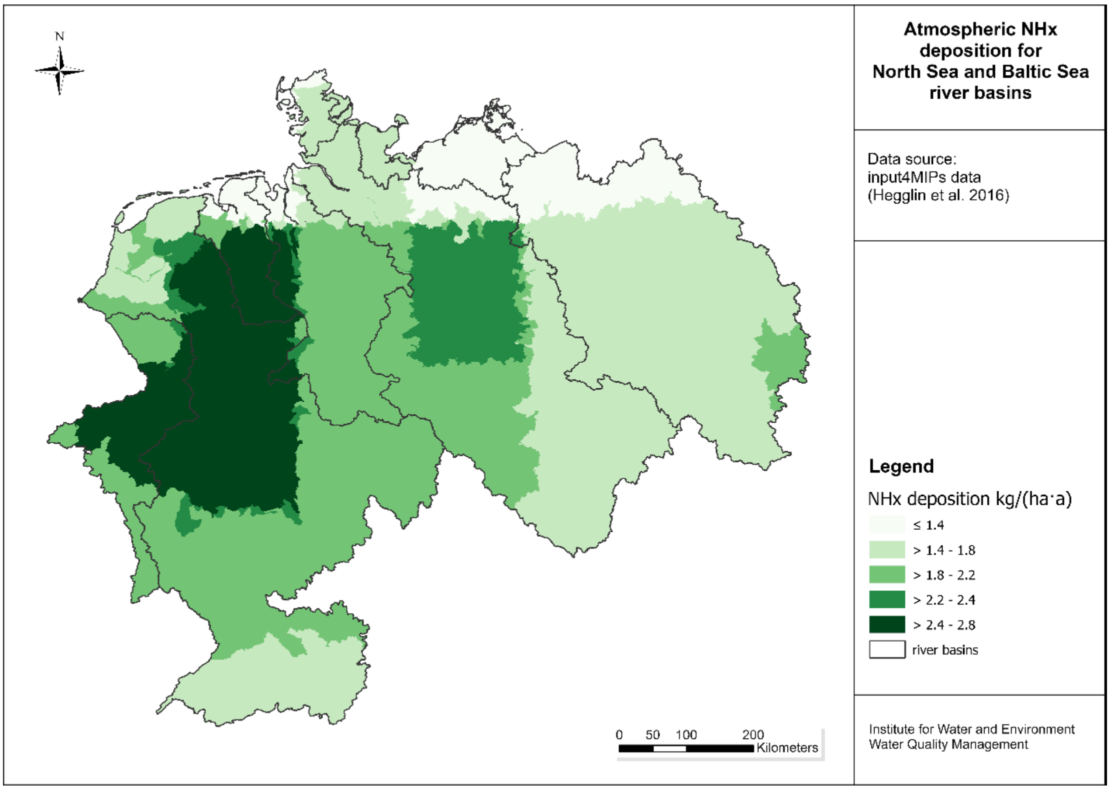

Source: own illustration, IWU-WG

Figure 15: Yearly NO_y deposition rates per MoRE analytical unit as obtained from input4MIPs dataset, averaged for the period 1873 – 1887.

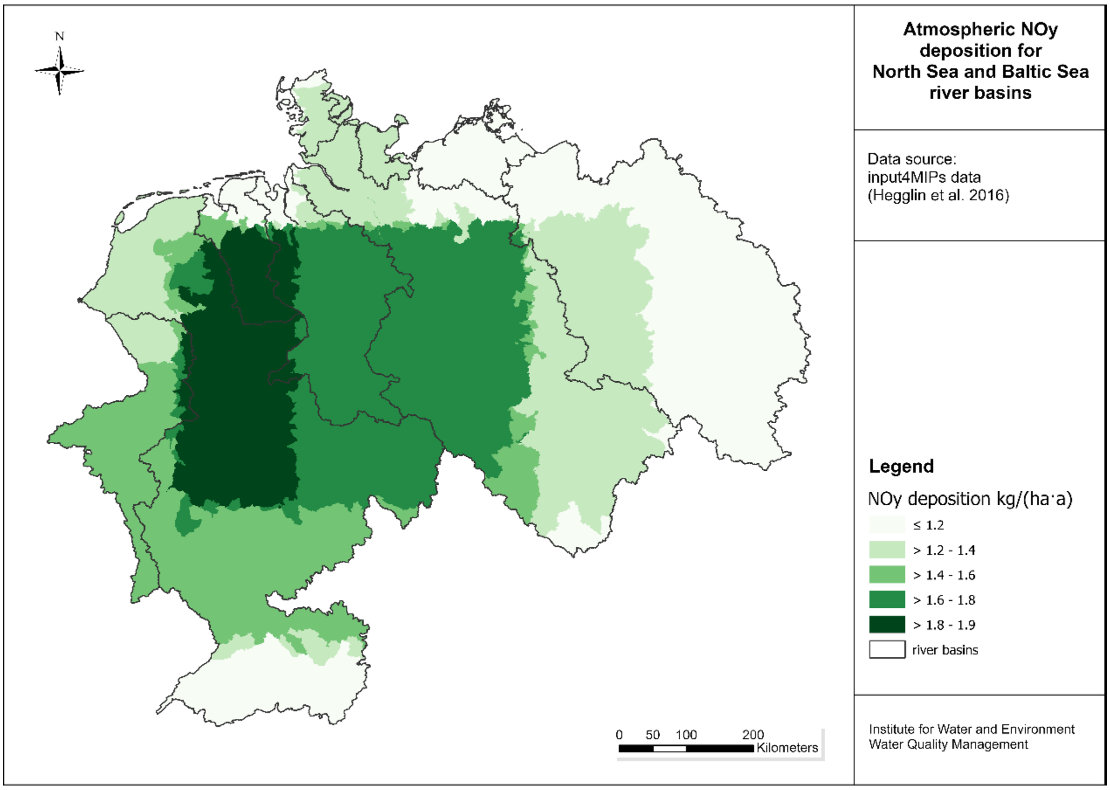

Source: own illustration, IWU-WG

5.1.2 Phosphorus deposition rates

For phosphorus (P), no comparable data on historic atmospheric deposition are available. Centennial changes in phosphorus deposition have been less pronounced compared to nitrogen (Mahowald et al. 2008). For modelling purposes, the assumption of Ruoho-Airola et al. (2012) is used, who estimated a phosphorus deposition rate of 75 g/(ha·a) for the Baltic Sea region in 1850. This is 66% higher than the deposition rate of 45 g/(ha·a) used by Gadegast & Venohr (2015).

5.1.3 Modelled emissions via atmospheric deposition onto water surfaces

Emissions via atmospheric deposition onto water surfaces are quantified by multiplying the area of water surfaces with the deposition rate specific for each substance. Modelled N emissions were roughly four times higher for North Sea basins than for Baltic Sea basins (Table 8). In addition to higher N deposition rates (Figure 14 and Figure 15), North Sea basins cover a larger area of inland waters such as Lake Constance and Mecklenburg Lake District. Accordingly, P emissions via atmospheric deposition are also higher for North Sea basins (Table 8).

Table 8: Modelled emissions via atmospheric deposition onto water surfaces for North and Baltic Sea basins in 1880.

Atmospheric deposition onto water surfaces	North Sea basins [t/a]	Baltic Sea basins [t/a]
Nitrogen	2 894	529
Phosphorus	66	15

5.2 Erosion

Erosion by water is an important pathway for substances transported as particles. The universal soil loss equation (USLE) forms the basis of the erosion pathway in MoRE. The USLE does not depict soil erosion by individual rain events but describes the long-term average soil erosion to be expected due to rainfall, which is in line with the MoRE approach of providing annual average substance emissions and loads. Not all of the eroded soil material is transported into surface waters but is deposited and retained on nearby areas along the transportation path. The sediment delivery ratio (SDR) refers to the relation of soil loss and the actual amount of sediment received by water bodies. Substance emissions via erosion are calculated by combining the sediment inputs with spatially and land use-differentiated topsoil contents and enrichment ratios (Fuchs et al. 2022; Morling et al. 2024).

5.2.1 Soil loss and sediment inputs

To determine the soil loss and sediment inputs for the historic scenario, different approaches were used for present Germany and foreign territories. The approach for Germany (see below) is derived from Fuchs et al. (2022) and could not extrapolated to the foreign parts as underlying data are not available in the same extent and resolution.

For **foreign territories**, a gridded dataset on historical soil loss in Europe (Fendrich et al. 2022) was used, which adapted the C and R factors for historical conditions. The dataset comprises soil loss rasters [t/(ha·a)] in different temporal resolution. We selected the decadal averages for the periods 1870 – 1879 and 1880 – 1889, both periods were averaged to obtain the long-term average erosion. Land use from HANZE 2.0 dataset (Paprotny & Mengel 2023, chapter 3.1) was used to obtain specific soil loss rates for each analytical unit and land use class.

For **present Germany**, the input data were adapted from results of a recent erosion modelling (Fuchs et al. 2022), for which up-to-date data and methodological approaches were used for calculating soil erosion and sediment inputs. These improved model statements and results for the erosion pathway were integrated into the modelling tool MoRE (Fuchs et al. 2022). The erosion modelling is based on the universal soil loss equation (USLE):

$$A = R \cdot K \cdot C \cdot L \cdot S \cdot P \tag{5}$$

whereby

A	[t/(ha·a)]	Average annual soil loss
R	[N/(ha·a)]	Rainfall erosivity factor
K	[(t·h)/(ha·N)]	Soil erodibility factor
C	[-]	Crop factor
L	[-]	Length factor
S	[-]	Slope factor
P	[-]	Management factor

Soil loss was calculated on the level of analytical units for different land use classes (arable land, pasture, fruits, wine and naturally covered areas) after adapting the individual USLE factors as described below. Therefore, changes in soil losses and sediment inputs essentially result not only from the adjusted USLE factors, but also from the historically different distribution of land use.

5.2.1.1 C factor

In 1880, roughly three quarters of the agricultural land were particularly erosive arable land compared to around two thirds today (proportion of arable land on agriculturally used land) (Paprotny & Mengel 2023; Rahlf 2022). Regarding crop types, approximately 50 % were winterised for both the period around 1880 and the period 2010 – 2017 (Kaiserliches Statistisches Amt 1884; Röder et al. 2022). Thus, no substantial changes in crop rotation and soil coverage by plants were assumed for the historical scenario. However, it is assumed that no conservation tillage took place, while the current proportion is 40 % (Häußermann et al. 2023) which leads to an average C factor of 0.12 (Fuchs et al. 2022). Wurbs & Steininger (2011) calculated an average C factor of 0.17 for recent conditions but with 100 % conventional tillage. For the 1880 scenario, the C factors on arable land were increased by around 41 % (ratio of C factors 0.17/0.12).

5.2.1.2 L and S factors

In 1883, farms of less than 20 ha controlled about 58 % of the total utilised area, while currently farms of more than 100 ha control almost the entire utilised area (93 %) (Kopsidis 2022). Overall, progressive mechanisation and land consolidation can be observed since 1880. Arable land in Germany has decreased from 50 % to 35 % since then due to the conversion of arable land into grassland, forest or settlements. In many cases, unprofitable hillside areas have been converted. This led us to the conclusion that the average S factor is lower today than in the past. At the same time, it can be assumed that the average L factor is higher today than it used to be due to increasing field sizes. Currently, the average slope on arable land is 2.24° (3.9 %) (Fuchs et al. 2022). The average erosive slope length corresponds to approx. 100 m according to an estimation based on the approach by Moore & Nieber (1989). If the erosive slope length is assumed to be halved, the LS factor is reduced by approx. 25 %. If we assume that the slope was historically 25 % higher, as more slopes were cultivated, the effect of halving the slope length would be equalised. Due to these contrary effects, the LS factor was not adjusted and adopted from Fuchs et al. (2022).

5.2.1.3 R factor

The R factor was recalculated at the level of the analytical units using the mean annual precipitation used for the historical water balance (refer to chapter 4.1). It was assumed that the relationship between annual rainfall and rainfall erosivity does not differ between the late 19th century and the late 20th century. The R factor was calculated according to DIN 19708 (2017):

$$R = 0.0788 \cdot N_j - 2.82 \tag{6}$$

whereby

N_j	[mm/a]	Mean annual precipitation for the period 1873 – 1887

5.2.1.4 P and K factors

The P factor is not taken into account and is left at one according to Fuchs et al. (2022) as no information is available. The K factor was determined on the basis of DIN 19708 (2017) as described in Fuchs et al. (2022) and was not changed for the 1880 scenario.

5.2.1.5 Sediment delivery ratio

The sediment delivery ratio (SDR) is the ratio of sediment delivered into surface waters to the total amount of eroded soil. For **present Germany**, the SDR is a function of crop management, slope, watercourse distance and connection probability (Fuchs et al. 2022). There are no digital elevation models available with a sufficiently high resolution for historical conditions. The changes due to settlements and measures for drainage or land consolidation etc. could not be reconstructed. Thus, adjustments of watercourse distance and connection probability involves too much uncertainty. For these reasons, the average SDR per analytical unit and land use class were kept as obtained by Fuchs et al. (2022) for calculating the sediment inputs in the analytical units of present Germany.

For **foreign territories**, a different approach for depicting the erosion pathway was used based on a dataset on historical soil loss (Fendrich et al. 2022). SDR was calculated from soil loss rates following the original MOENRIS approach of Venohr et al. (2011). SDR depends on the average slope (obtained from current digital elevation model, Appendix A.1) and the proportion of arable land per analytical unit.

5.2.1.6 Alpine areas and glaciers

For alpine open areas and glaciers, it is assumed that all eroded material (SDR = 100 %) is entering surface waters (Fuchs et al. 2022). A sediment input of 5.39 t/(ha·a) and of 26.9 t/(ha·a) is assumed for alpine open areas and glaciers, respectively.

5.2.2 Enrichment ratios

The ratio of nutrient content in suspended sediments to that in the bulk soil is referred to as enrichment ratio. For the 1880 scenario, the approach of Fuchs et al. (2022) for the enrichment ratio was kept to calculate both nitrogen and phosphorus emissions via erosion. Enrichment ratios depend on the clay and silt content of the topsoil material (Appendix A.1). For 1880, it is assumed that these soil properties did not change over time.

5.2.3 Topsoil contents

Long-term agricultural experiments are a valuable source of information and some of them run for more than 100 years. However, they provide only site-specific results depending on the local soil characteristics, fertilization treatment and variation of crops. Changes in topsoil contents are usually not in the focus of these experiments and show even opposing results. For instance, total N increased by 52 % and 181 % in upper soil (0 – 23 cm) depending on treatment with farmyard manure in Rothamsted experiments in southern England (Rothamsted Research 2018). Nitrogen contents also increased by 11 – 24 % in the period 1949 – 1961 at the Halle experimental site in central Germany (Stumpe 1967). Decreasing N concentrations were observed regardless of fertilizer regime over a 56-year period (1940 – 1998) in the Danish Sandmarken long-term experiment (Hu et al. 2019). Thereby, changes in soil N are highly coupled to changes in organic carbon content in soils (Hu et al. 2019; Rothamsted Research 2018, 2021; Stumpe 1967).

C:N ratios in soils are likely to have changed from past to present due to different cultivation methods and fertilizer applications. Thus, highly complex processes, involving local soil properties, crop rotation, fertilization and soil tillage, affect nitrogen topsoil contents. Data on these are not available in detail for the whole study area. Thus, input data for nitrogen were not adapted. For both present Germany and foreign territories, the currently implemented nitrogen topsoil contents (Morling et al. 2024) were used for modelling 1880 emissions via erosion.

For phosphorus, a 20 % – 106 % increase was found in upper soil (0 – 23 cm) in Rothamsted experiments (Rothamsted Research 2016). Likewise, up to two times higher soil P contents were found after 110 years of fertilization in German Bad Lauchstädt experiment (Medinski et al. 2018). At the same experimental site, the P content decreased continuously without fertilization in upper soil (0 – 20 cm) in a 42-year period (1949 – 1991, Stumpe et al. 1994). Similar to nitrogen, only a few observations with highly variable results are available. Modelling studies intended to depict changes for soil phosphorus considering different P pools. Zhang et al. (2017) modelled a 31 % increase of the total P per hectare between 1900 and 2010 in soils of Europe. Similarly, Ringeval et al. (2024) reconstructed past and present distributions of P in cropland and grassland soils on the global scale assuming recent P contents in (semi-)natural soils (He et al. 2021) as initial conditions in 1900 agricultural soils for their modelling. However, data of He et al. (2021) are on average higher than the currently implemented P contents of natural areas derived from recent soil measurements by Fuchs et al. (2022) for the model area. For the 1880 scenario, it was assumed that P contents in agriculturally used soils are predominantly regulated by background conditions and no over-fertilization due to cultivation occurred. The currently implemented P content of naturally covered areas (Fuchs et al. 2022) was used as P contents for agriculturally used land (arable land, fruits, vineyards, pasture) in 1880.

5.2.4 Modelled sediment inputs and nutrient emissions via erosion

Modelled sediment inputs are clearly linked to topography and land use. Higher sediment inputs can be found in the low mountain ranges of the study area, the highest ones in the alpine areas of the Rhine basin (Figure 16).

Most sediment input is delivered from arable land (Table 9) as the dominant land use in both North Sea and Baltic Sea basins. Sediment input from open areas (mountains and glaciers) occurs only in North Sea basins, where they make up roughly 36 % of the total sediment input into surface waters. This is due to the model settings with very high soil loss for mountains and glaciers in combination with a SDR of 100 % (refer to chapter 5.2.1.6). Thus, open areas show also the highest area-specific values for sediment inputs (Table 9).

Differences in area-specific sediment inputs between arable land and other land use categories (Table 9, Figure 17) reflect soil cover (assumptions on C factor) and spatial patterns of land use. Special crops (fruits and wine) show higher specific sediment inputs as they are typically grown on slopes. In contrast, area-specific sediment inputs from pasture and naturally covered areas tend towards zero in the flat North German Plain.

Modelled nutrient emissions via erosion partly reflect the sediment inputs. Most of the emissions are delivered from arable lands for both nitrogen and phosphorus in North Sea and Baltic Sea basins (Table

10, Table 11). Special crops show high area-specific sediment inputs but cover much less area than other land use classes, thus contributing ≤ 2 % of nutrient emissions via erosion. Open areas contribute 42 % of P emissions via erosion, but only 2 % of N emissions in North Sea basins (Table 10, Table 11). P emissions are approximately five times larger than N emissions for open areas, which can be attributed to the comparably higher P content of 660 mg P/kg for mountains and glaciers (Fuchs et al. 2022) compared to N contents of 150 mg N/kg and 100 mg N/kg for mountains and glaciers, respectively, in the model settings (Morling et al. 2024).

Figure 16: Modelled total area-specific sediment inputs into surface waters per MoRE analytical unit in 1880.

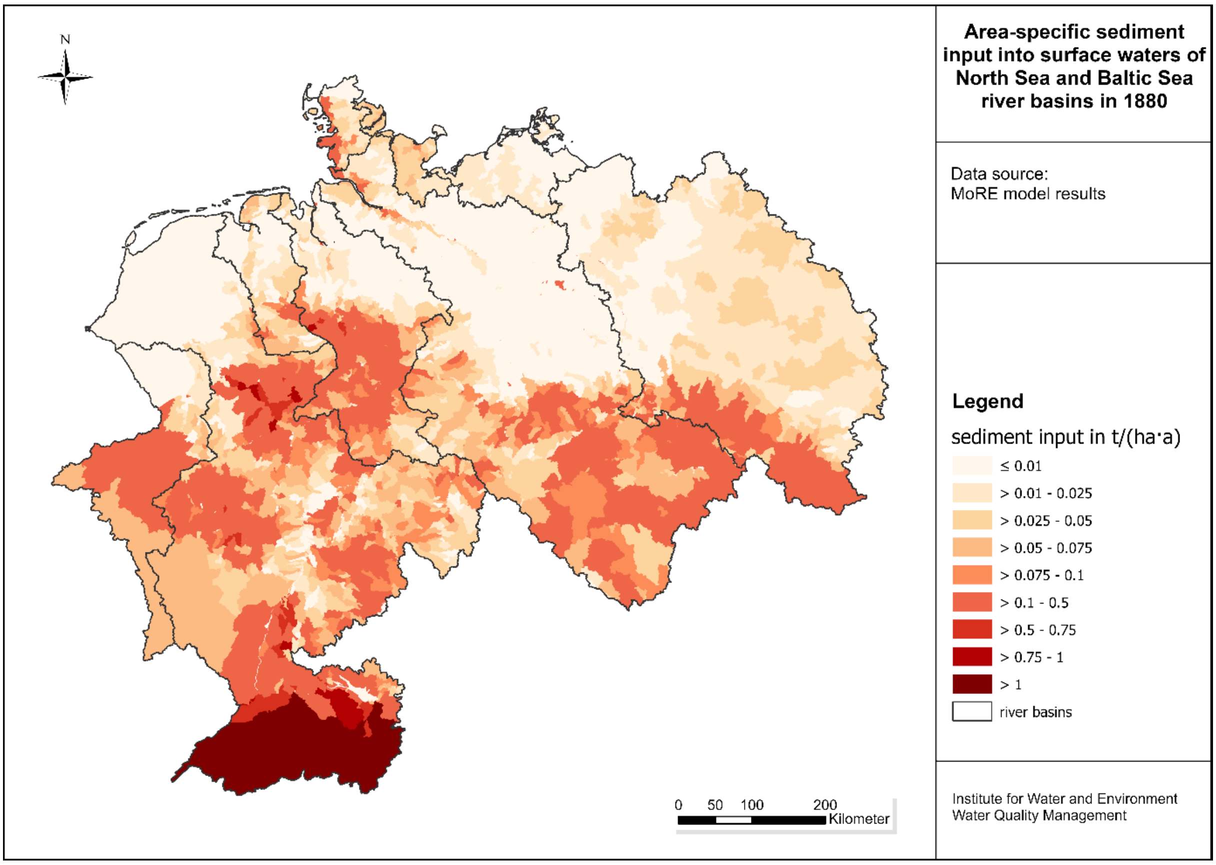

Source: own illustration, IWU-WG

Table 9: Modelled sediment inputs into surface water bodies for North and Baltic Sea basins in 1880, values rounded.

	North Sea basins		Baltic Sea basins	
Erosion via	**[t/a]**	**[t/(ha·a)]**	**[t/a]**	**[t/(ha·a)]**
Arable land	3 489 300	0.160	474 500	0.058
Pasture	698 900	0.117	57 900	0.042
Special crops (fruits and wine)	112 200	0.324	600	0.048
Naturally covered areas	65 400	0.005	57 900	0.007
Open areas	2 508 200	8.030	0	0
Total	**6 874 000**	**0.167**	**560 600**	**0.041**

Figure 17: Land use and area-specific sediment inputs into surface waters per river basin in 1880.[a]

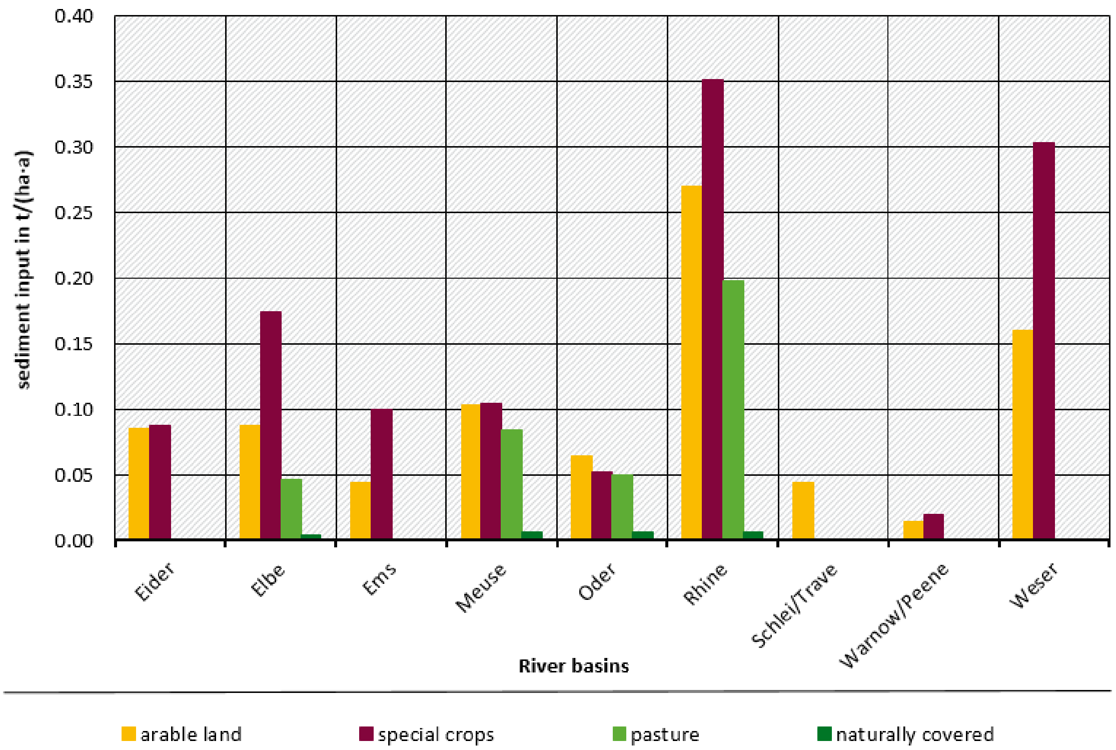

Source: own illustration, IWU-WG

[a] – Open areas are not shown (refer to chapter 5.2.1.6)

Table 10: Modelled nitrogen emissions via erosion for North and Baltic Sea basins in 1880.

	North Sea basins		Baltic Sea basins	
Erosion	**[t N/a]**	**[%]**	**[t N/a]**	**[%]**
Arable land	9 134	62	1 577	77
Pasture	4 597	31	306	15
Special crops (fruits and wine)	266	2	2	<1
Naturally covered areas	327	2	169	8
Open areas	335	2	0	0
Total	**14 660**	**100**	**2 054**	**100**

Table 11: Modelled phosphorus emissions via erosion for North and Baltic Sea basins in 1880.

	North Sea basins		Baltic Sea basins	
Erosion	[t P/a]	[%]	[t P/a]	[%]
Arable land	1 924	48	318	79
Pasture	332	8	43	11
Special crops (fruits and wine)	90	2	1	<1
Naturally covered areas	36	<1	39	10
Open areas	1 655	41	0	0
Total	**4 038**	**100**	**401**	**100**

5.3 Urban systems

Several input data are required for modelling emissions via urban systems. Information on total population, urban areas and impervious surfaces was taken from HANZE 2.0 dataset (refer to chapters 3.1 and 3.2). Precipitation and water consumed by population are parts of the water balance (see chapter 4).

To estimate the emissions via wastewater disposal, the following approach was considered (Figure 18): total population is divided into urban population connected to sewers and population not connected (both urban and rural). The approach for deriving the **connection rate** is explained in chapter 5.3.1. Nutrient amounts were calculated from total population and **daily inhabitant excretion rates** (chapter 5.3.2). These nutrient amounts are collected and treated in form of **wastewater** and were divided onto the sub-pathways of sewer systems, cesspit soil infiltration and cesspit cleanout (chapter 5.3.3).

Figure 18: Scheme for wastewater disposal and nutrient removal via urban systems in 1880.

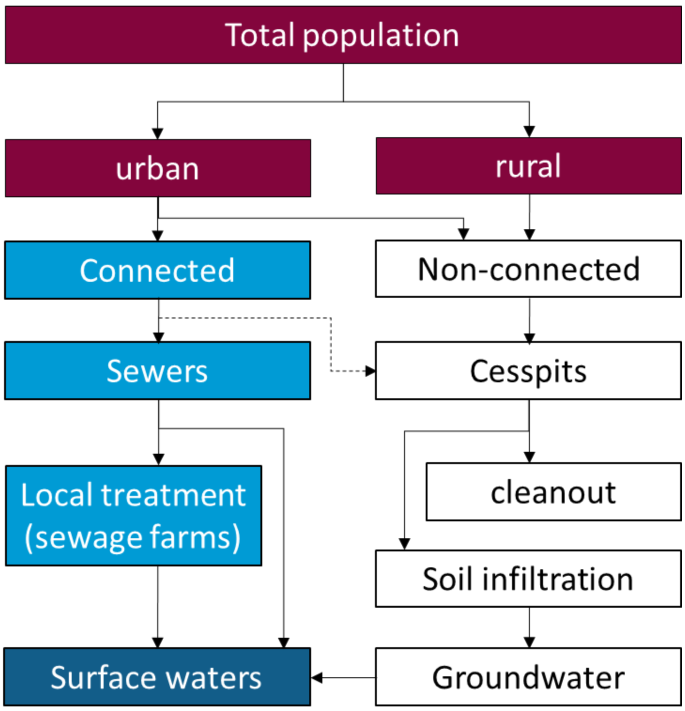

Source: own illustration, IWU-WG

Runoff from impervious areas connected to sewers contributes to nutrient emissions via urban systems as well. For impervious areas, the same connection rate as for population was assumed. To quantify emissions from street runoff, **surface loads** are needed as input data (chapter 5.3.4) and are multiplied with the connected impervious area.

Both rainwater runoff from connected impervious areas as well as wastewater by the connected population, contribute to the water volumes transported via sewers. These volumes were used to calculate **nutrient concentrations in the sewers** and compared to reported observed ones from historical literature (chapter 5.3.5).

5.3.1 Population connected to sewers

In many cities, gutters existed in the streets to collect kitchen swills and cleaning waters. Channels had been built for decades in an unsystematic manner in order to reach water bodies by the shortest route (Bärthel 2003; Büschenfeld 1997; Dunbar 1998; Evans 1990; Franzius et al. 1893; Gordon; Hobrecht 1868; Hötte 1992; Lange 2002; Mittermaier 1870; Mohajeri 2005; Salomon 1906, 1907; Soyka 1885; Weyl 1894; Architekten- und Ingenieur-Verein zu Hannover 1891). Ditches, streams and smaller rivers flowing through urban areas served as open sewer channels and were progressively built over in the late 19th century (Gordon 1874; Ladd 1990; Lange 2002). The new discipline of city planning emerging in the 1870s in Germany relied largely on sanitation needs (Ladd 1990). The construction of sewer systems according to consistent plans were indispensable for any city and started in the 1880 – 1890s and afterwards for the majority of German cities (Brix et al. 1934; Ladd 1990; Salomon 1906, 1907).

The need for urban drainage and wastewater disposal becomes stronger the more inhabitants live in a city. Accordingly, population density has been used for estimating population connected to sewer systems in historical scenarios before (Blauw et al. 2019; Naden et al. 2016). For instance, Blauw et al. (2019), assumed that 100 % of the urban population is connected to a sewer at a population density of > 5 inh/ha for their 1900 scenario. This estimation appears to be not applicable for 1880 conditions in Germany, as cities were tremendously growing and showed much higher population densities (Schott 1912, refer to Appendix A.3).

Table 12: Percentage of urban population connected to any kind of sewer used for modelling purposes.

Population density[a] [inh/ha]	Urban population connected to sewers [%]
≤ 9	0
10 – 35	30
≥ 36	80

[a] – For choosing the population density classes, refer to Appendix A.3

The population connected to sewers was estimated as follows: Present administrative boundaries for cities (ACT 2024; BKG 2020; CBS 2024a, b; DINUM 2024; GAPD 2023; Główny Urząd Geodezji i Kartografii 2024; Lacko 2023; Statbel 2023; Statistik Austria 2024; swisstopo 2024) with more than 20,000 inhabitants were used as a template to separate urban and rural areas of the HANZE 2.0 population density raster for the year 1880 (Paprotny & Mengel 2023). Further, areas of < 1 km^2 were eliminated from the selection of urban areas to exclude small settlements detached from larger urban centres. The percentages in Table 12 were multiplied with the selected urban areas of the population density raster. In contrast to Blauw et al. (2019), a maximum of 80 % instead of 100 % connection was assumed as most urban areas were not likely to meet a complete sewer connection at that time. Consequently, the population connected to sewers was summarized for each analytical unit. As a result, around 13 % of the total population was connected to any kind of urban sewer (Table 13). A higher amount of the population was connected in the North Sea basins, which corresponds well with the distribution of larger cities and industrial centres in these river basins (Figure 19).

This approach resulted in a slightly higher percentage of connected population (Table 13) than the estimated 9 % for the North Sea basins of Gadegast & Venohr (2015), who estimated the population connected to urban sewers according to the year of construction as given by Salomon (1906, 1907) and Brix et al. (1934).

Table 13: Total population and population connected to any kind of urban sewer in 1880 as obtained from the HANZE 2.0 dataset North and Baltic Sea basins, values rounded.

	Total population [inh]	Population connected to sewers [inh]	Population connected to sewers [%]
North Sea basins	44 107 000	6 011 000	14
Baltic Sea basins	9 786 000	769 000	8
Total	**53 893 000**	**6 780 000**	**13**

Figure 19: Percent population connected to any kind of sewers in the 1880 scenario for the MoRE analytical units.

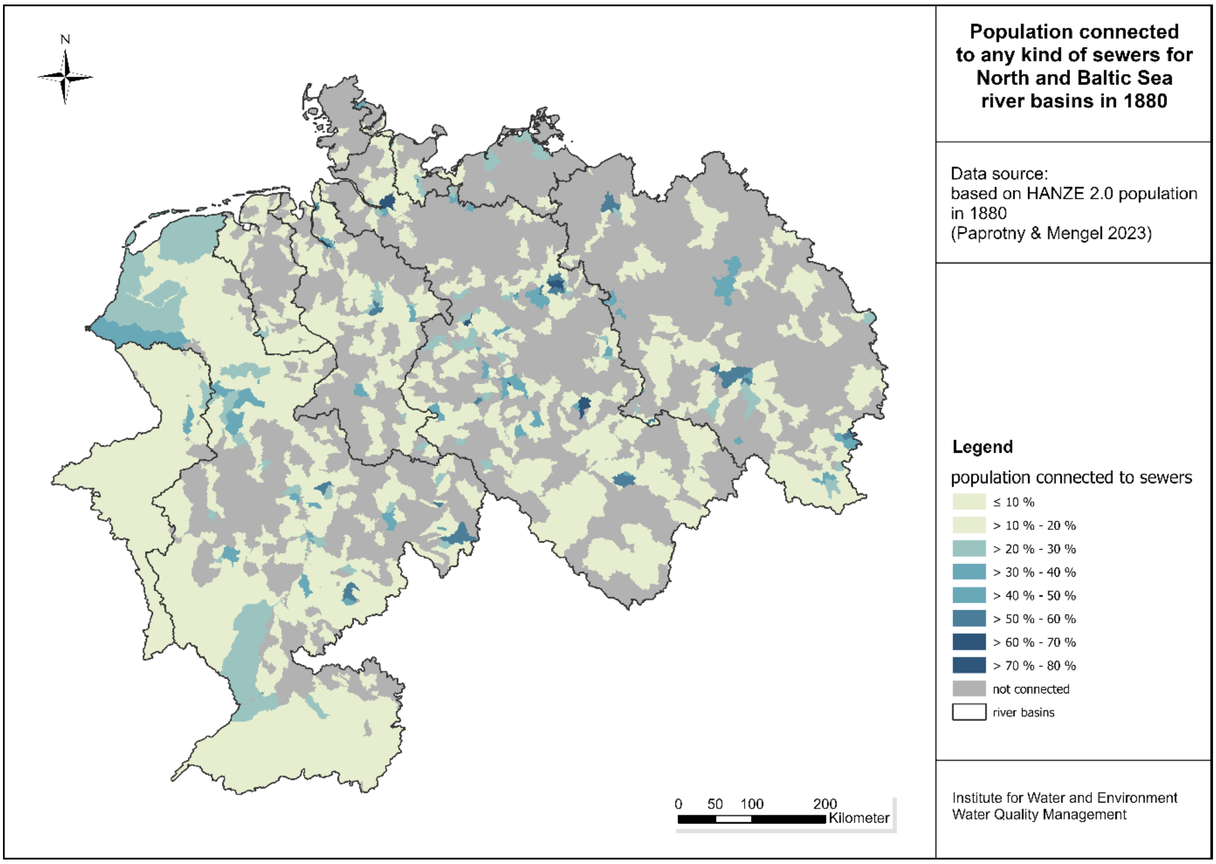

Source: own illustration, IWU-WG

Validation of historical connection rates is hampered by a lack of reliable data. Hardly any quantitative information was available about older channel systems before the construction of new sewers according to consistent plans started. Even after the new sewers were constructed, information for individual cities refer often not to the amount of people connected, but to the number of water connections or the number of connected properties within city borders. Inhabitants per water connection were around 60 for the largest German city of Berlin in the period 1882 – 1886 (Mohajeri 2005) and ranged from 20 to 30 for Munich (Soyka 1885). Cities were growing tremendously at that time, whereby inhabitants doubled or even tripled during a few years. For instance, the number of inhabitants of Hamburg city increased more than 3-fold from roughly 290,000 in 1880 to 931,000 in 1910 (Preiksch 2021).

An exemplary assessment revealed that estimated connection rates are in adequate agreement to literature information (Table 14). A very good agreement between the derived values and literature sources was achieved for the cities of Berlin (69 % compared to 70 % of population connected) and Munich (52 % compared to 54 % of population connected). For other cities, the derived percentages of connected inhabitants were lower than the ones given in literature. One reason is that these literature references refer to years after the construction of sewers in the 1880s, e.g. for the cities of Wrocław and Brunswick. Although the approach might not accurately reflect the situation for individual cities in 1880, it was assumed to provide a good agreement on the average situation on population connected to any kind of sewer.

Table 14: Estimated population connected to any kind of urban sewer for exemplary cities compared to literature data (year of reference for the connected population is given in brackets according to the literature references).

City	Estimated population connected in 1880 [%]	Population connected by literature [%] (year)	Building time of sewer system	References
Berlin	69	70 (1880)	1852 – 1874	Mohajeri (2005)
Wrocław	66	93 (1888)	1874 – 1881	Salomon (1907), Statistisches Amt der Stadt Breslau (1889/91)
Munich	52	54 (1880)	Older sewers since 1811, combined sewer system since 1890	Soyka (1885), Landeshauptstadt München (2024)
Frankfurt/Main	46	63 (1880)	1867	Salomon (1906), Bauer (1998)
Brunswick	45	76 (1894)	1886	Blasius (1894), braunschweiger forum e.V. (2022)
Würzburg	50	79 (1880)	1860	Salomon (1906), Hügel (1886)

5.3.2 Daily inhabitant excretion rates

Data were collected for daily excretion rates of nitrogen and phosphorus from literature (Figure 20; see also Appendix A.7). As the ranges of literature values cover the values already implemented in MoRE [12 g N/(inh·d) and 1.9 g P/(inh·d) for the sum of faeces and urine], these were used for the historical modelling. These input data also lie between the assumptions of other historical scenarios. Jensen (2017) assumed 4 kg N/(inh·a), which corresponds to ~11 g N/(inh·d), for Denmark in 1900. Gadegast & Venohr (2015) used a higher value of 14.2 g N/(inh·d) for modelling North Sea basins in 1880 but reduced the excretion rate for phosphorus to 1.09 g P/(inh·d).

Figure 20: Daily inhabitant excretion rates for nitrogen (top) and phosphorus (bottom) taken from literature (refer to Appendix A.7).

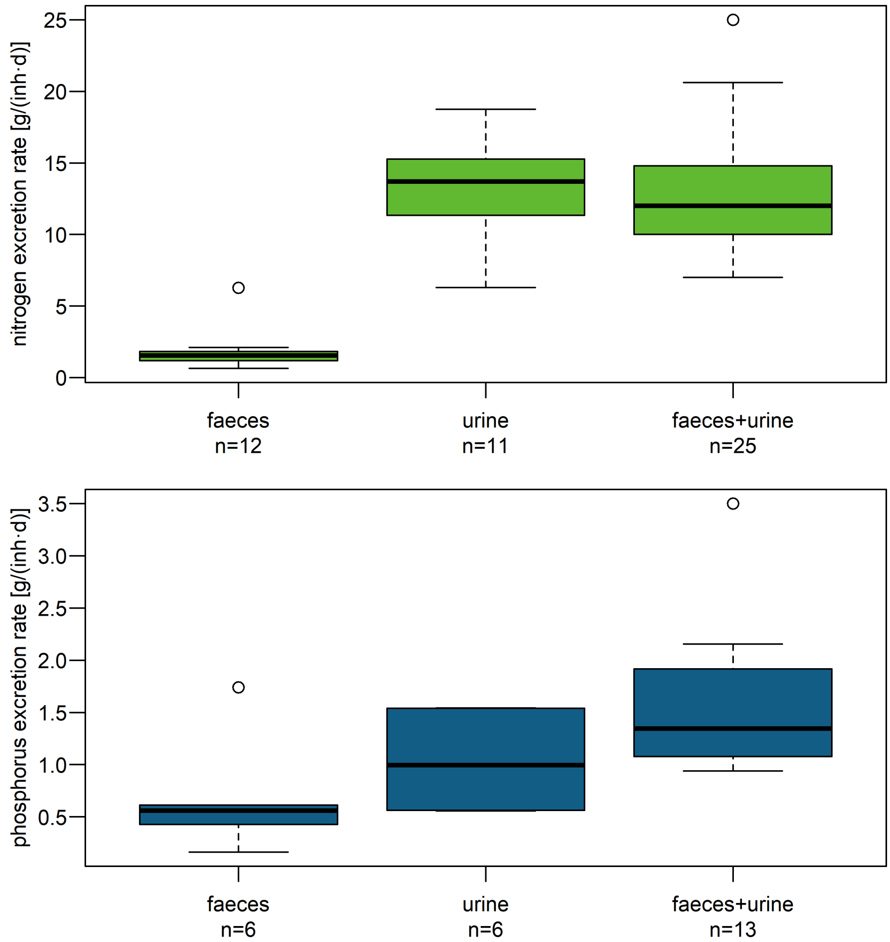

Source: own illustration, IWU-WG

5.3.3 Wastewater collection and treatment

Although the discharge of faeces into sewers was prohibited in many cities, these were partly disposed in this way (Lange 2002). In the city of Berlin, women earned their living by carrying buckets nightly from latrines to the Spree River (Ladd 1990). For the cities of Dresden and Stuttgart, it was assumed that only roughly 50 % and 75 % of total faeces were removed from cesspits, respectively, the rest getting into sewers and soils (Architekten- und Ingenieur-Verein zu Hannover 1891). Mohajeri (2005) reported that 29 % of the flats in Berlin were equipped with a WC in 1880. Similar, Plate (1998) refers to 25 % of urban households in Germany being equipped with a WC in 1880. Once a household had a WC, it is most likely that faeces were introduced into sewers and no longer collected separately. For modelling purposes, it was assumed that 25 % of the connected population discharged both urine and faeces into sewers. For the remaining connected population, it was assumed that one third of urine and the total faeces were collected in cesspits (König 1887).

The dissolved fraction of nutrient amounts entering cesspits was considered to infiltrate the soil and reach the groundwater (Figure 18). For soil retention, the settings already implemented in the MoRE model system were used (Fuchs et al. 2010), whereby soil retention varies from 50 – 90 % depending on permeability. Cesspit cleanout describes the amount of nutrients from collected faeces and was not considered to be discharged into surface waters but used for fertilizer production. Note that emissions via cesspit soil infiltration consider soil retention, while no retention was considered for cesspit cleanout.

The first wastewater treatment plant in Germany operated from 1887 in Frankfurt-Niederrad and covered mechanical treatment only (SEF 2024). Hence, point sources of municipal wastewater treatment plants were not modelled in the 1880 scenario. However, local wastewater treatment existed in terms of sewage farms. Many of these were implemented in the 1890s and afterwards in the German Empire (Salomon 1906, 1907). Only few of these facilities existed earlier than 1880 e.g. in Berlin and Gdańsk. Also, the small city of Bolesławiec in Lower Silesia was known for its use of wastewater for irrigation purposes since the mid of the 16th century (Dunbar 1998; Salomon 1907).

Sewage farms could usually not treat the total amount of wastewater of the connected inhabitants as the fields had to be running dry occasionally (Salomon 1906, 1907). In contrast to the British approach, sewage farms in Germany were based on soil infiltration with artificial drainage by default (Dunbar 1998). The drainage assured fast infiltration and allowed oxygen to enter the soil for mineralization of organic compounds. Further, swamp formation on the fields was prevented by discharging the drainage waters into the receiving water bodies. The performance of sewage farms depended on many factors, e.g. local soil characteristics, operation modes, crop types, which makes quantitative assessments of their efficiency difficult (Dunbar 1998).

The sewage farms of Berlin were implemented in the 1870s and expanded in the 1880s (Mohajeri 2005, Bärthel 2003, Dunbar 1998). In 1885, the fields received roughly 22.5 hm^3/a of wastewater (Mohajeri 2005). It was the largest facility of this kind at that time in the study area, acting as a role model for implementation in many other German cities in the following decades (Salomon 1906, 1907; Dunbar 1998). Thus, a local wastewater treatment of emissions via sewer systems was considered in the modelling for the analytical units covering Berlin. The few available comparisons of inflowing sewage and drained water at the sewage farms in Berlin and Wrocław revealed around 64 – 68 % retention of total nitrogen and 90 – 98 % retention of phosphoric acid (König 1887, 1899; Mohajeri 2005). For modelling 1880, a retention of 65 % was assumed for nitrogen. For phosphorus, the same retention as for soil infiltration was used (90 % for analytical units covering Berlin).

5.3.4 Surface loads

Substance loads from impervious surfaces contribute to the runoff from urban areas and to urban emissions into water bodies. Litter contained 0.472 % of nitrogen and 0.173 % of phosphorus (Weyl 1893). Using the per capita litter amount of 80 kg/(inh·a) (Weyl 1894) and applying this value to the population and urban area from HANZE 2.0 dataset (see chapters 3.1 and 3.3), resulted in surface loads for nitrogen and phosphorus of 4.49 kg N/(ha·a) and 1.64 kg P/(ha·a), respectively. The obtained nitrogen surface load for historical conditions is close to the 4.6 kg N/(ha·a) by Gadegast & Venohr (2015).

5.3.5 Modelled emissions via urban systems and concentrations in sewer systems

As much more connected population was located in North Sea basins compared to the Baltic Sea basins (Table 13, Figure 19), modelled nutrient emissions via urban sewers were generally higher for North Sea basins than for Baltic Sea basins (Table 15, Table 16). Most of the nutrient emissions can be attributed to cesspits.

Based on modelled nutrient inputs into sewers and water volumes, nutrient concentrations of the transported wastewater in the sewer systems were calculated for each analytical unit. Modelled concentrations were compared with concentrations reported in historical literature for some German cities (Baumeister 1890; König 1887, 1899; refer to Appendix A.1), showing an overall acceptable agreement of the concentration ranges (Figure 21). Modelled concentrations also matched the range of observed concentrations in untreated wastewater today.

Figure 21: Comparison of modelled nitrogen (top) and phosphorus (bottom) concentrations in urban sewer systems per analytical unit with concentrations reported in literature (refer to Appendix A.1).

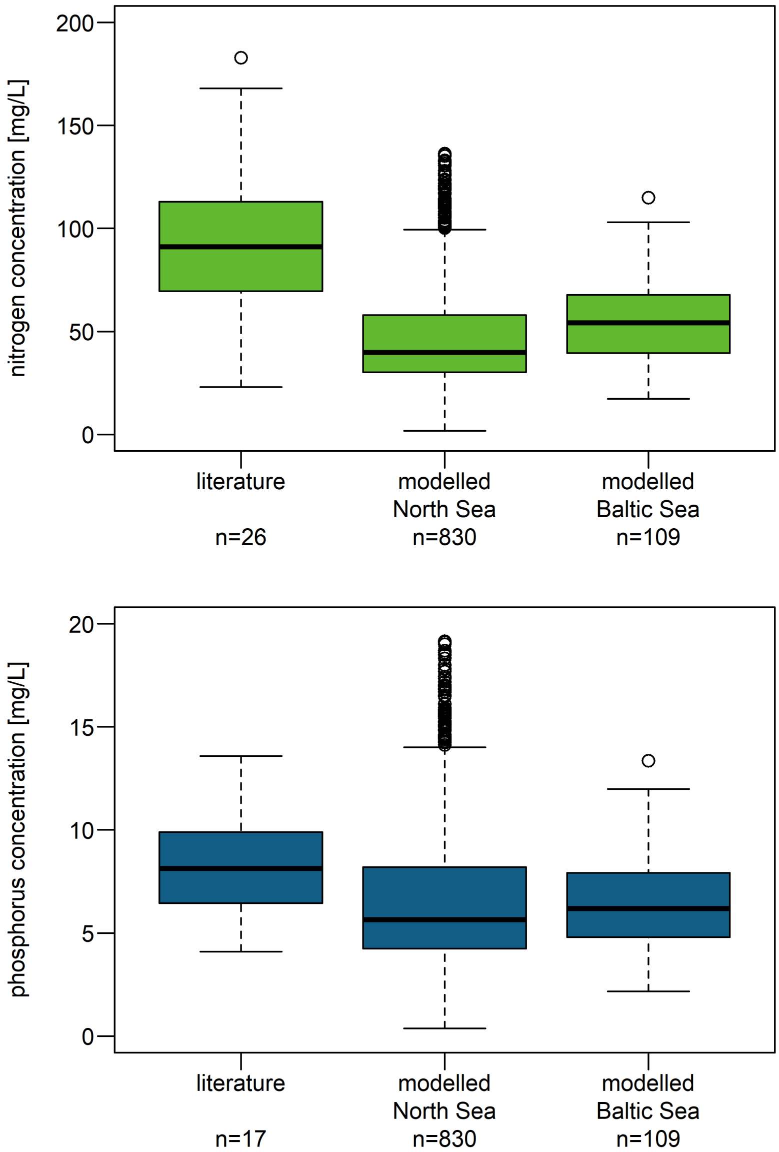

Source: own illustration, IWU-WG

Table 15: Nitrogen emissions via urban systems for North Sea and Baltic Sea basins in 1880.

	North Sea basins		Baltic Sea basins	
Urban system	**[t N/a]**	**[%]**	**[t N/a]**	**[%]**
Sewer systems	14 973	26	2 166	19
Cesspit soil infiltration	11 179	19	1 722	15
Cesspit cleanout	31 292	54	7 399	66

Table 16: Phosphorus emissions via urban systems for North Sea and Baltic Sea basins in 1880.

Urban system	North Sea basins [t P/a]	[%]	Baltic Sea basins [t P/a]	[%]
Sewer systems	1 851	17	263	12
Cesspit soil infiltration	1 241	11	170	7
Cesspit cleanout	7 823	72	1 850	81

5.4 Surface runoff

Unlike erosion, surface runoff comprises the transport of dissolved substances from non-built-up areas. Emissions via surface runoff are calculated by multiplying nutrient concentrations with surface runoff (as obtained from the water balance, refer to chapter 4). Concentrations are obtained differently for nitrogen and phosphorus and were adapted separately to 1880 conditions.

5.4.1 Nitrogen

Concentrations in surface runoff are usually dominated by atmospheric nitrogen deposition on arable land, pasture, naturally covered areas and open areas. For the 1880 scenario, the CCMI v2.0 dataset for input4MIPs on nitrogen deposition was implemented in MoRE (refer to chapter 5.1.1).

In addition to deposition, a nitrogen concentration of 0.3 mg N/L is assumed for arable land in current MoRE modelling to represent leaching from fertilizer additions. This was reduced to 0.1 mg N/L in 1880 to represent historical agriculture. We assumed that soils were not over-fertilized to the same extent they are nowadays. Further, mainly manure and human excreta were used as fertilizers in 1880, which are less soluble than mineral fertilizers. For alpine areas, the currently implemented N concentration of 0.1 mg N/L was kept.

5.4.2 Phosphorus

Fuchs et al. (2022) derived phosphorus concentrations in surface runoff from agricultural land depending on soil phosphate contents. This approach cannot be applied for the 1880 scenario as phosphate contents in agricultural soils most likely changed due to cultivation and fertilizer practice. Instead, the phosphorus concentration in surface runoff from all vegetated areas was set to 0.0125 mg P/L based on average phosphorus leaching from unproductive vegetation (Prasuhn et al. 1996), assuming that surface runoff concentrations differ not much from leaching concentrations due to the high soil phosphorus sorption capacity.

5.4.3 Modelled emissions via surface runoff

Table 17 summarises the modelled emissions for North Sea and Baltic Sea basins. Since North Sea basins cover a larger area, they have higher emissions for both nitrogen and phosphorus.

Table 17: Modelled emissions via surface runoff for North Sea and Baltic Sea basins in 1880.

Surface runoff	North Sea basins [t/a]	Baltic Sea basins [t/a]
Nitrogen	8 210	1 058
Phosphorus	254	31

5.5 Tile drainage

Emissions via tile drainage are calculated by multiplying the drainage concentrations with the runoff via tile drainage for each substance. Runoff via tile drainage is obtained by using the drained agricultural area and the runoff heights provided from LARSIM-ME water balance for arable land and pasture as described in Morling et al. (2024). Nutrient concentrations are derived differently for nitrogen and phosphorus and were adapted for the historical scenario.

5.5.1 Drained agricultural land and runoff via tile drainage

In the recent version of MoRE, the proportions of drained areas derived by Behrendt et al. (2000) are used. Information on drained areas is barely available for the period of the German Empire. In their modelling of historic nitrogen emissions into the Oder River, Gadegast et al. (2012) stated that approximately 9 % of the agricultural land was artificially drained in 1880. However, Gadegast & Venohr (2015) mention that 8 % of arable land and 6 % of agriculturally used areas were drained around 1880.

Due to a lack of reliable data, we adopted the approach of Gadegast & Venohr (2015) to derive the historical proportion of drained agricultural land (arable land and pasture) based on the currently implemented input data used in MoRE. By retaining the proportion of drained area for each AU to the total drained area, the current values were reduced to meet a total drained area of the entire MoRE model area of 6 % for the year 1880. This implies that areas with a currently high proportion of drainage also have comparatively high values in the year 1880.

5.5.2 Drainage concentrations

5.5.2.1 Nitrogen

In the current MoRE version, nitrogen concentrations via tile drainage are derived from nitrogen balance (Venohr et al. 2011). According to Batool et al. (2022), N balances in 1880 were mostly negative in the study area. Gadegast & Venohr (2015) estimated an average N surplus of 2 kg N/(ha·a) without nitrogen fixation and an average of 22 kg N/(ha·a) with nitrogen fixation for their 1880 scenario of the North Sea basins. Hirt et al. (2014) and Gadegast et al. (2012) estimated a mean N surplus without considering N fixation fluctuating around 5 kg N/(ha·a) before 1893 for Baltic Sea basins, but negative N surpluses for the following period, which were scaled up to a low positive N surplus (0.1 kg N/(ha·a)). Similar, Muhammed et al. (2018) obtained an overall mean average N balance of 0.5 kg N/(ha·a) for arable land and 0.98 kg N/(ha·a) for grass land in the United Kingdom considering the period 1800 – 1950.

Such low and even negative N surpluses cannot be used with the currently implemented approach of Venohr et al. (2011) in MoRE. Negative N surpluses would result in negative concentrations. Low N surpluses (≤ 1 kg N/(ha·a)) would lead to drainage N concentrations < 0.5 mg N/L, which is similar or even less than what can be assumed to leach from natural vegetation.

Therefore, a simple approach was chosen for modelling 1880: A nitrate concentration of 10 mg/L (2.257 mg N/L) was assumed as tile drainage concentration. This corresponds to the assumed unaffected conditions for groundwater concentrations (refer to chapter 5.6.1).

5.5.2.2 Phosphorus

In the current MoRE version, the P concentrations in tile drainage are differentiated according to four different soil structures following the approach of Venohr et al. (2011). For 2016 – 2018, the average concentration is 0.36 mg P/L.

Gadegast & Venohr (2015) and Hirt et al. (2014) adapted the P concentration in tile drainage and groundwater to 0.02 mg P/L to reflect undisturbed conditions in 1880. Fuchs et al. (2022) derived P concentrations in groundwater from recent phosphate measurements, averaging to 0.022 mg P/L for

Germany. Similar to nitrogen, these groundwater concentrations were also used for modelling tile drainage P emissions in 1880 (refer also to chapter 5.6.2).

5.5.3 Modelled emissions via tile drainage

Table 18 summarises the modelled tile drainage emissions for North Sea and Baltic Sea basins. Since North Sea basins cover a larger area, they have higher emissions for both nitrogen and phosphorus.

Table 18: Modelled emissions via tile drainage for North and Baltic Sea basins in 1880.

Tile drainage	North Sea basins [t/a]	Baltic Sea basins [t/a]
Nitrogen	5 863	2 476
Phosphorus	53	24

5.6 Interflow and Base flow

Emissions via interflow and base flow are quantified by multiplying the corresponding concentrations and runoff components (from historical water balance, chapter 4).

5.6.1 Nitrogen concentrations

In current MoRE modelling, interflow concentrations for nitrogen are derived depending on N surpluses and retention in soils according to their properties (Morling et al. 2024). For base flow, the N concentrations derived by Knoll et al. (2020) are used for Germany in MoRE.

A drinking water analysis in 1915 in Germany revealed nitrate concentrations below 10 mg/L in 91 % of samples (n = 278, UBA 1994). However, the exact distribution and representativeness of the samples are unknown. Groundwater being the most common source of raw water in Germany and a nitrate concentration of 10 mg/L (2.257 mg N/L) is typically considered to represent groundwater conditions unaffected by human activity (by current standards). The upper class boundary of 2.257 mg N/L was chosen as upper limit of N concentration in interflow and base flow for modelling purposes. For the currently implemented base flow concentrations per analytical unit in MoRE (Knoll et al. 2020; Morling et al. 2024), all concentrations below 2.257 mg N/L were kept as is and all concentrations above 2.257 mg N/L were replaced with this value. These adapted concentrations were transferred to the analytical units outside present Germany using the average N concentration per aquifer type of the International Hydrogeological Map of Europe (IHME1500 v1.2, BGR & UNESCO 2019). Hydrogeological units were identified as one of the most important predictors of N concentrations in groundwater (Knoll et al. 2020).

N concentrations lower than 2.257 mg N/L are typically found in the North German Plains and large parts of Eastern Germany due to strongly anaerobic conditions and long residence times in these groundwater bodies (Knoll et al. 2020). This pattern is transferred to N concentrations used for 1880 modelling of interflow and base flow emission pathways (Figure 22).

Historical N surpluses were found to be mostly negative (Batool et al. 2022) which cannot directly used with current modelling approaches (refer also to chapter 5.5.2.1). Therefore, we used the nitrogen base flow concentration for the interflow as well.

Figure 22: Nitrogen concentrations in interflow and base flow per MoRE analytical unit in 1880.

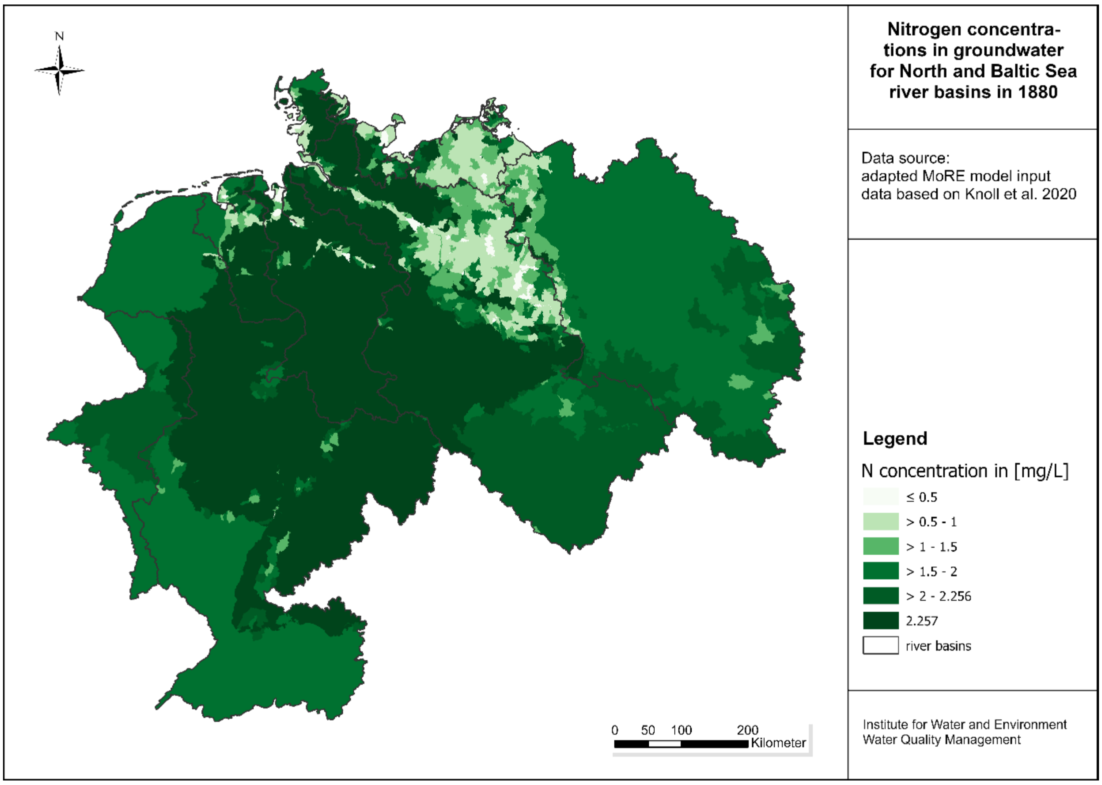

Source: own illustration, IWU-WG

Figure 23: Phosphorus concentrations in interflow and base flow per MoRE analytical unit in 1880.

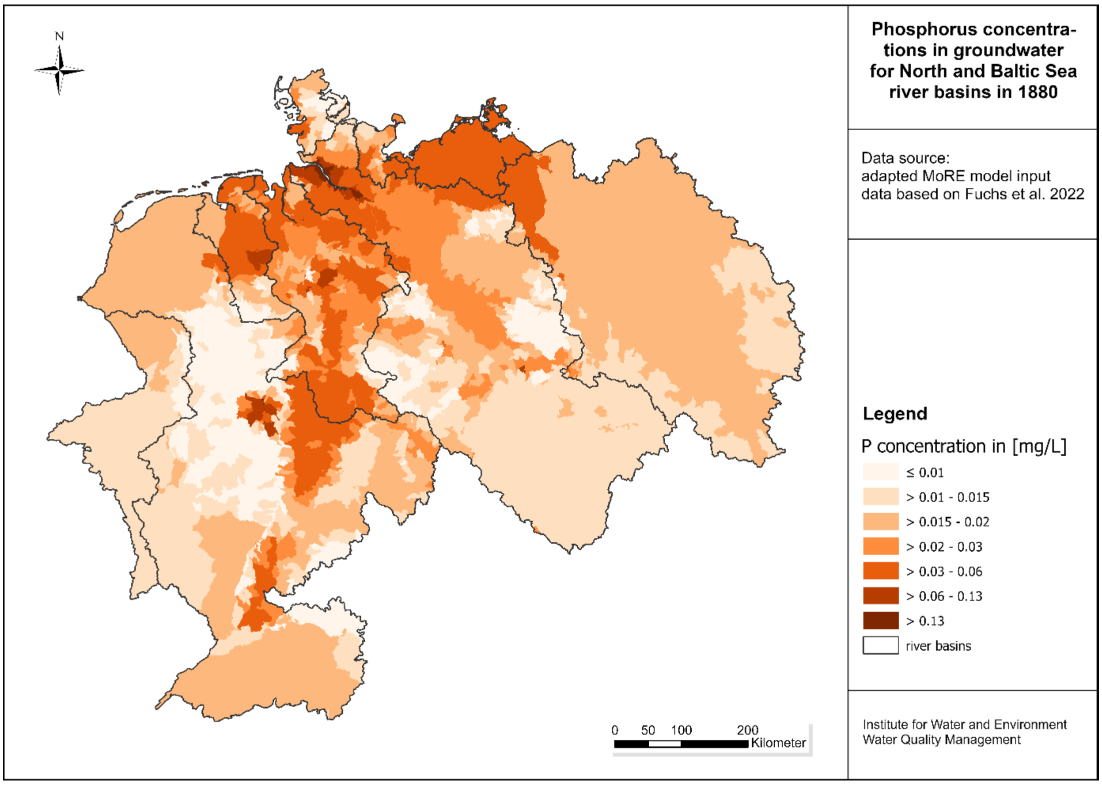

Source: own illustration, IWU-WG

5.6.2 Phosphorus concentrations

For both interflow and base flow, P concentrations derived from recent phosphate measurements are currently used for modelling in MoRE (Fuchs et al. 2022). For Germany, these P concentrations are on average 0.022 mg P/L, which is close to the 0.02 mg P/L previously used for historical modelling (Gadegast et al. 2012; Gadegast & Venohr 2015; Hirt et al. 2014). It is assumed that P concentrations in groundwater are predominantly depending on geological properties instead of agricultural practices since P is immobile and remains in the soils instead of leaching into the groundwater unlike nitrogen. Thus, the currently implemented input data by Fuchs et al. (2022) were kept for the 1880 scenario (Figure 23). Like nitrogen, phosphorus concentrations were extrapolated to the analytical units outside present Germany using the average P concentration per aquifer type (BGR & UNESCO 2019).

5.6.3 Modelled emissions via interflow and base flow

As base flow runoff is generally larger than interflow runoff (chapter 4.3), also modelled emissions via base flow are larger for both nitrogen and phosphorus (Table 19, Table 20). Baltic Sea basins show a higher share of base flow runoff (Table 7) and thus nutrient emissions via base flow are also larger than via interflow for Baltic Sea basins (Table 19, Table 20).

Table 19: Nitrogen emissions via interflow and base flow for North Sea and Baltic Sea basins in 1880.

	North Sea basins		Baltic Sea basins	
	[t N/a]	[%]	[t N/a]	[%]
Interflow	90 456	43	10 023	36
Base flow	119 939	57	17 532	64
Total	**210 395**	**100**	**27 555**	**100**

Table 20: Phosphorus emissions via interflow and base flow for North Sea and Baltic Sea basins in 1880.

	North Sea basins		Baltic Sea basins	
	[t P/a]	[%]	[t P/a]	[%]
Interflow	835	43	121	37
Base flow	1 111	57	210	63
Total	**1 946**	**100**	**331**	**100**

5.7 Retention in surface water bodies

In-stream retention is needed to transfer modelled emissions into surface water loads and concentrations. For nitrogen, the THL approach by Venohr (2006) is used in MoRE, which considers water temperature (T) and hydraulic load (HL). For the historical scenario, currently implemented average water temperatures were reduced by 1 K to reflect the generally cooler climate conditions of the past (see chapter 4.1.1). Phosphorus retention is modelled as a function of hydraulic load following Venohr et al. (2011).

Average surface water concentrations are obtained for each analytical unit by dividing the transported load by the total runoff, cumulated according to the runoff routing. The currently used runoff routing was not changed in the MoRE model.

6 Results of historical nutrient emission modelling

This chapter summarizes the model results on nutrient emissions, transported loads and concentrations in surface waters in 1880. For details on general and specific input data, historical water balance as well as model settings of the individual emission pathways refer to chapters 3 to 5 as well as Appendix A and B.

The results of this project are visualized for North Sea and Baltic Sea basins of present Germany in the MoRE toolbox (https://stoffeintraege-more.de/), which allows to interactively explore selected input data and results in more detail. The model results of the 1880 scenario as well as the geometry of the modeling units can be downloaded from the ZENODO repository: https://doi.org/10.5281/zenodo.15227585

6.1 Total emissions into surface waters

Total nitrogen emissions amount to roughly 257 kt N/a and 36 kt N/a for North Sea and Baltic Sea basins in 1880, respectively (Table 21). Almost half of the emissions originate from base flow, interflow being the second largest emission pathway for nitrogen. Even though the pathways erosion and urban systems together contribute to only 12 % of total nitrogen emissions (Table 21), they are locally of great importance. Mountainous areas as well as densely populated areas such as the cities of Berlin, Hamburg or Prague reach high area-specific emissions (Figure 24). In contrast, the lowest area-specific emissions can be found in the Oder basin and in large parts of the Elbe and Warnow/Peene basins (Figure 24). These areas combine a low population density (Figure 7) with low groundwater concentrations (Figure 22).

Total phosphorus emissions amount to 8.2 kt P/a and 1 kt P/a for North Sea and Baltic Sea basins in 1880, respectively (Table 22). Erosion is the most important emission pathway for phosphorus, making up almost half of the modelled emissions for the North Sea basins (Table 22). Urban systems contribute with 23 – 25 % as the second largest emission pathway for phosphorus. Similar to nitrogen, mountainous areas and densely populated areas show high area-specific phosphorus emissions (Figure 25). The lowest area-specific emissions occur in sparsely populated lowland regions.

6.2 Surface water loads and concentrations

River basins emit around 180 kt N/a and 4.2 kt P/a into the North Sea (Table 23). This corresponds to a retention of total emissions of 30 % and 49 % for nitrogen and phosphorus, respectively. The Baltic Sea basins emit around 22 kt N/a and 0.46 kt P/a into the sea (Table 23), which equals an emission retention of 38 % and 58 % for nitrogen and phosphorus, respectively. The higher retention in the Baltic Sea basins is related to the generally drier conditions with lower runoff compared to the North Sea basins (Table 23, refer also to chapter 4) leading to lower hydraulic loads and higher residence times.

The nutrient concentration in analytical units was calculated by dividing the transported load by total runoff. For both nitrogen and phosphorus, the modelled concentrations follow only partly the pattern of emissions. The highest concentrations were modelled in densely populated urban areas (Figure 26, Figure 27). For nitrogen, wide areas reflect the groundwater concentrations used as input data. Regions with the lowest groundwater concentrations in the Northeastern basins show the lowest modelled concentrations (Figure 26). As 2.257 mg N/L was set the upper limit of nitrogen concentration in groundwater (chapter 5.6.1), large parts of the study area show modelled surface water concentrations between 1.5 mg N/L and 2 mg N/L (Figure 26). For phosphorus, the modelled concentrations are mostly below 0.05 mg P/L (Figure 27). Higher concentrations can be found in urban areas and in mountainous areas, which have higher emissions via erosions.

Modelled concentrations per analytical units vary between river basins. Baltic Sea basins show on average lower nitrogen concentrations in surface waters (Figure 28, Table 23). For phosphorus, differences are less pronounced. On average, lowest P concentrations were modelled for Eider basin (Figure 29, Table 23).

Table 21: Total and pathway-specific nitrogen emissions for the North Sea and Baltic Sea basins in 1880.

Pathway	North Sea basins [t N/a]	North Sea basins [%]	Baltic Sea basins [t N/a]	Baltic Sea basins [%]
Atmospheric deposition onto water surfaces	2 894	1	529	2
Erosion	14 660	6	2 054	6
Urban systems	14 973	6	2 166	6
Surface runoff	8 210	3	1 058	3
Tile drainage	5 863	2	2 476	7
Interflow	90 456	35	10 023	28
Base flow	119 939	47	17 532	49
Total	**256 994**	**100**	**35 838**	**100**

Figure 24: Total area-specific nitrogen emissions into surface waters in 1880.

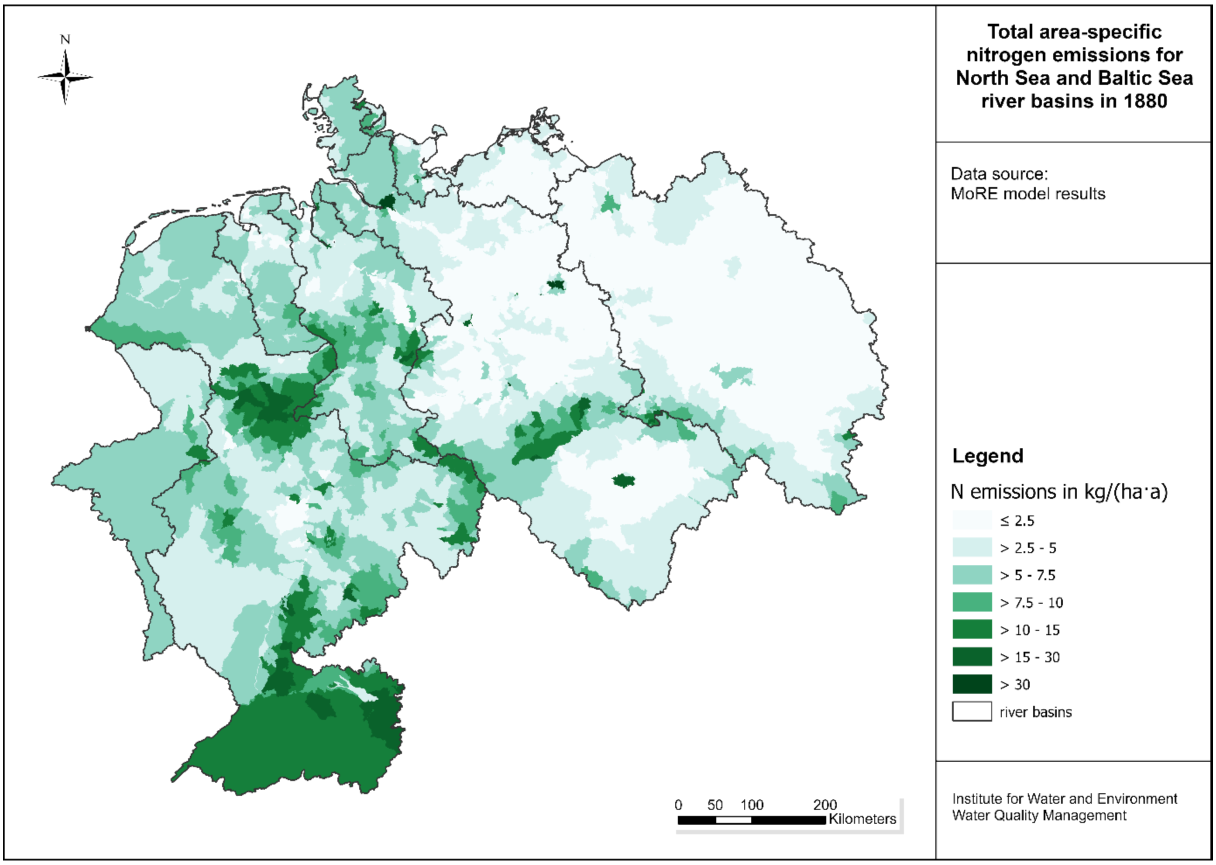

Source: own illustration, IWU-WG

Table 22: Total and pathway-specific phosphorus emissions for North Sea and Baltic Sea basins in 1880.

Pathway	North Sea basins [t P/a]	North Sea basins [%]	Baltic Sea basins [t P/a]	Baltic Sea basins [%]
Atmospheric deposition onto water surfaces	66	<1	15	1
Erosion	4 038	49	401	38
Urban systems	1 851	23	263	25
Surface runoff	254	3	31	3
Tile drainage	53	<1	24	2
Interflow	835	10	121	11
Base flow	1 111	14	210	20
Total	**8 208**	**100**	**1 065**	**100**

Figure 25: Total area-specific phosphorus emissions into surface waters in 1880.

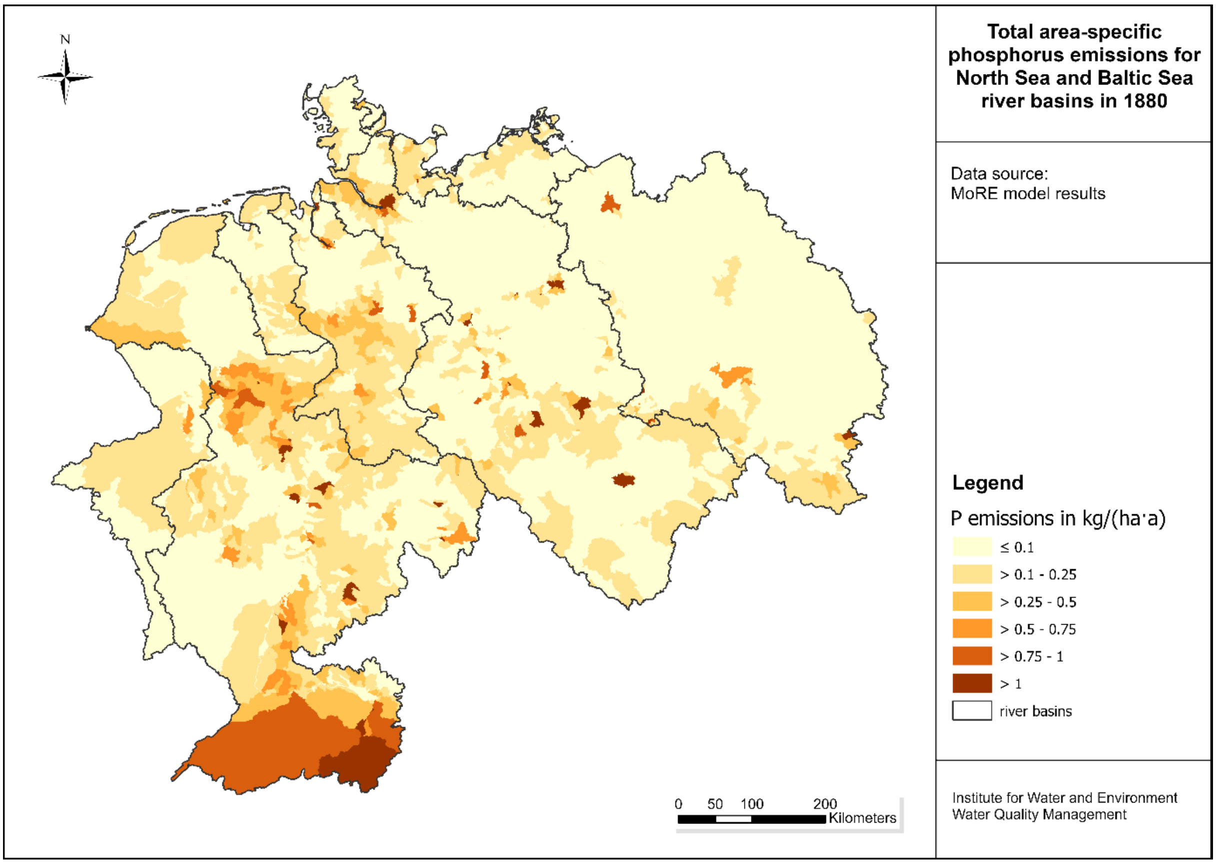

Source: own illustration, IWU-WG

Table 23: Nutrient surface water loads and outlet concentrations for North Sea and Baltic Sea basins in 1880.

River basin	Total runoff [m³/s]	Nitrogen [t N/a]	Nitrogen [%]	Nitrogen [mg/L][a]	Phosphorus [t P/a]	Phosphorus [%]	Phosphorus [mg/L][a]
Eider	53	2 501	1	1.51	23	<1	0.014
Elbe	841	37 339	18	1.41	839	18	0.032
Ems	133	6 421	3	1.54	99	2	0.024
Meuse	331	16 915	8	1.62	272	6	0.026
Rhine	2 417	95 970	47	1.26	2 546	55	0.033
Weser	414	21 244	10	1.63	426	9	0.033
Oder	487	17 955	9	1.17	320	7	0.021
Schlei/Trave	60	2 000	<1	1.05	56	1	0.029
Warnow/Peene	85	2 098	1	0.78	70	2	0.026
Total	**4 820**	**202 443**	**100**	**1.33**	**4 678**	**100**	**0.031**

[a] – average concentrations were calculated from surface water loads and total runoff per river basin

Figure 26: Total nitrogen concentrations in surface waters in 1880.

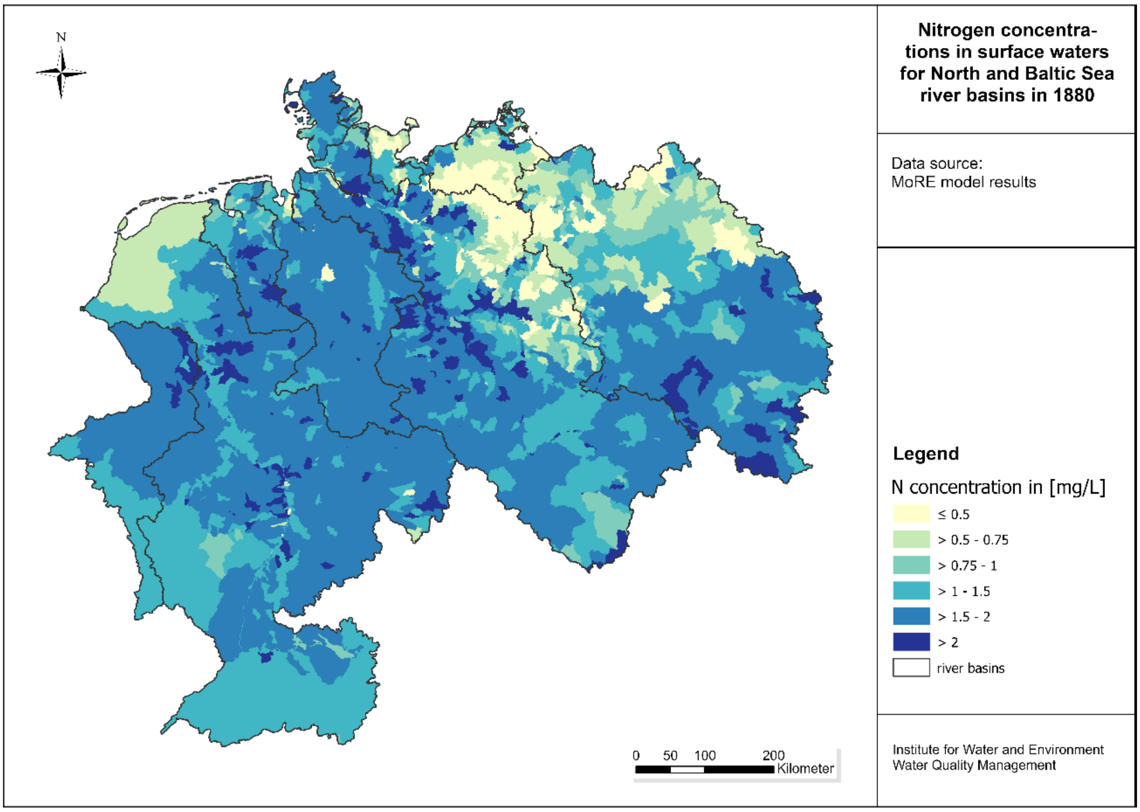

Source: own illustration, IWU-WG

Figure 27: Total phosphorus concentrations in surface waters in 1880.

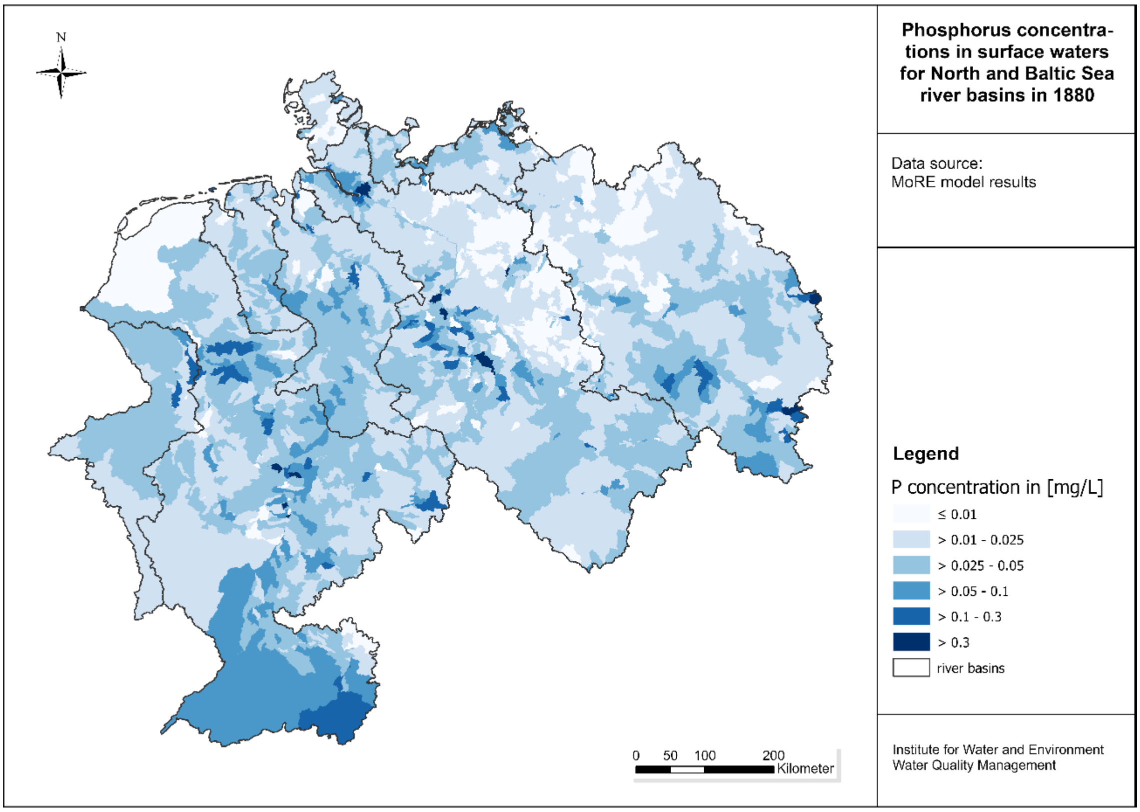

Source: own illustration, IWU-WG

Figure 28: Distribution of total nitrogen concentrations in surface waters per analytical unit in river basins in 1880.

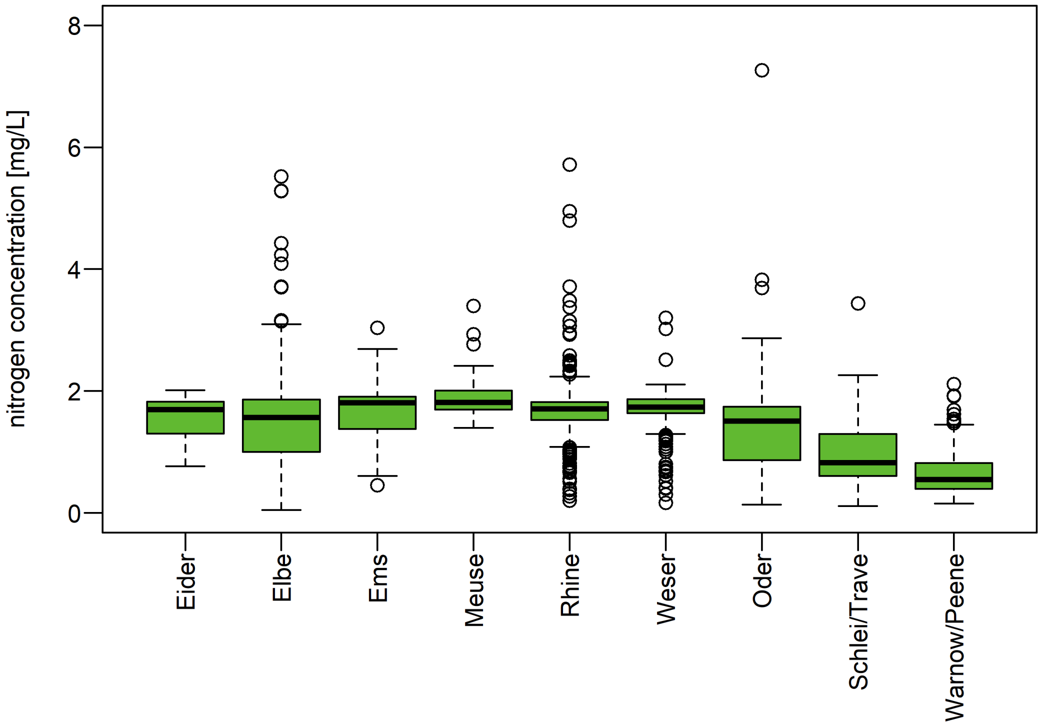

Source: own illustration, IWU-WG

Figure 29: Distribution of total phosphorus concentrations in surface waters per analytical unit in river basins in 1880. Note, that the y axis is displayed on a logarithmic scale.

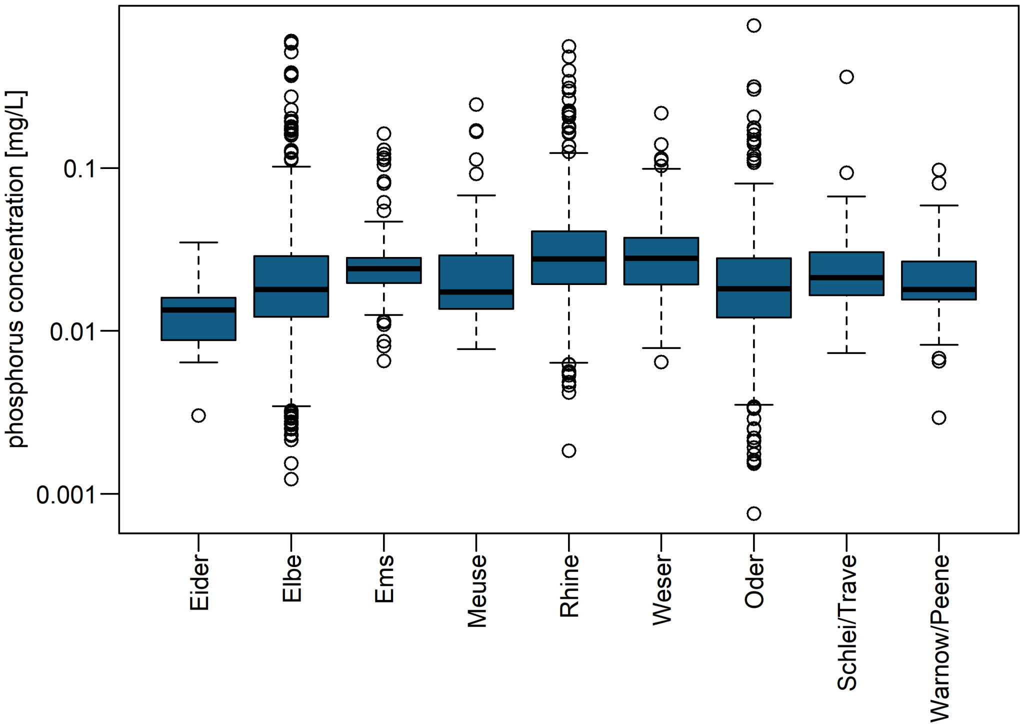

Source: own illustration, IWU-WG

The validation of modelled concentrations was hampered by a lack of suitable data. Only a few measurements have been reported in historical literature. They represent mostly individual records or averages over short time periods (≤ 1 – 2 years) and/or are valid for specific sites only, making them hardly suitable for deriving conditions of whole river basins. Analytical procedures differed in the past from present ones and might not have been standardized in the same way as today. It is often unclear if and how samples were treated (e.g. filtered) before analysis. Thus, it is not always clear if reported values refer to total or partial nutrient concentrations. For these reasons, a comparison to reported data from literature was conducted mainly to assure that modelled concentrations are in the same order of magnitude rather than fitting individual data.

Reported measurements of riverine samples within the study area were obtained from literature (Fischer 1914; Hirt et al. 2014; König 1887). Most of the collected records (n = 125) were available for nitrogen species (n = 113), the majority of these being located within the river basins of Elbe, Rhine and Oder (n = 81). These are compared to modelled concentrations per analytical unit (Figure 30), showing an overall good agreement of magnitude. Higher nitrogen concentrations were observed in urban areas especially downstream of sewer inflows or tributaries used for wastewater discharges (Fischer 1914; König 1887).

The modelled concentrations are on average in good agreement with results of further historical modelling approaches. For instance, Jensen (2017) found 1 – 2 mg N/L plausible for Danish rivers in 1900. Gadegast & Venohr (2015) obtained 1.41 – 2.5 mg N/L for their 1880 scenario of North Sea basins. Hirt et al. (2014) modelled concentrations ranging from 0.1 – 3 mg N/L for German Baltic Sea tributaries, which is similar to the ones obtained in this project (Figure 26, Figure 28).

Figure 30: Observed historical nitrate-N and nitrogen concentrations obtained from literature compared to modelled total nitrogen concentrations in surface waters in 1880 (Figure 28). Single values of the literature data overlay the boxplots as grey dots.

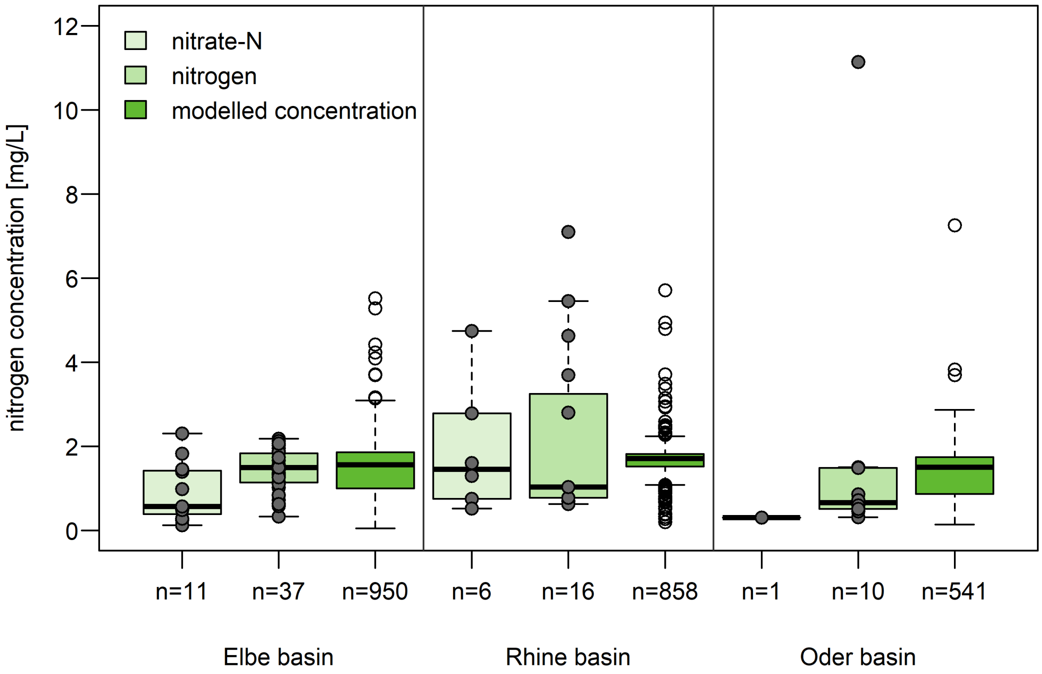

Source: own illustration, IWU-WG

Only a few measurements on phosphorus or phosphate concentrations are reported in historic literature (Fischer 1914; Hirt et al. 2014; König 1887). Most of them refer to sites with distinct urban influence or flood conditions showing concentrations above 0.07 mg P/L. For undisturbed or pristine conditions, concentrations below 0.05 mg P/L are typically considered for temperate rivers (Hirt et al. 2014; Topcu et al. 2011).

Gadegast & Venohr (2015) modelled average concentrations ranging from 0.02 – 0.05 mg P/L for North Sea basins in 1880, which are higher than the ones (0.01 – 0.03 mg P/L) obtained in this study (Table 23). Hirt et al. (2014) estimated for Baltic Sea tributaries 0.01 – 0.2 mg P/L, which is in the same range of concentrations modelled in this study (Figure 27, Figure 29), although differences most likely exist locally due to different input data.

7 Comparison to further historical modelling scenarios

The results of the 1880 MoRE modelling were compared to other historical scenarios on the level of river basins. This includes the previous 1880 MONERIS modelling of North Sea and Baltic Sea areas (Gadegast et al. 2012; Gadegast & Venohr 2015; Hirt et al. 2014), for which data on emissions, loads, and concentrations were kindly provided by M. Venohr (IGB Berlin). Further, loads and concentrations for some German North Sea basins were available from the regional E-HYPE 1900 modelling scenario (Blauw et al. 2019). Beusen et al. (2016) provided data of their global modelling study on riverine N and P transport to oceans in 1900. Further aspects of historical modelling comparison are discussed in Gericke et al. (2025).

Individual modelled **nutrient emission** pathways vary between the MoRE and MONERIS applications which provides some insight into differences (refer to Appendix C.1 for details). Total nitrogen emissions obtained with MoRE are consistently lower for all basins (Figure 31 upper panel). In general, lower emissions in tile drainage and surface runoff are modelled with MoRE. The sum of interflow and base flow showed slightly lower N emissions than the groundwater pathway of MONERIS for most of the basins. However, these two pathways (interflow and base flow) were proportionally more significant for total nitrogen emissions than tile drainage in the MoRE 1880 scenario compared to MONERIS (Appendix C.1).

Differences in total phosphorus emissions are more pronounced. While most basins exhibit similar or lower total phosphorus emissions in the MoRE modelling, there are 29 % more total phosphorus emissions for the Rhine basin compared to MONERIS (Figure 31 lower panel). Erosion is contributing the most to the overall higher emissions of the Rhine basin (Appendix C.1). Since the Rhine basin is covering alpine areas, the differences are most likely due to different model assumptions on nutrient emissions from these areas. The individual pathways differ in their relative importance between MoRE and MONERIS results. Phosphorus emissions via urban systems are higher for the MoRE modelling in the larger and more populated river basins. In contrast, phosphorus emissions via interflow and base flow are generally lower for the MoRE modelling than MONERIS results of the groundwater pathway for almost all river basins (Appendix C.1).

A comparison of MoRE and MONERIS results for the Upper Danube basin can be found in appendix D.3.

Differences in modelled **surface water loads** of MoRE and MONERIS applications are less prominent compared to the results of the regional and global modelling studies (Blauw et al. 2019, Beusen et al. 2016). Total nitrogen loads modelled with MoRE are the lowest ones in this comparison (Figure 32 upper panel). The largest differences exist for Rhine and Elbe basins. The reported nitrogen load for the Rhine River from the global modelling (Beusen et al. 2016) is almost double that obtained in MoRE and MONERIS modelling. Further, the results of the regional E-HYPE model show a 72 % higher nitrogen load for the Elbe basin compared to our study.

Total phosphorus loads modelled with MoRE are mostly lower compared to MONERIS results (Figure 32 lower panel). Similar to nitrogen, the largest differences exist for Elbe, Rhine and Oder basins compared to the global model data (Beusen et al. 2016). Especially for the Rhine basin, Beusen et al. (2016) estimated phosphorus loads almost 10 times higher. In fact, their 1900 phosphorus load of 21,035 t/a is almost equal to that reported for 2000 in their dataset (20,920 t/a; Beusen et al. 2016).

Figure 31: Comparison of total nitrogen (upper panel) and total phosphorus (lower panel) emissions for individual river basins between MoRE and MONERIS model in 1880.

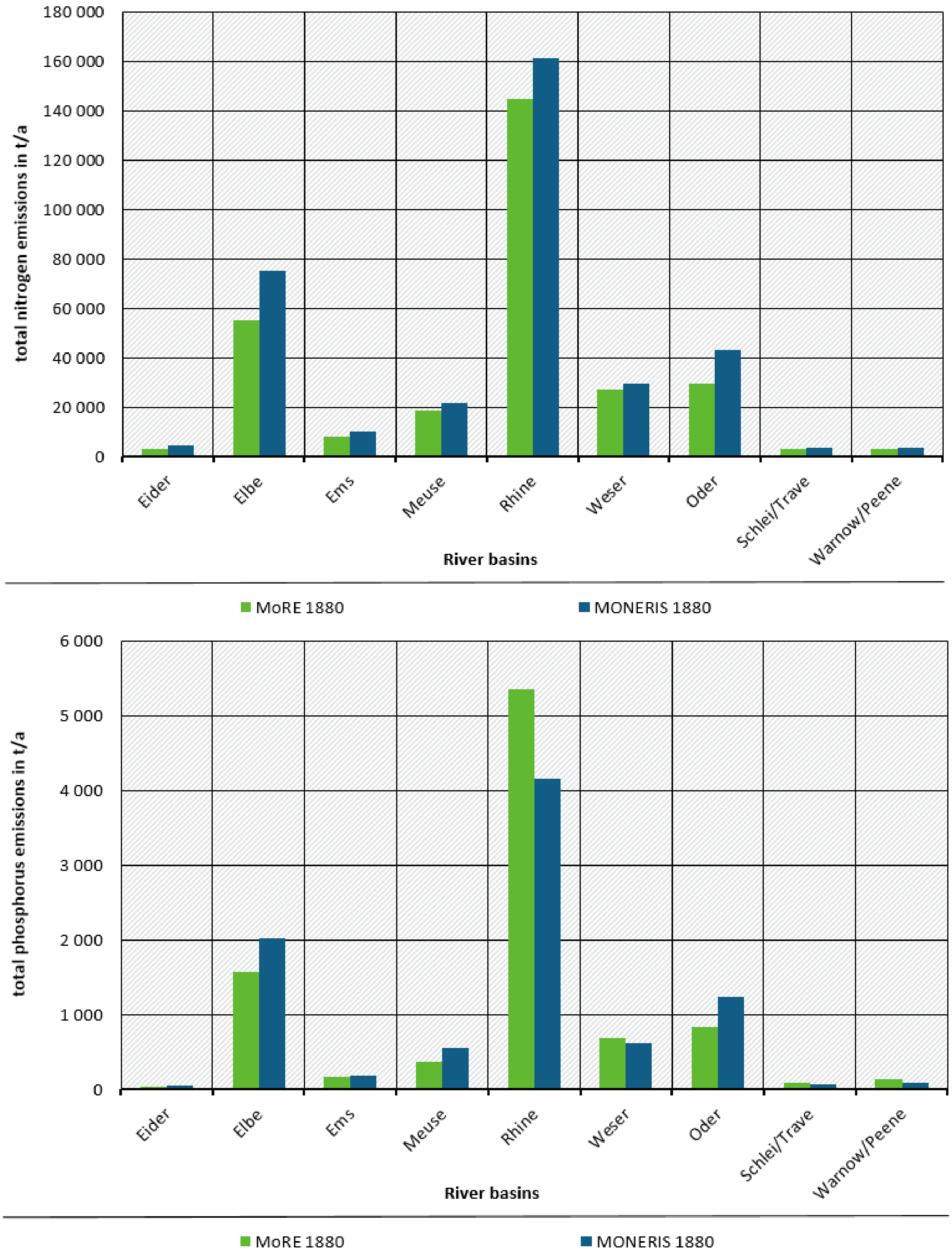

Source: own illustration, IWU-WG

Figure 32: Comparison of total nitrogen (upper panel) and total phosphorus (lower panel) surface water loads for individual river basins between different historical model scenarios.

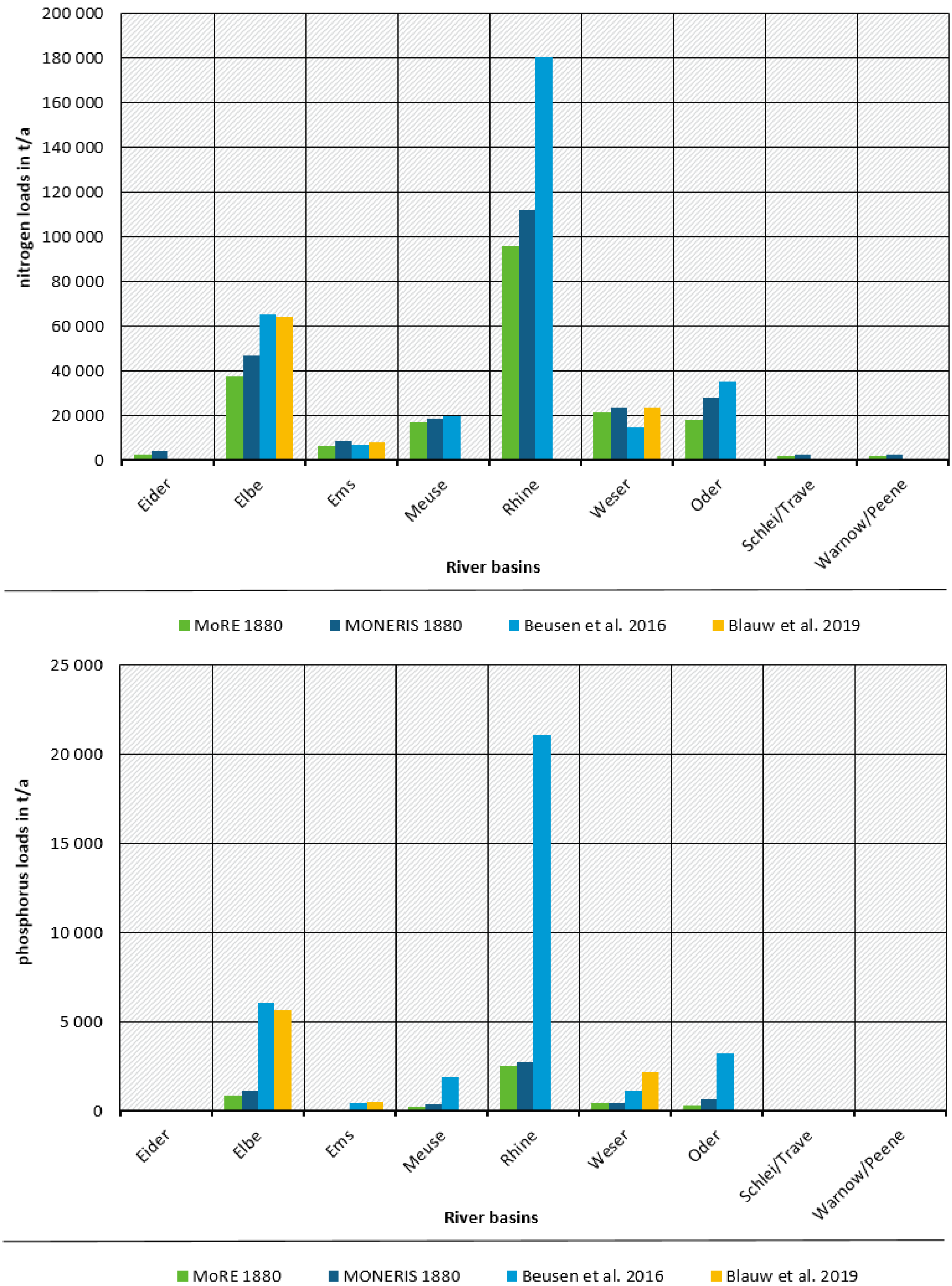

Source: own illustration, IWU-WG

Retention of emissions was calculated for MoRE and MONERIS results considering each river basin. It was also available for river mouths from Beusen et al. (2016). For nitrogen, the MoRE and MONERIS results are in the same order of magnitude, but do not show a consistent pattern (Figure 33 upper panel). The global data from Beusen et al. (2016) show generally lower nitrogen retention except for the Meuse basin. The lowest retention is given for the Rhine basin (Figure 33 upper panel), which might be one reason for the observed higher loads (Figure 32). For phosphorus, the retention modelled with MoRE is mostly higher than MONERIS results (Figure 33 lower panel), which also relates to the generally lower phosphorus loads modelled with MoRE compared to MONERIS (Figure 32 lower panel). Like nitrogen, the phosphorus retention from Beusen et al. (2016) dataset is generally lower than MoRE results except for Meuse basin.

Average nutrient concentrations were calculated for each river basin by dividing the total transported nutrient load by total runoff (see also Appendix C.3). MoRE results show generally the lowest nitrogen concentrations (Figure 34 upper panel). However, they are close to MONERIS results, ranging consistently between 0.8 – 2.5 mg N/L (Figure 34 upper panel). This corresponds well with the range of reported historical measurements (chapter 6.2). Resulting nitrogen concentrations of the regional E-HYPE model are generally higher, between 2 – 3 mg N/L for Elbe, Ems and Weser basin. Nitrogen concentrations obtained from the global modelling of Beusen et al. (2016) are partly in the same range. However, Oder and Elbe basins show the highest concentrations (Figure 34 upper panel), exceeding 4 mg N/L and even 5 mg N/L, respectively. One reason for such high concentrations is certainly the ~50 % lower total runoff for these river basins in the Beusen et al. (2016) data compared to the other model studies (Appendix C.3). Such high average concentrations contradict our assumptions of historically less eutrophic conditions in surface waters and available observations from historical literature (chapter 6.2). Indeed, concentrations obtained from Beusen et al. (2016) data exceed present water quality measurements in Oder and Elbe Rivers (refer to Appendix E). For Oder River, yearly average concentrations of total nitrogen are recently below 3 mg N/L. For Elbe River, present yearly average total nitrogen concentrations range from 3 to 4 mg N/L.

Phosphorus concentrations for MoRE and MONERIS results are generally similar but do not show such a consistent pattern as for nitrogen (Figure 34 lower panel). Both models predicted concentrations of total phosphorus below 0.05 mg P/L, which corresponds to non-eutrophic and rather pristine conditions. In contrast, the E-HYPE model application resulted in already higher phosphorus concentrations (Figure 34 lower panel), which are comparable to recently observed riverine concentrations (refer to Appendix E). The major river basins of Elbe, Rhine and Oder show extremely high concentrations (Figure 34 lower panel) for the global modelling of Beusen et al. (2016). In the case of the Elbe basin, the phosphorus concentration is even 10 times higher than MoRE and MONERIS results. The estimated concentrations from Beusen et al. (2016) data even exceed measurements of total phosphorus in recent years (yearly averages ≤ 0.20 mg P/L; see also Appendix E). For phosphorus, less historical measurements are available compared to nitrogen and higher concentrations could be expected in sites with distinct urban influence (Hirt et al. 2014). However, it seems very unlikely that average concentrations per river basin would meet the ones obtained by Beusen et al. (2016).

Figure 33: Comparison of total nitrogen (upper panel) and total phosphorus (lower panel) retention for individual river basins between different historical model scenarios.

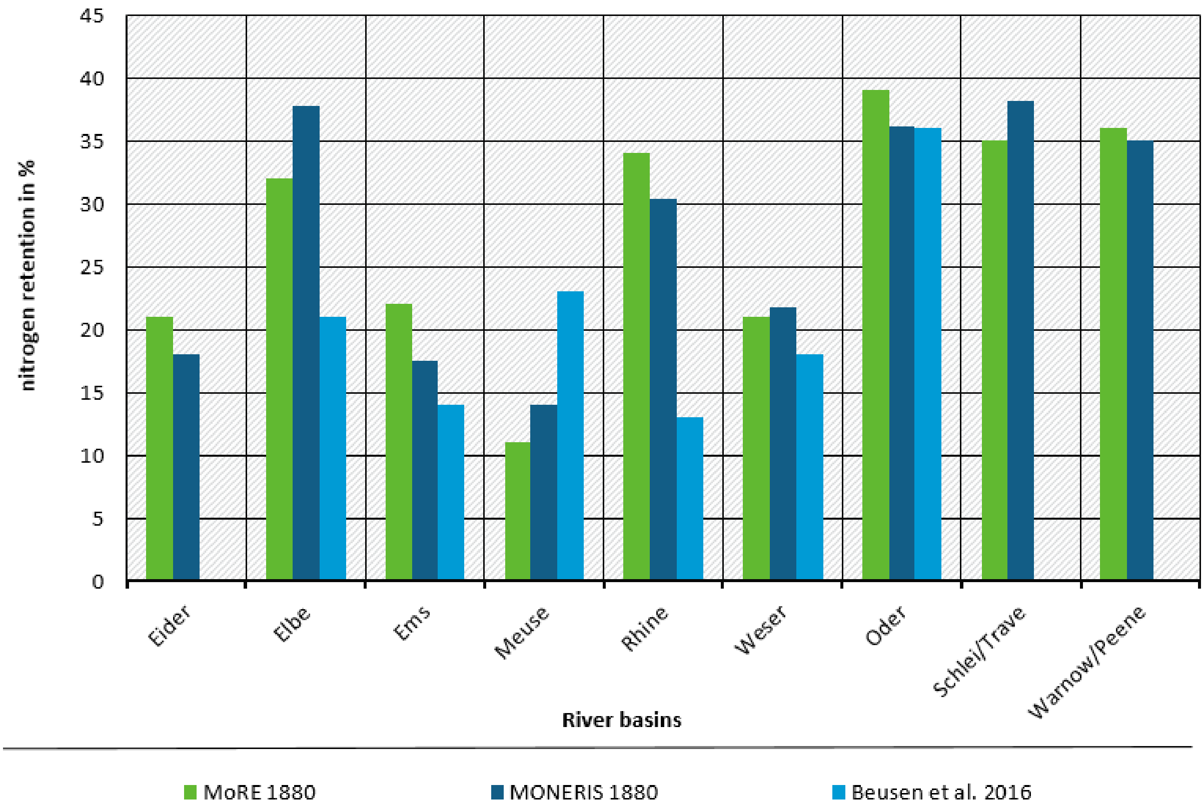

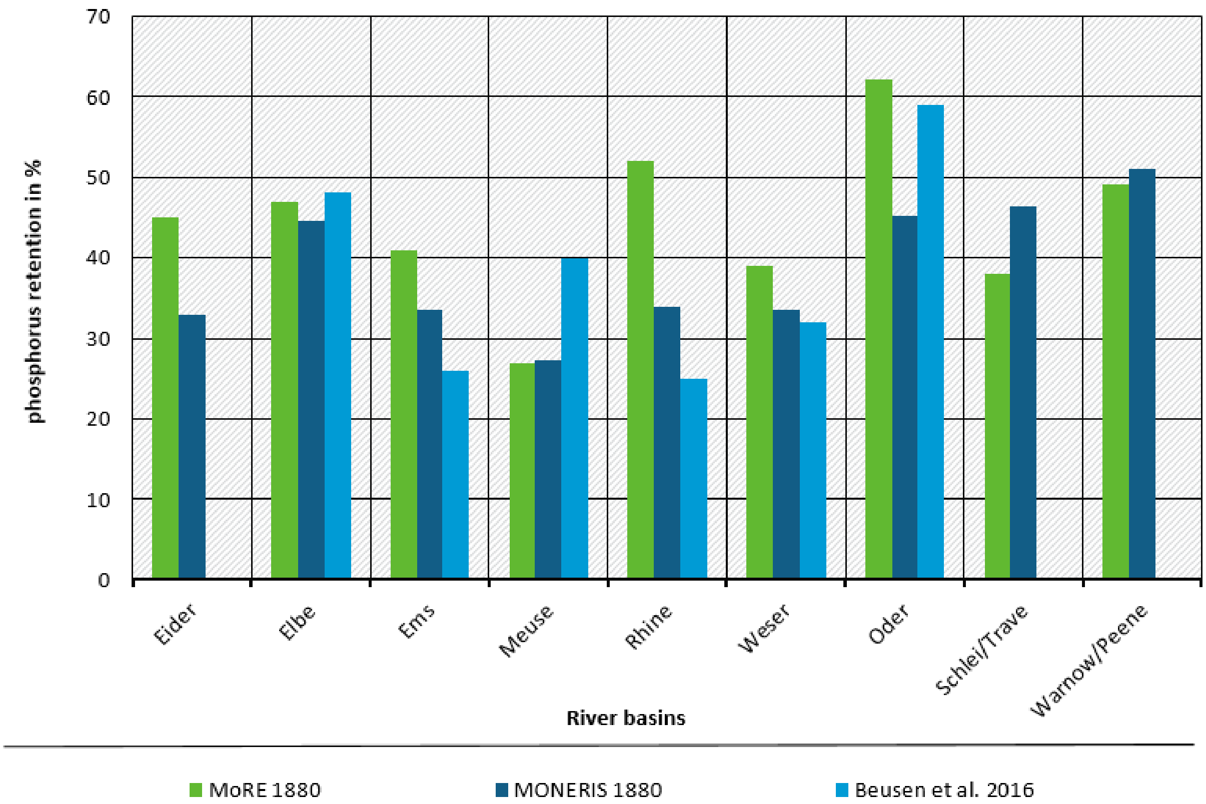

Source: own illustration, IWU-WG

Figure 34: Comparison of average total nitrogen (upper panel) and total phosphorus (lower panel) concentration for individual river basins between different historical model scenarios.

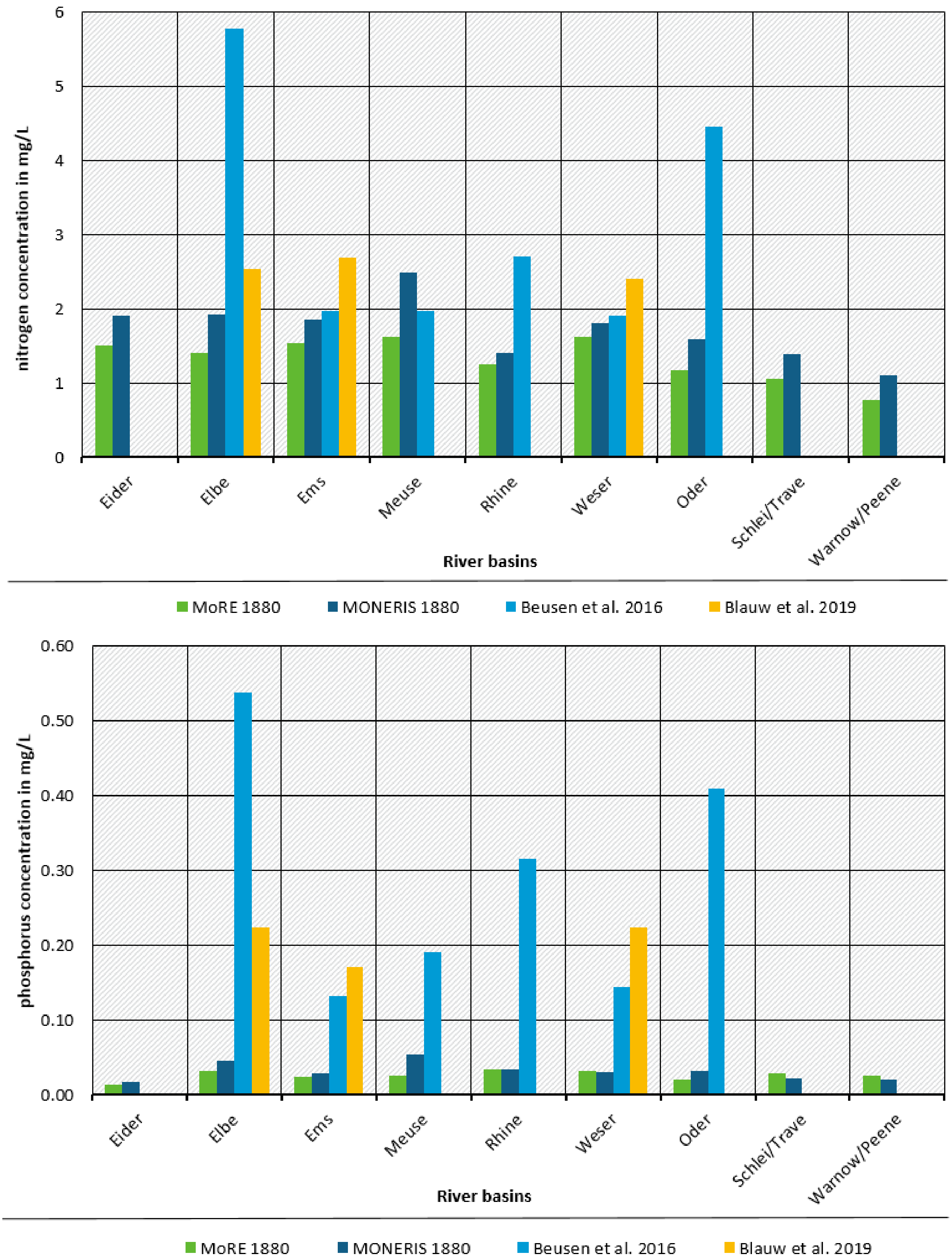

Source: own illustration, IWU-WG

The comparison revealed significant discrepancies between different historical scenarios. Results of MoRE and MONERIS modelling are much more alike compared to results from regional E-HYPE and global modelling (Beusen et al. 2016) for all parameters considered (emissions, loads, retention and surface water concentrations). Input data and modelling approaches differ for all four of these modelling studies and further evaluation is needed to detangle the reasons behind such varying results. Only limited measurements exist for historical nutrient concentrations in surface waters. In comparison to these, concentrations predicted by MoRE and MONERIS models fit historical conditions the best.

8 Limitations and uncertainties in historical nutrient emission modelling

Modelling is generally subject to many uncertainties. Reproducing past conditions is additionally challenged by lack of historical data, necessary model assumptions and simplifications as well as very limited validation options. The choice of input data highly influences model results and might lead to over- or underestimation of emissions and loads. Especially the most basic input data for land use, population and climate affect model results in the first place and already induce regional patterns throughout the study area. Each emission pathway depends on specific input data and variables. Thus, the contributions of individual emission pathways to the total emissions differ and their relative importance varies spatially as well. Therefore, a full uncertainty assessment from the great number of input data and adjustments of modelling approaches is not feasible. Instead, we focus on some important aspects.

Uncertainties of the **water balance** are mainly owing to model inadequacies as well as uncertainties of meteorological forcing and imperviousness of the 1880 scenario. The most prominent limitation of LARSIM-ME is an oversimplification of snow and ice processes in high altitude alpine regions, which leads to noticeable errors of the water balance in the highest parts of the Swiss Alps (chapter 4.3.1). This particular source of uncertainty could be mitigated by using the LARSIM glacier module in future versions of LARSIM-ME. The meteorological forcing for the 1880 scenario is based on climate change vectors ccv, which were derived from NOAA re-analysis data. The overall mean of the ccv agreed well with data of the German Meteorological Service DWD. However, the spatial pattern and seasonal distribution of the NOAA re-analysis data could not be confirmed by independent data. Therefore, temporarily and spatially constant ccv were used, which is surely an oversimplification (chapter 4.1.1.2). Furthermore, the unknown uncertainty of the HANZE 2.0 land use and imperviousness data for 1880 directly contribute to uncertainties of the water balance. Despite these limitations, the water balance for 1880, can be viewed as a reliable foundation for emission modelling (cf. chapter 4.3.4).

For nitrogen, interflow and base flow are the major emission pathways (chapter 6.1). Next to the water volumes, nitrogen concentration is the main driver for these pathways. A simple approach was used and currently implemented **groundwater concentrations** adapted according to an upper limit of 2.257 mg N/L (10 mg/L of nitrate, see chapter 5.6.1) based on a drinking water analysis in 1915 reported in literature (UBA 1994). This assumption is associated with a high degree of uncertainty as the exact distribution and representativeness of the samples is unknown. Groundwater concentrations are not known for 1880 and thus are certainly over- or underestimated in the modelling scenario in different regions of the study area.

Erosion is the main emission pathway for phosphorus (chapter 6.1), affected by assumptions on topography, soil types, land cover and management as well as connection probability. Topsoil P content is one main variable affecting the resulting emissions via this pathway. The real situation of **topsoil contents** of arable land and pastures in 1880 for the whole study area remains unknown. We assumed that current topsoil P contents of naturally covered areas are representative for agricultural soils as these were not over-fertilized in 1880 (refer to chapter 5.2.3). Phosphorus emissions via erosion are 2.5-fold higher for the Rhine basin compared to MONERIS results (Figure 40 in Appendix C.1). This is most likely due to differing model assumptions on **soil loss and delivery** for alpine areas, for which we assumed that all eroded material is entering surface waters (chapter 5.2.1.6). This example highlights the importance of land use specific assumptions for river basin modelling.

Urban systems contribute as the second largest emission pathway for phosphorus. High area-specific emissions are modelled in densely populated areas for both nitrogen and phosphorus (chapter 6.1). While it is known where cities already existed at that time, it is mostly uncertain how many inhabitants were actually connected to a sewer system. We chose a population density approach for deriving input data on

connected population (chapter 5.3.1). Due to the overlapping developments of urban population and sewer constructions, literature referring to the 1890s or 1900s likely does not well reflect the conditions in 1880 for a given city. The sparse data from different years highlight local characteristics of the individual cities. The chosen approach is simple and might not accurately reflect the situation for each individual city in 1880, but is conceptually in line with previous model applications (Blauw et al. 2019; Naden et al. 2016) and offers simple adjustments if necessary.

Emissions from urban areas are likely underestimated in this study as no **commercial and industrial wastewaters** potentially delivering nutrients to surface waters were included in the modelling due to a lack of suitable data on wastewater volumes and nutrient concentrations.

Lange (2002) estimated industrial wastewaters along the High and Upper Rhine around 1900 to more than 371,000 m^3/d. BASF Company in Ludwigshafen was known as the largest direct discharger in the 1880s at Upper Rhine, releasing ~75,000 m^3/d of wastewater into the river (Berhorst 2017; Lange 2002). Besides such single observations, quantification of wastewater amounts is complicated due to water extraction from headwaters or upstream areas and return to rivers after processing.

The composition of commercial and industrial wastewaters is only roughly known for the considered historical period. König (1887) and Fischer (1914) gathered measurements of different types of industrial wastewaters before and after various treatments. Typically, wastewater rich in organic matter also contained high concentrations of (organic) nitrogen. These originate predominantly from breweries, malt houses, slaughterhouses, dairy and starch factories as well as sugar refineries. Further, wastewater related to textile industry, e.g. from (wool) laundries, tanneries and wool/cloth factories, contained high amounts of nitrogen. Less reported data are available for phosphorus. Although these sources provide valuable insights into historical conditions, they report usually single measurements of a limited number of sites. Further, they refer to different treatments whose general efficacy, dissemination and application in the study area are unknown. Wastewater from different production stages and processes were discharged together and therefore its exact composition remained mostly unknown (Büschenfeld 1997). This hampers the derivation of reliable substance concentrations for commercial and industrial wastewaters besides the quantification of emitted volumes. Further, it can be expected that industrial emissions were much more decentralized compared to today.

Brudler et al. (2020) estimated urban nutrient emissions in Denmark in 1900 via flow path analyses, which included also industrial wastewaters. They assumed for 29 towns with more than 5,000 inhabitants to have dairies and slaughterhouses. Wastewater volumes and nutrient loads for these towns were based on a combination of historical and current data. They estimated that this industry contributed to 6 % and 9 % of urban nitrogen and phosphorus emissions, respectively. They also assumed that coastal cities delivered 95 % – 100 % of the industrial wastewater to surface water bodies; while this proportion was only 10 % for inland cities (assuming the majority of wastewater infiltrated the soil via landfills). While this kind of analysis provides a general idea of historical industrial nutrient emissions, it includes only two sources of very different types of industrial wastewater. A similar analysis of estimating industrial nutrient emissions for the study area considered here was not possible as specific operation modes and the dissemination of wastewater treatments (infiltration or direct discharge into water bodies) are not known.

Around 1880, industrialization was in full swing in the German Empire. Coal and ore mining allowed for growing iron and steel industry, promoting also metallurgy (Andersen 1996) as important industrial sectors. Potassium mining led to salination of rivers in Elbe and Weser basins (Büschenfeld 1997; Weyl 1894). German chemical producers held a 50 % share of the global market (North 2000) and produced worldwide half of all synthetic dyes at the beginning of the 1880s (Berhorst 2017). Bleaching agents and dyes were required by textile industry, being prominent in different parts of the study area (Büschenfeld 1997; North 2000). Operators of sugar, paper and textile factories discharged untreated wastewater but complained about the water pollution of upstream municipalities or industrial plants leading to several local conflicts (Büschenfeld 1997; Lange 2002). Consequently, agreements on time limits for contamination and precisely defined usage rights arose (Lange 2002). The discussion about **river pollution** centred mainly on direct discharges from industry and ultimately led to the development of first water acts in Germany in the late 19th and early 20th century (Büschenfeld 1997; Dunbar 1998; Lange 2002).

Retention in surface water bodies was modelled with currently implemented approaches in this study (chapter 5.7), neglecting changes due to the many hydraulic engineering measures carried out over the last one and a half centuries. They mainly include the regulation of watercourses (e.g. straightening and deepening), canalisation, drainage and land reclamation. Such measures might have led not only to changes in discharge conditions but also affected the nutrient retention capacity of rivers and estuaries. Nutrient retention might have been higher in the past due to less flow regulations by hydraulic measures and more wetlands in the past (Jensen 2017). A reconstruction of the water network and coastal morphology around 1880 was not possible in this study and would have required extensive adaptations and calibrations in both MoRE and LARSIM-ME models. Similar to previous MONERIS modelling (Gadegast et al. 2012; Gadegast & Venohr 2015; Hirt et al. 2014), settings on hydraulic load were not adapted in MoRE for modelling 1880 retention in surface waters (chapter 5.7).

Further, retention depends on biological processes, being also impaired by potentially toxic untreated wastewater emissions from industry and saline mine waters in the 1880s (see above), whose effects cannot be quantified. For the 1880 scenario, temperature was decreased in the model settings (refer to chapter 5.7). However, temperature is of minor importance for nitrogen retention compared to hydraulic load.

9 Conclusions

To reduce water pollution, substance emissions must be quantified related to their sources in spatially sufficient resolution. Models used for this purpose should provide plausible results, reflecting regional differences. The German Environment Agency (UBA) uses the MoRE model for estimating substance emissions into surface waters. MoRE is continuously developed (Fuchs et al. 2010; Fuchs et al. 2017a; Fuchs et al. 2017b; Fuchs et al. 2018; Fuchs et al. 2022; Morling & Fuchs 2021) and was lately extended to integrate runoff components from the hydrological model LARSIM-ME (Morling et al. 2024). Building on this existing cooperation, we modelled the historical conditions for nitrogen and phosphorus emissions as well as their loads and concentrations in 1880.

In comparison to previous work, the 1880 scenario is more consistent across the North Sea and Baltic Sea basins, more consistent with the recent datasets as well as the modelling approaches used by UBA for the national reporting. In contrast to previous historical modelling studies, a historical water balance was developed with LARSIM-ME model accounting for changes in climate, land use and imperviousness.

The model results represent a pre-industrial state with distinct anthropogenic impacts before the intensification of agricultural production by use of mineral fertilizers. Calculated nutrient concentrations in surface waters in 1880 are thus higher than those for an undisturbed (pristine) state (Hirt et al. 2014; Topcu et al. 2011), and are lower than presently observed ones. The modelled concentrations are in the same order of magnitude as observed historical measurements for the considered period.

The comparison to further historical modelling studies revealed that the 1880 results of the MoRE model are more similar to that of previous MONERIS (Gadegast et al. 2012; Gadegast & Venohr 2015; Hirt et al. 2014) than to regional (Blauw et al. 2019) and global applications (Beusen et al. 2016). Despite all the differences in input data and modelling approaches between MoRE and MONERIS, the total nutrient emissions and loads changed hardly – at least on the level of river basins. However, individual pathways differed in their importance and spatial representation between the two models. For nitrogen, the sum of interflow and base flow pathways of MoRE contributed proportionally more to total emissions than the groundwater pathway in MONERIS. For phosphorus, the importance of emissions via erosion varied among the river basins between the two models, which reflects differences in land use specific modelling assumptions.

Despite the overall similarities of MoRE and MONERIS results, average nutrient concentrations at the outlet of the river basins modelled with MoRE are on average lower. In fact, lower nutrient concentrations imply stronger requirements for reduction needs to protect marine and coastal waters. In this sense, our work may also enable a critical revision of currently implemented target values for total nitrogen and total phosphorus for North Sea and Baltic Sea tributaries of Germany for their validity.

The results of this project are visualized for the area of present Germany in the **MoRE toolbox**, which allows to interactively explore selected input data and results in more detail: https://stoffeintraege-more.de/

The model results of the 1880 scenario presented here as well as the geometry of the modeling units can be downloaded from the **ZENODO repository**: https://doi.org/10.5281/zenodo.15227585.

10 Acknowledgements

The authors would like to express their sincere thanks to numerous individuals and institutions who have contributed to this work by providing data, information and advice. We would like to thank the staff of KIT Library and Baden State Library in Karlsruhe for their help as well as the following individuals by name (in alphabetical order of the surnames):

Masooma Batool, Helmholtz Centre for Environmental Research (UFZ)

Michael Baumecker, Humboldt University Berlin

Anouk Blauw, Deltares

Claudius Fleischer, Federal Institute of Hydrology (BfG)

Michaela Hegglin, University of Reading

Florian Imbery, German Meteorological Service (DWD)

Karolin Kunz, Martin-Luther-University Halle-Wittenberg

Sarah Perryman, Rothamsted Research

Bruno Ringeval, French National Research Institute for Agriculture, Food and Environment (INRAE)

Markus Venohr, Leibniz Institute of Freshwater Ecology and Inland Fisheries (IGB)

11 List of references

Aas, W.; Fagerli, H.; Alastuey, A.; Cavalli, F.; Degorska, A.; Feigenspan, S. et al. (2024): Trends in Air Pollution in Europe, 2000–2019. In: *Aerosol Air Qual. Res.* 24 (4), P. 230237. Online available at https://doi.org/10.4209/aaqr.230237 [last access on 29.10.2024]

Administration du cadastre et de la topographie (ACT) (2024): Limites administratives du Grand-Duché de Luxembourg. Online available at https://data.public.lu/en/datasets/limites-administratives-du-grand-duche-de-luxembourg/#resources [last access on 25.01.2024]

Andersen, A. (1996): Historische Technikfolgenabschätzung am Beispiel des Metallhüttenwesens und der Chemieindustrie 1850-1933. Zugl.: Darmstadt, Techn. Hochsch., Habil.-Schr., 1995. Stuttgart: Steiner (Zeitschrift für Unternehmensgeschichte / Beiheft, 90).

Anonymus (1889a): Bericht einer französischen Kommission über die Reinigung der Kanalwasser von Berlin durch Rieselfelder. In: *Gesundheits-Ingenieur: Zeitschrift für die gesamte Städtehygiene* (7), P. 219–224. Online available at https://play.google.com/store/books/details?id=AprmAAAAMAAJ&rdid=book-AprmAAAAMAAJ&rdot=1 [last access on 13.05.2025]

Anonymus (1889b): Berliner Wasserwerke. Kleine Mitteilungen. In: *Gesundheits-Ingenieur: Zeitschrift für die gesamte Städtehygiene* (23), P. 785–790. Online available at https://play.google.com/store/books/details?id=AprmAAAAMAAJ&rdid=book-AprmAAAAMAAJ&rdot=1 [last access on 13.05.2025]

Architekten- und Ingenieurverein für Niederrhein und Westfalen (Ed.) (1888): Köln und seine Bauten. Festschrift zur VIII. Wanderversammlung des Verbandes deutscher Architekten- und Ingenieur-Vereine in Köln; vom 12. bis 16. August 1888. Köln: DuMont Schauberg. Online available at https://archive.org/details/kolnundseinebaut00arch/mode/2up?view=theater [last access on 29.04.2024]

Architekten- und Ingenieur-Verein zu Hannover (Ed.) (1891): Die Kanalisation von Hannover. Hannover: Schmorl & von Seefeld (Zeitschrift des Architekten- und Ingenieur-Vereins zu Hannover, 37). Online available at https://www.digitale-sammlungen.de/de/view/bsb11452583?page=234,235 [last access on 29.04.2024]

Ballabio, C.; Panagos, P.; Monatanarella, L. (2016): Mapping topsoil physical properties at European scale using the LUCAS database. In: *Geoderma* 261, P. 110–123. Online available at https://doi.org/10.1016/j.geoderma.2015.07.006 [last access on 04.08.2022]

Barles, S. (2007): Feeding the city: Food consumption and flow of nitrogen, Paris, 1801–1914. In: *Science of The Total Environmen*t 375 (1), P. 48–58. Online available at https://doi.org/10.1016/j.scitotenv.2006.12.003 [last access on 21.06.2024]

Barles, S.; Lestel, L. (2007): The Nitrogen Question: Urbanization, Industrialization, and River Quality in Paris, 1830—1939. In: Journal of Urban History 33 (5), P. 794–812. Online available at https://doi.org/10.1177/0096144207301421 [last access on 21.06.2024]

Bärthel, H. (Ed.) (2003): Geklärt! 125 Jahre Berliner Stadtentwässerung. 1. Aufl. Berlin: Huss-Medien Verl. Bauwesen. ISBN 3-345-00806-8.

Batool, M.; Sarrazin, F. J.; Attinger, S.; Basu, N. B.; van Meter, K.; Kumar, R. (2022): Long-term annual soil nitrogen surplus across Europe (1850–2019). In: *Scientific data* 9 (1), P. 612. Online available at https://doi.org/10.1038/s41597-022-01693-9 [last access on 18.08.2023]

Bauer, T. (1998): Im Bauch der Stadt. Kanalisation und Hygiene in Frankfurt am Main 16. - 19. Jahrhundert. Zugl.: Frankfurt (Main), Univ., Diss., 1996/97 u.d.T.: Bauer, Thomas: „Frankfurt ist rein!“. Frankfurt am Main: Kramer (Studien zur Frankfurter Geschichte, 41). ISBN 3-7829-0480-X.

Baumeister, R. (1890): Städtisches Strassenwesen und Städtereinigung. Berlin: Ernst Toeche (Handbuch der Baukunde Abt. 3, Baukunde des Ingenieurs). Online available at https://play.google.com/store/books/details?id=ddQCja0i7KsC&rdid=book-ddQCja0i7KsC&rdot=1 [last access on 23.07.2024]

Becker (1887): Die Entwässerung von Wiesbaden. Hierzu ein Lageplan. In: *Wochenblatt für Baukunde* (91), P. 455–457. Online available at https://opus4.kobv.de/opus4-btu/frontdoor/index/index/searchtype/series/id/29/docId/4075/start/4/rows/10 [last access on 29.04.2024]

Behrendt, H.; Huber, P.; Kornmilch, M.; Opitz, D.; Schmoll, O.; Scholz, G.; Uebe, R. (2000): Nutrient Emissions into River Basins. With collaboration of Wolf-Gunther Pagenkopf, Martin Bach and Ulrike Schweikart, 1. Aufl. Berlin: Federal Environment Agency (Umweltbundesamt) (TEXTE, 23/00). Online available at https://www.umweltbundesamt.de/sites/default/files/medien/publikation/long/1837.pdf [last access on 07.11.2023]

Belgian statistical office (Statbel) (2023): Population by place of residence, nationality, marital status, age and sex. Online available at https://statbel.fgov.be/en/open-data/population-place-residence-nationality-marital-status-age-and-sex-13 [last access on 25.01.2024]

Berhorst, R. (2017): Die Giftmacher. In: *Geo Epoche Kollektion* (7).

Beusen, A. H. W.; Bouwman, A. F.; Van Beek, L. P. H.; Mogollón, J. M.; Middelburg, J. J. (2016): Global riverine N and P transport to ocean increased during the 20th century despite increased retention along the aquatic continuum. In: *Biogeosciences* 13 (8), P. 2441–2451. Online available at https://doi.org/10.5194/bg-13-2441-2016 [last access on 21.10.2025]

BGR & UNESCO (2019): International hydrogeological map of Europe 1:1,500,000 (IHME1500). Digital map data 1.2. Hannover/Paris. Online available at http://data.europa.eu/88u/dataset/341255a9-180f-4bf9-b96f-d085339ea86d [last access on 06.08.2024]

Blasius, R. (Ed.) (1894): Die Errichtung von Rieselfeldern für die Stadt Braunschweig in Steinhof. Gutachten des Kaiserlichen Gesundheitsamtes. Braunschweig: Meyer. Online available at http://www.digibib.tu-bs.de/?docid=00022732 [last access on 02.05.2024]

Blauw, A.; Eleveld, M.; Prins, T.; Zijl, F.; Groenenboom, J.; Winter, G. et al. (2019): Coherence in assessment framework of chlorophyll a and nutrients as part of the EU project 'Joint monitoring programme of the eutrophication of the North Sea with satellite data'. (Ref: DG ENV/MSFD Second Cycle/2016). Activity 1 Report, 2019. Online available at https://www.informatiehuismarien.nl/publish/pages/163016/1_coherent_assessment.pdf [last access on 24.07.2023]

BLMP (2011): Konzept zur Ableitung von Nährstoffreduzierungszielen in den Flussgebieten Ems, Weser, Elbe und Eider aufgrund von Anforderungen an den ökologischen Zustand der Küstengewässer gemäß Wasserrahmenrichtlinie, 2011. Online available at https://www.schleswig-holstein.de/DE/fachinhalte/W/wasserrahmenrichtlinie/Downloads/weitere_Dokumente/12_Ableitungskonzept?nn=361421d9-6f5c-46d8-9ff9-d6a5b89fa18e [last access on 06.11.2024]

BMU (Ed.) (2003): Hydrologischer Atlas Deutschland. Online available at http://www.hydrology.uni-freiburg.de/forsch/had/had_bezug.htm [last access on 27.02.2025]

Bundesamt für Kartographie und Geodäsie (BKG) (2017): Digitales Geländemodell für Deutschland im 10-m-Raster: DGM10/BKG/2017.

Bundesamt für Kartographie und Geodäsie (BKG) (2023): NUTS-Gebiete 1:250 000. NUTS250. Product as of 31.12.2023. Online available at https://gdz.bkg.bund.de/index.php/default/digitale-geodaten/verwaltungsgebiete/nuts-gebiete-1-250-000-stand-31-12-nuts250-31-12.html [last access on 29.04.2025]

DIN 19708 (2017): Bodenbeschaffenheit - Ermittlung der Erosionsgefährdung von Böden durch Wasser mit Hilfe der ABAG – 2017-08, Deutsches Institut für Normung e. V.; Beuth (Berlin). DOI: 10.31030/2676773

braunschweiger forum e.V. (2022): Beginn einer planmäßigen Schmutzwasserableitung (Kläranlagen). Online available at https://www.braunschweigerzeitschiene.de/de/zeitreise/dekade-1878-1887/1886-beginn-einer-planmaessigen-schmutzwasserableitung.php [last access on 12.06.2024]

Bremicker, M. (2000): Das Wasserhaushaltsmodell LARSIM – Modellgrundlagen und Anwendungsbeispiele. Freiburg (Freiburger Schriften zur Hydrologie, 11). Online available at https://www.hydrology.uni-freiburg.de/publika/band11.html [last access on 06.09.2023]

Bremicker, M.; Homagk, P.; Ludwig, K. (2004): Operationelle Niedrigwasservorhersage für das Neckareinzugsgebiet. In: *Wasserwirtschaft* 94 (7-8), P. 40–46.

Bremicker, M.; Brahmer, G.; Demuth, N.; Holle, F.-K.; Haag, I. (2013): Räumlich hoch aufgelöste LARSIM Wasserhaushaltsmodelle für die Hochwasservorhersage und weitere Anwendungen. In: *KW Korrespondenz Wasserwirtschaft* (6/9), P. 509–519.

Brix, J.; Imhoff, K.; Weldert, R. (Ed.) (1934): Die Stadtentwässerung in Deutschland. 2 Bände. Jena: Fischer.

Brudler, S.; Arnbjerg-Nielsen, K.; Jeppesen, E. B.; Bitsch, C.; Thelle, M.; Rygaard, M. (2020): Urban Nutrient Emissions in Denmark in the Year 1900. In: *Water* 12 (3), P. 789. Online available at https://doi.org/10.3390/w12030789 [last access on 17.12.2024]

Bund/Länder-Ausschuss Nord- und Ostsee (BLANO) (2015): Harmonisierte Hintergrund- und Orientierungswerte für Nährstoffe und Chlorophyll-a in den deutschen Küstengewässern der Ostsee sowie Zielfrachten und Zielkonzentrationen für die Einträge über die Gewässer. Konzept zur Ableitung von Nährstoffreduktionszielen nach den Vorgaben der Wasserrahmenrichtlinie, der Meeresstrategie-Rahmenrichtlinie, der Helsinki-Konvention und des Göteborg-Protokolls. Stand: 6. Oktober 2014, 2015. Online available at https://www.schleswig-holstein.de/DE/fachinhalte/W/wasserrahmenrichtlinie/Downloads/weitere_Dokumente/13_HarmonisierteOrientierungswerte [last access on 06.11.2024]

Bundesamt für Geowissenschaften und Rohstoffe (BGR) (2020): Bodenübersichtskarte der Bundesrepublik Deutschland 1:200.000 (BUEK200): Bundesanstalt für Geowissenschaften und Rohstoffe (BGR). Online available at https://www.bgr.bund.de/DE/Themen/Boden/Informationsgrundlagen/Bodenkundliche_Karten_Datenbanken/BUEK200/buek200_node.html [last access on 21.01.2022]

Bundesamt für Kartographie und Geodäsie (BKG) (2017): DGM10 - Digitales Geländemodell in Gitterweite 10 m. Online available at https://gdz.bkg.bund.de/index.php/default/digitales-gelandemodell-gitterweite-10-m-dgm10.html [last access on 13.02.2020]

Bundesamt für Kartographie und Geodäsie (BKG) (2020): Administrative Areas 1:250,000 (VG250). Status of 01.01.2019. Online available at https://gdz.bkg.bund.de/index.php/default/digitale-geodaten/verwaltungsgebiete/verwaltungsgebiete-1-250-000-ebenen-stand-01-01-vg250-ebenen-01-01.html [last access on 09.07.2020]

Bundesamt für Kartographie und Geodäsie (BKG) (2023): NUTS-Gebiete 1:250 000. NUTS250. Product as of 31.12.2023. Online available at https://gdz.bkg.bund.de/index.php/default/digitale-geodaten/verwaltungsgebiete/nuts-gebiete-1-250-000-stand-31-12-nuts250-31-12.html [last access on 29.04.2025]

Bundesamt für Landestopografie (swisstopo) (2024): swissBOUNDARIES3D. Grenzen schweizweit in 3D. Online available at https://www.swisstopo.admin.ch/de/landschaftsmodell-swissboundaries3d [last access on 22.01.2024]

Bundesanstalt für Gewässerkunde (BfG) (2024): Global Runoff Data Centre (GRDC). Online available at https://grdc.bafg.de/ [last access on 25.04.2025]

Büschenfeld, J. (1997): Flüsse und Kloaken. Umweltfragen im Zeitalter der Industrialisierung (1870 - 1918). Zugl.: Bielefeld, Univ., Diss., 1994-1995. Stuttgart: Klett-Cotta (Industrielle Welt, 59). ISBN 3-608-91822-1.

Centraal Bureau voor de Statistiek (CBS) (2024a): Dataset: CBS Gebiedsindelingen. Gebiedsindelingen 2023 (WFS). Online available at https://www.pdok.nl/introductie/-/article/cbs-gebiedsindelingen [last access on 26.01.2024]

Centraal Bureau voor de Statistiek (CBS) (2024b): Population dynamics; birth, death and migration per region. Online available at https://opendata.cbs.nl/statline/portal.html?_la=en&_catalog=CBS&tableId=37259eng&_theme=1164 [last access on 26.01.2024]

Deutscher Wetterdienst (DWD) (2023): Open data. Online available at https://opendata.dwd.de/climate_environment/CDC/grids_germany/monthly/ [last access on 05.12.2024]

Direction interministérielle du Numérique (DINUM) (2024): Découpage administratif communal français issu d'OpenStreetMap. communes-20220101-shp. Online available at https://www.data.gouv.fr/en/datasets/decoupage-administratif-communal-francais-issu-d-openstreetmap/ [last access on 25.01.2024]

Dunbar, W. P. (Ed.) (1998): Leitfaden für die Abwasserreinigungsfrage. Abwassertechnische Vereinigung, 4. Aufl; Faks.-Dr. der Ausg. 1912. Hennef: GFA Ges. zur Förderung der Abwassertechnik.

European Centre for Medium-Range Weather Forecasts (ECMWF) (2023): Reanalysis datasets. Online available at https://www.ecmwf.int/en/forecasts/datasets/browse-reanalysis-datasets.

European Environment Agency (EEA) (2016): European Digital Elevation Model (EU-DEM), version 1.1. Copernicus Land Monitoring Service. Online available at https://land.copernicus.eu/imagery-in-situ/eu-dem/eu-dem-v1.1 [last access on 05.03.2020]

Evans, R. J. (1990): Tod in Hamburg. Stadt, Gesellschaft und Politik in den Cholera-Jahren 1830 - 1910. 1. Aufl. Reinbek bei Hamburg: Rowohlt. ISBN 3-498-01648-2

Fendrich, A. N.; Ciais, P.; Lugato, E.; Carozzi, M.; Guenet, B.; Borrelli, P. et al. (2022): Matrix representation of lateral soil movements: scaling and calibrating CE-DYNAM (v2) at a continental level. In: *Geoscientific Model Development* 15 (20), P. 7835–7857. Online available at https://doi.org/10.5194/gmd-15-7835-2022 [last access on 23.07.2024]

Fischer, F. (1914): Das Wasser. Seine Gewinnung, Verwendung und Beseitigung mit besonderer Berücksichtigung der Flussverunreinigung. Leipzig: Otto Spamer (Chemische Technologie in Einzeldarstellungen).

FPS Finance - General Administration of Patrimonial Documentation (GAPD) (2023): Administrative units - situation on January 1st. With collaboration of Florian Van Aubel. Schaarbeek, Belgium. Online available at https://www.geo.be/catalog/details/629ad470-71dc-11eb-af47-3448ed25ad7c?l=en [last access on 25.01.2024]

Franzius, L.; Frühling, A.; Schlichting, J.; Sonne, E. (Ed.) (1893): Handbuch der Ingenieurwissenschaften. Dritter Band: Der Wasserbau. Wasserversorgung und Entwässerung der Städte. Unter Mitarbeit von F. Lincke, 3., verm. Aufl. Leipzig: Engelmann.

Freudenberg (1873): Die Canalisation der Stadt Witten. In: *Zeitschrift für Bauwesen* 23 (3-5), P. 136–152. Online available at https://digital.zlb.de/viewer/image/15239363_1873/74/ [last access on 26.04.2024]

Frings (1889): Die Kanalisation von Düsseldorf. In: *Gesundheits-Ingenieur: Zeitschrift für die gesamte Städtehygiene* 12 (1), P. 11–18. Online available at https://play.google.com/store/books/details?id=AprmAAAAMAAJ&rdid=book-AprmAAAAMAAJ&rdot=1 [last access on 13.05.2024]

Frühwirth, A. (1896): Die Breslauer Rieselfelder. In: *Zeitschrift des österreichischen Ingenieur- und Architekten-Vereins* 48 (37), P. 521–525. Online available at https://opus4.kobv.de/opus4-btu/files/1784/H._36_39.pdf [last access on 30.04.2024]

Fuchs, S.; Scherer, U.; Wander, R.; Behrendt, H.; Venohr, M.; Opitz, D. et al. (2010): Calculation of Emissions into Rivers in Germany using the MONERIS Model. Nutrients, heavy metals and polycyclic aromatic hydrocarbons. 1. Aufl. 1 Band. Dessau-Roßlau: Federal Environment Agency (Umweltbundesamt) (TEXTE, 46/2010). Online available at http://www.umweltbundesamt.de/sites/default/files/medien/461/publikationen/4018.pdf [last access on 07.11.2023]

Fuchs, S.; Weber, T.; Wander, R.; Toshovski, S.; Kittlaus, S.; Reid, L. et al. (2017a): Effizienz von Maßnahmen zur Reduktion von Stoffeinträgen. Endbericht. 1. Aufl. 1 Band. Dessau-Roßlau: Umweltbundesamt (TEXTE, 05/2017). Online available at https://www.umweltbundesamt.de/sites/default/files/medien/1968/publikationen/2017-01-17_texte_05-2017_masnahme_neffizienz-stoffeintrage_komp.pdf [last access on 07.11.2023]

Fuchs, S.; Kaiser, M.; Kiemle, L.; Kittlaus, S.; Rothvoß, S.; Toshovski, S. et al. (2017b): Modeling of Regionalized Emissions (MoRE) into Water Bodies. An Open-Source River Basin Management System. In: *Water* 9 (4), P. 239. Online available at https://doi.org/10.3390/w9040239 [last access on 16.07.2018]

Fuchs, S.; Rothvoß, S.; Toshovski, S. (2018): Ubiquitäre Schadstoffe – Eintragsinventare, Umweltverhalten und Eintragsmodellierung. Abschlussbericht (Forschungskennzahl 3714 21 200 0), 2018 (52/2018). Online available at https://www.umweltbundesamt.de/publikationen/ubiquitaere-schadstoffe-eintragsinventare [last access on 21.10.2025]

Fuchs, S.; Hilgert, S.; Sotiri, K.; Wagner, A.; Ishikawa, M.; Kern, J. et al. (2019): Sustainable management of reservoirs - defining minimum data needs and model complexity. In: Proceedings of the GRoW Midterm Conference – Global analyses and local solutions for sustainable water resources management. GRoW - Water as a Global Resource. Frankfurt/Main, 20.02.2019 – 21.02.2019: adelphi. Online available at https://publikationen.bibliothek.kit.edu/1000105514 [last access on 05.12.2024]

Fuchs, S.; Brecht, K.; Gebel, M.; Bürger, S.; Uhlig, M.; Halbfaß, S. (2022): Phosphoreinträge in die Gewässer bundesweit modellieren. Neue Ansätze und aktualisierte Ergebnisse von MoRE-DE. Dessau-Roßlau, 2022 (142/2022). Online available at https://www.umweltbundesamt.de/publikationen/phosphoreintraege-in-die-gewaesser-bundesweit [last access on 14.12.2022]

Gadegast, M.; Hirt, U.; Opitz, D.; Venohr, M. (2012): Modelling changes in nitrogen emissions into the Oder River System 1875-1944. In: *Regional Environmental Change* 12 (3), P. 571–580. Online available at https://doi.org/10.1007/s10113-011-0270-5 [last access on 10.01.2019]

Gadegast, M.; Hirt, U.; Venohr, M. (2014): Changes in Waste Water Disposal for Central European River Catchments and Its Nutrient Impacts on Surface Waters for the Period 1878–1939. In: *Water Air Soil Pollut* 225 (4), P. 1914. Online available at https://doi.org/10.1007/s11270-014-1914-0 [last access on 28.09.2023]

Gadegast, M.; Venohr, M. (2015): Modellierung historischer Nährstoffeinträge und -frachten zur Ableitung von Nährstoffreferenz- und Orientierungswerten für mitteleuropäische Flussgebiete. Erstellt im Auftrag des

Niedersächischen Landesbetriebs für Wasserwirtschaft, Küsten- und Naturschutz. Berlin, 2015. Online available at https://www.nlwkn.niedersachsen.de/download/98787 [last access on 24.07.2023]

Garcier, R. J. (2007): Rivers we can't bring ourselves to clean – historical insights into the pollution of the Moselle River (France), 1850–2000. In: Hydrol. Earth Syst. Sci. 11 (6), P. 1731–1745. Online available at https://doi.org/10.5194/hess-11-1731-2007 [last access on 02.05.2024]

Gericke, A.; Morling, K.; Haag, I.; Gebel, M.; Krumm, J.; Bruns, G. et al. (2025): Are historical conditions reference conditions? Revising the modeled riverine nutrient input into the German North Sea and Baltic Sea around 1880. In: *Environ Sci Eur* 37 (133). Online available at https://doi.org/10.1186/s12302-025-01185-8 [last access on 01.08.2025]

Ghiggi, G.; Humphrey, V.; Seneviratne, S. I.; Gudmundsson, L. (2021): G-RUN ENSEMBLE: A Multi-Forcing Observation-Based Global Runoff Reanalysis. In: *Water Resources Research* 57 (5), P. 129. Online available at https://doi.org/10.1029/2020WR028787 [last access on 06.11.2024]

Glasauer, H.; Arndt, K. (1995): Die Entwicklung der Trinkwasserversorgung - dargestellt am Beispiel der Stadt Frankfurt am Main. Kassel: Projekt WasserKultur, Koordinationsstelle, Arbeitsgruppe Empirische Planungsforschung (WasserKultur-Texte, 3). Online available at https://kobra.uni-kassel.de/bitstream/handle/123456789/2008051921590/wakutexte3.pdf?sequence=1 [last access on 13.05.2024]

Główny Urząd Geodezji i Kartografii (2024): Państwowy Rejestr Granic (PRG). Administrative Boundaries. Online available at https://www.geoportal.gov.pl/pl/dane/panstwowy-rejestr-granic-prg/ [last access on 23.01.2024]

Gordon, J.: Canalisation der Stadt Heilbronn. Bericht. Heilbronn: Schell'sche Buchdruckerei. Online available at https://play.google.com/store/books/details?id=1lza3HZavD4C&rdid=book-1lza3HZavD4C&rdot=1 [last access on 15.05.2024]

Gordon, J. (1874): Erläuterungsbericht zu dem Dispositions-Plan über die Anlage von Spülkanälen in der Kgl. Haupt- und Residenzstadt Stuttgart incl. Heslach und Berg. Stuttgart: Kohlhammer. Online available at https://play.google.com/store/books/details?id=Oi9CAQAAIAAJ&rdid=book-Oi9CAQAAIAAJ&rdot=1 [last access on 29.04.2024]

Grohmann, O. (2005): Stadtentwässerung Hannover. Die Geschichte. Hannover: Stadtentwässerung Hannover. ISBN 3-938769-01-7.

Gustafsson, B. G.; Schenk, F.; Blenckner, T.; Eilola, K.; Meier, H. E. M.; Müller-Karulis, B. et al. (2012): Reconstructing the development of Baltic sea eutrophication 1850-2006. In: *Ambio* 41 (6), P. 534–548. Online available at https://doi.org/10.1007/s13280-012-0318-x [last access on 02.05.2024]

Haag, I.; Luce, A. (2008): The integrated water balance and water temperature model LARSIM-WT. In: *Hydrol. Process.* 22 (7), P. 1046–1056. Online available at https://doi.org/10.1002/hyp.6983 [last access on 05.12.2024]

Haag, I.; Luce, A.; Henn, N.; Demuth, N. (2016): Berücksichtigung räumlich differenzierter Abflussprozesskarten im Wasserhaushaltsmodell LARSIM. In: *Forum für Hydrologie und Wasserbewirtschaftung* (36.16), P. 51–62. Online available at https://hdl.handle.net/20.500.11970/113232 [last access on 27.02.2025]

Haag, I.; Aigner, D.; Raffeiner, G. (2019): Ein robustes Gletschermodul für die Hochwasservorhersage in hochalpinen Gebieten: Entwicklung, Parametrisierung und Validierung auf der Basis unterschiedlicher verfügbarer Daten. In: *Forum für Hydrologie und Wasserbewirtschaftung*, P. 99–104. Online available at https://hdl.handle.net/20.500.11970/113340 [last access on 27.02.2025]

Haag, I.; Krumm, J.; Aigner, D.; Steinbrich, A.; Weiler, M. (2022): Simulation von Hochwasserereignissen in Folge lokaler Starkregen mit dem Wasserhaushaltsmodell LARSIM. In: *Hydrologie und Wasserbewirtschaftung: HyWa* 66 (1), P. 6–27. Online available at https://doi.bafg.de/HyWa/2022/HyWa_2022.1_1.pdf [last access on 05.12.2024]

Haag, I.; Teltscher, K.; Aigner, D. (2023): 2-Grad-Ziel für unsere Bäche - Wassertemperatur und Beschattung. KLIWA-Kurzbericht, 2023. Online available at https://www.kliwa.de/_download/KLIWA_Kurzbericht_Wassertemperatur_und_Beschattung.pdf [last access on 05.12.2024]

Häußermann, U.; Bach, M.; Klement, L.; Knoll, L.; Breuer, L.; Strassemeyer, J. et al. (2023): Auswirkungen des Anbaus nachwachsender Rohstoffe und der Verwendung von Gärresten auf die Oberflächen- und Grundwasserbeschaffenheit in Deutschland. Abschlussbericht. Dessau-Roßlau, 2023 (163/2023). Online available at https://www.umweltbundesamt.de/publikationen/auswirkungen-des-anbaus-nachwachsender-rohstoffe [last access on 06.03.2024]

Hegglin, M.; Kinnison, D.; Lamarque, J-F. (2016). CCMI nitrogen surface fluxes in support of CMIP6 - version 2.0. https://doi.org/10.22033/ESGF/input4MIPs.1125 [last access on 22.08.2023]

He, X.; Augusto, L.; Goll, D. S.; Ringeval, B.; Wang, Y.; Helfenstein, J. et al. (2021): Global patterns and drivers of soil total phosphorus concentration. In: *Earth Syst. Sci. Data* 13 (12), P. 5831–5846. Online available at https://doi.org/10.5194/essd-13-5831-2021 [last access on 02.08.2024]

Hirt, U.; Mahnkopf, J.; Gadegast, M.; Czudowski, L.; Mischke, U.; Heidecke, C. et al. (2014): Reference conditions for rivers of the German Baltic Sea catchment: reconstructing nutrient regimes using the model MONERIS. In: *Regional Environmental Change* 14 (3), P. 1123–1138. Online available at https://doi.org/10.1007/s10113-013-0559-7 [last access on 04.08.2023]

Hobrecht, J. (1868): Kanalisation der Stadt Stettin. Stettin: von der Nahmer. Online available at https://kpbc.umk.pl/dlibra/publication/212793/edition/225201?language=en [last access on 29.04.2024]

Hötte, H. (Ed.) (1992): Wasser für Hamburg. Zur Geschichte der Hamburger Wasserversorgung und -entsorgung; Katalogbuch einer Ausstellung; [eine Ausstellung des Museumspädagogischen Dienstes der Kulturbehörde Hamburg in Zusammenarbeit mit den Hamburger Wasserwerken und der Umweltbehörde - Amt für Stadtentwässerung; Wasserturm/Planetarium im Stadtpark, 14. September - 29. November 1992]. Hamburg; Planetarium - Stadtpark - Wasserturm. Hamburg: Dölling & Galitz.

Hügel, L. F. (1886): Kanalisation und Abfuhr in Würzburg. Inaugural-Dissertation. Würzburg, Univ., Diss., 1886. Würzburg: Stahel. Online available at https://play.google.com/store/books/details?id=1XcNf0-1vUwC&rdid=book-1XcNf0-1vUwC&rdot=1&pli=1 [last access on 26.04.2024]

Hu, T.; Taghizadeh-Toosi, A.; Olesen, J. E.; Jensen, M. L.; Sørensen, P.; Christensen, B. T. (2019): Converting temperate long-term arable land into semi-natural grassland: decadal-scale changes in topsoil C, N, 13 C and 15 N contents. In: *Eur J Soil Sci* 70 (2), P. 350–360. Online available at https://doi.org/10.1111/ejss.12738 [last access on 01.08.2024]

International Comission for the Protection of the Rhine (ICPR) (2010): Internationally Coordinated Management Plan for the International River Basin District of the Rhine. Koblenz, 2010. Online available at https://www.iksr.org/fileadmin/user_upload/Dokumente_en/Inventory_Parts/bwp_endversion-en_komplett.pdf [last access on 06.02.2025]

ISIMIP (2022): The Inter-Sectoral Impact Model Intercomparison Project. Online available at https://www.isimip.org/ [last access on 06.11.2024]

Jankiewicz, P.; Neumann, J.; Duijnisveld, W. H.M.; Wessolek, G.; Wycisk, P.; Hennings, V. (2005): Abflusshöhe - Sickerwasserrate - Grundwasserneubildung - Drei Themen im Hydrologischen Atlas von Deutschland. In: *Hydrologie und Wasserbewirtschaftung: HyWa* 49 (1), P. 2–13. Online available at https://www.hywa-online.de/?p=2389 [last access on 04.07.2019]

Jensen, P. N. (Ed.) (2017): Estimation of nitrogen concentrations from root zone to marine areas around the year 1900. Aarhus University, DCE – Danish Centre for Environment and Energy (Scientific Report from DCE –

Danish Centre for Environment and Energy, 241). Online available at https://dce2.au.dk/pub/sr241.pdf [last access on 01.08.2024]

Kaiserliches Statistisches Amt (1884): Statistisches Jahrbuch für das Deutsche Reich. Berlin: Puttkammer & Mühlbrecht. Online available at https://www.digizeitschriften.de/id/514401303_1883|log1 [last access on 01.12.2023]

Klein Goldewijk, K.; Beusen, A.; van Drecht, G.; Vos, M. de (2011): The HYDE 3.1 spatially explicit database of human-induced global land-use change over the past 12,000 years. In: *Global Ecology and Biogeography* 20 (1), P. 73–86. Online available at https://doi.org/10.1111/j.1466-8238.2010.00587.x [last access on 04.08.2023]

Klein Goldewijk, K.; Beusen, A.; Doelman, J.; Stehfest, E. (2017): Anthropogenic land use estimates for the Holocene - HYDE 3.2. In: *Earth System Science Data* 9 (2), P. 927–953. Online available at https://doi.org/10.5194/essd-9-927-2017 [last access on 02.08.2023]

Knoll, L.; Breuer, L.; Bach, M. (2020): Nation-wide estimation of groundwater redox conditions and nitrate concentrations through machine learning. In: *Environmental Research Letters* 15 (6), P. 64004. Online available at https://doi.org/10.1088%2F1748-9326%2Fab7d5c [last access on 08.06.2020]

König, J. (1887): Die Verunreinigung der Gewässer, deren schädliche Folgen, nebst Mitteln zur Reinigung der Schmutzwässer. Berlin: Julius Springer. Online available at https://digital.zbmed.de/gesundheitspflege/content/titleinfo/6439020 [last access on 01.12.2023]

König, J. (1899): Die Verunreinigung der Gewässer, deren schädliche Folgen sowie die Reinigung von Trink- und Schmutzwasser. 2., vollst. umgearb. und verm. Aufl. Berlin: Springer.

Kopáček, J.; Hejzlar, J.; Posch, M. (2013): Factors Controlling the Export of Nitrogen from Agricultural Land in a Large Central European Catchment during 1900–2010. In: *Environ. Sci. Technol*. 47 (12), P. 6400–6407. Online available at https://doi.org/10.1021/es400181m [last access on 15.12.2023]

Kopsidis, M. (2022): Landwirtschaft. In: Thomas Rahlf (Ed.): Deutschland in Daten. Zeitreihen zur Historischen Statistik. 2. Aufl. Bonn: Bundeszentrale für politische Bildung/bpb. Online available at http://www.deutschland-in-daten.de/landwirtschaft/ [last access on 22.03.2024]

Korn, O. (1898): Die Rieselfelder der Stadt Freiburg i. B. Chemische und bacteriologische Untersuchungen der Kanalflüssigkeit und der Drainwässer. In: *Archiv für Hygiene* (32), P. 173–218. Online available at https://digital.zbmed.de/gesundheitspflege/periodical/structure/5975564 [last access on 29.02.2024]

Kosztra, B., Büttner, G., Hazeu, G., & Arnold, S. (2017). Updated CLC illustrated nomenclature guidelines. European Environment Agency: Vienna, Austria, 1-124. Online available at https://land.copernicus.eu/content/corine-land-cover-nomenclature-guidelines/docs/pdf/CLC2018_Nomenclature_illustrated_guide_20190510.pdf [last access on 21.10.2025]

Krieger, J. (Ed.) (1885): Topographie der Stadt Strassburg nach ärztlich-hygienischen Gesichtspunkten bearbeitet. Festschrift für die diesjährige, in Strassburg tagende Versammlung deutscher Naturforscher und Aerzte. Strassburg: C. F. Schmidt's Univ. Buchhdlg (Archiv für öffentliche Gesundheits-Pflege in Elsass-Lothringen, 10). Online available at https://play.google.com/books/reader?id=02smurh8FHQC&pg=GBS.PR2&hl=de [last access on 30.04.2024]

Krumm, J.; Haag, I.; Teltscher, K.; Hänsler, A.; Schmit, M.; Steinbrich, A.; Weiler, M. (in press): Der Sturzflutindex (SFI) und seine Anwendung auf rezente Überflutungsereignisse in vier Bundesländern. In: *Hydrologie und Wasserbewirtschaftung*.

Lacko, J. (2023): RCzechia: Spatial Objects of the Czech Republic. In: *JOSS* 8 (83), S. 5082. Online available at https://doi.org/10.21105/joss.05082 [last access on 24.01.2024]

Ladd, B. (1990): Urban planning and civic order in Germany. 1860 - 1914. Cambridge, Mass.: Harvard Univ. Press (Harvard historical studies). ISBN 0-674-93115-7.

Landeshauptstadt München (2024): Stadtentwässerung in München. Online available at https://stadt.muenchen.de/infos/abwasserentsorgung-muenchen.html [last access on 12.06.2024]

Lange, J. (2002): Zur Geschichte des Gewässerschutzes am Ober- und Hochrhein. Eine Fallstudie zur Umwelt- und Biologiegeschichte. Dissertation. Albert-Ludwigs-Universität Freiburg. Online available at https://freidok.uni-freiburg.de/fedora/objects/freidok:635/datastreams/FILE1/content [last access on 25.08.2023]

LARSIM Entwicklergemeinschaft (LEG) (2024): Das Wasserhaushaltsmodell LARSIM – Modellgrundlagen und Anwendungsbeispiele, 2024. Online available at https://larsim.info/dokumentation/LARSIM-Dokumentation.pdf [last access on 24.10.2024]

Lubberger (1889): Kläranlagen und Rieselfelder. Ein Beitrag zur Untersuchung der Leistungen und der Kosten beider Systeme. In: *Gesundheits-Ingenieur: Zeitschrift für die gesamte Städtehygiene* (16), S. 521–534. Online available at https://play.google.com/store/books/details?id=AprmAAAAMAAJ&rdid=book-AprmAAAAMAAJ&rdot=1 [last access on 13.05.2025]

Luce, A.; Haag, I.; Bremicker, M. (2006): Einsatz von Wasserhaushaltsmodellen zur kontinuierlichen Abflussvorhersage in Baden-Württemberg. In: *Hydrologie und Wasserbewirtschaftung* (50/2), P. 58–66. Online available at https://www.hywa-online.de/?p=2244 [last access on 21.10.2025]

Lundstad, E.; Brugnara, Y.; Pappert, D.; Kopp, J.; Samakinwa, E.; Hürzeler, A. et al. (2023): The global historical climate database HCLIM. In: *Scientific data* 10 (1), P. 44. Online available at https://doi.org/10.1038/s41597-022-01919-w [last access on 05.12.2024]

Mahowald, N.; Jickells, T. D.; Baker, A. R.; Artaxo, P.; Benitez-Nelson, C. R.; Bergametti, G. et al. (2008): Global distribution of atmospheric phosphorus sources, concentrations and deposition rates, and anthropogenic impacts. In: *Global Biogeochem. Cycles* 22 (4), GB4026. Online available at https://doi.org/10.1029/2008GB003240 [last access on 27.05.2013]

Medinski, T.; Freese, D.; Reitz, T. (2018): Changes in soil phosphorus balance and phosphorus-use efficiency under long-term fertilization conducted on agriculturally used Chernozem in Germany. In: *Can. J. Soil. Sci.* 98 (4), P. 650–662. Online available at https://doi.org/10.1139/cjss-2018-0061 [last access on 23.07.2024]

Meißner, D.; Klein, B.; Ionita, M. (2017): Development of a monthly to seasonal forecast framework tailored to inland waterway transport in central Europe. In: *Hydrol. Earth Syst. Sci.* 21 (12), P. 6401–6423. Online available at https://doi.org/10.5194/hess-21-6401-2017 [last access on 05.12.2024]

Mittermaier, K. (1870): Die Reinigung und Entwässerung der Stadt Heidelberg nebst einem Anhang über die Wasserversorgung der Stadt. Denkschrift der … ärztl. Commission. Heidelberg: Bassermann. Online available at https://play.google.com/store/books/details?id=7CsQc32fFVUC&rdid=book-7CsQc32fFVUC&rdot=1 [last access on 15.05.2024]

Mohajeri, S. (2005): 100 Jahre Berliner Wasserversorgung und Abwasserentsorgung 1840 - 1940. Zugl.: Berlin, Techn. Univ., Diss., 2002. Steiner, Stuttgart. ISBN 3-515-08541-6.

Moore, I. D.; Nieber, J. L. (1989): Landscape assessment of soil erosion and nonpoint source pollution. In: *J. Minnesota Acad. Sci.* (55), P. 18–25. Online available at https://digitalcommons.morris.umn.edu/jmas/vol55/iss1/4 [last access on 14.05.2025]

Morling, K.; Fuchs, S. (2021): Modelling copper emissions from antifouling paints applied on leisure boats into German water bodies. In: *Environmental Pollution* 289, P. 117961. Online available at https://doi.org/10.1016/j.envpol.2021.117961 [last access on 18.08.2021]

Morling, K.; Fuchs, S.; Krumm, J.; Haag, I. (2024): Zusammenführung der bundesweiten Modellierung von Wasserhaushalt (LARSIM-ME) und Stoffeinträgen (MoRE). Dessau-Roßlau, 2024 (37/2024). Online available at https://www.umweltbundesamt.de/publikationen/zusammenfuehrung-der-bundesweiten-modellierung-von [last access on 06.03.2024]

Muhammed, S. E.; Coleman, K.; Wu, L.; Bell, V. A.; Davies, J. A. C.; Quinton, J. N. et al. (2018): Impact of two centuries of intensive agriculture on soil carbon, nitrogen and phosphorus cycling in the UK. In: *The Science of the total environment* 634, P. 1486–1504. Online available at https://doi.org/10.1016/j.scitotenv.2018.03.378 [last access on 14.05.2025]

Naden, P.; Bell, V.; Carnell, E.; Tomlinson, S.; Dragosits, U.; Chaplow, J. et al. (2016): Nutrient fluxes from domestic wastewater: A national-scale historical perspective for the UK 1800–2010. In: *Science of The Total Environment* 572, P. 1471–1484. Online available at https://doi.org/10.1016/j.scitotenv.2016.02.037 [last access on 15.12.2023]

National Aeronautics and Space Administration (NASA) (2005): Shuttle Radar Topography Mission (SRTM) Digital Elevation Model. Online available at http://www2.jpl.nasa.gov/srtm/index.html [last access on 30.07.2014]

North, M. (Ed.) (2000): Deutsche Wirtschaftsgeschichte. Ein Jahrtausend im Überblick. Unter Mitarbeit von Gerold Ambrosius. München: Beck. ISBN 3406460933.

Paprotny, D.; Mengel, M. (2023): Population, land use and economic exposure estimates for Europe at 100 m resolution from 1870 to 2020. In: *Scientific data* 10 (1), P. 372. Online available at https://doi.org/10.1038/s41597-023-02282-0 [last access on 24.07.2023]

Plate, U. (1998): Der Landgraben in Karlsruhe. In: *Denkmalpflege in Baden-Württemberg – Nachrichtenblatt der Landesdenkmalpflege* 27 (4). Online available at https://journals.ub.uni-heidelberg.de/index.php/nbdpfbw/article/view/13230 [last access on 15.04.2024]

Prasuhn, V.; Spiess, E.; Braun, M. (1996): Methoden zur Abschätzung der Phosphor- und Stickstoffeinträge aus diffusen Quellen in den Bodensee. Reichenau (Bericht / Internationale Gewässerschutzkommission für den Bodensee, 45). Online available at https://www.igkb.org/fileadmin/user_upload/Downloads/Publikationen/Blaue_Berichte/blauer_bericht_45.pdf [last access on 14.05.2025]

Preiksch, C. (2021): Hamburgs Weg zu einer modernen Großstadt. Künstlerischer Akt oder Notwendigkeit? Online available at https://www.shmh.de/journal-hamburgs-weg-zu-einer-modernen-grossstadt/ [last access on 12.06.2024]

Rahlf, T. (Ed.) (2022): Deutschland in Daten. Zeitreihen zur Historischen Statistik. 2. Aufl. Bonn: Bundeszentrale für politische Bildung/bpb. Online available at http://www.deutschland-in-daten.de/ [last access on 22.03.2024]

Ringeval, B.; Demay, J.; Goll, D. S.; He, X.; Wang, Y.-P.; Hou, E. et al. (2024): A global dataset on phosphorus in agricultural soils. In: *Scientific data* 11 (1), P. 17. Online available at https://doi.org/10.1038/s41597-023-02751-6 [last access on 18.07.2024]

Röder, N.; Ackermann, A.; Baum, S.; Böhner, H. G. S.; Laggner, B.; Lakner, S. et al. (2022): Evaluierung der GAP-Reform von 2013 aus Sicht des Umweltschutzes anhand einer Datenbankanalyse von InVeKoS-Daten der Bundesländer. Abschlussbericht. Abschlussdatum: April 2022. Dessau-Roßlau, 2022 (75/2022). Online available at https://www.umweltbundesamt.de/publikationen/evaluierung-der-gap-reform-von-2013-aus-sicht-des [last access on 06.03.2024]

Rothamsted Research (2016): Broadbalk changes in Olsen P in top soil, 1843-2010. In collaboration with Sarah Perryman, Margaret Glendining, Andrew Macdonald, Paul Poulton, Daniel Hampshire, Sadia Beg et al., 2016. Online available at https://www.era.rothamsted.ac.uk/dataset/rbk1/01-OAOlsenP1844 [last access on 09.08.2024]

Rothamsted Research (2018): Broadbalk Soil Total % Nitrogen Content, 1843-2010. In collaboration with Sarah Perryman, Margaret Glendining, Andrew Macdonald, Paul Poulton, Ruth Skilton and Nathalie Castells, 2018. Online available at https://www.era.rothamsted.ac.uk/dataset/rbk1/01-Nitro1843 [last access on 09.08.2024]

Rothamsted Research (2021): Broadbalk soil organic carbon content 1843-2015. In collaboration with Sarah Perryman, Margaret Glendining, Andrew Macdonald, Paul Poulton, Richard Ostler, Ruth Skilton et al., 2021. Online available at https://www.era.rothamsted.ac.uk/dataset/rbk1/02-BKSOC1843 [last access on 09.08.2024]

Ruoho-Airola, T.; Eilola, K.; Savchuk, O. P.; Parviainen, M.; Tarvainen, V. (2012): Atmospheric Nutrient Input to the Baltic Sea from 1850 to 2006: A Reconstruction from Modeling Results and Historical Data. In: *Ambio* 41 (6), P. 549–557. Online available at https://doi.org/10.1007/s13280-012-0319-9 [last access on 30.09.2024]

Salomon, H. (1906): Die städtische Abwässerbeseitigung in Deutschland. Wörterbuchartig angeordnete Nachrichten und Beschreibungen städtischer Kanalisations- und Kläranlagen in deutschen Wohnplätzen. Jena: Fischer (1). Online available at https://archive.org/details/diestdtischeabw00salogoog/mode/2up [last access on 23.10.2023]

Salomon, H. (1907): Die städtische Abwässerbeseitigung in Deutschland. Wörterbuchartig angeordnete Nachrichten und Beschreibungen städtischer Kanalisations- und Kläranlagen in deutschen Wohnplätzen. (Abwässerlexikon.): G. Fischer (2). Online available at https://archive.org/details/bub_gb_FbB9AAAAIAAJ/mode/2up [last access on 23.10.2023]

Schernewski, G.; Friedland, R.; Carstens, M.; Hirt, U.; Leujak, W.; Nausch, G. et al. (2015): Implementation of European marine policy: New water quality targets for German Baltic waters. In: *Marine Policy* 51, P. 305–321. Online available at https://doi.org/10.1016/j.marpol.2014.09.002 [last access on 02.05.2024]

Schott, S. (1912): Großstädtische Agglomerationen des Deutschen Reichs, 1871-1910: GESIS Datenarchiv, Köln. ZA8674 Datenfile Version 1.0.0. Online available at https://doi.org/10.4232/1.12929 [last access on 22.01.2024]

Slivinski, L.; Compo, G.; Whitaker, J.; Sardeshmukh, P.; Giese, B.; McColl, C. et al. (2019): NOAA-CIRES-DOE Twentieth Century Reanalysis Version 3. Unter Mitarbeit von University Corporation For Atmospheric Research (UCAR): National Center for Atmospheric Research (NCAR): Computational and Information Systems Laboratory (CISL): Information Services Division (ISD): Data Engineering and Curation Section (DECS), 2019. Online available at https://doi.org/10.5065/H93G-WS83 [last access on 05.12.2024]

Slivinski, L. C.; Compo, G. P.; Sardeshmukh, P. D.; Whitaker, J. S.; McColl, C.; Allan, R. J. et al. (2021): An Evaluation of the Performance of the Twentieth Century Reanalysis Version 3. In: *Journal of Climate* 34 (4), P. 1417–1438. Online available at https://doi.org/10.1175/JCLI-D-20-0505.1 [last access on 05.12.2024]

ISO 11263, 1994: Soil quality - Determination of phosphorus - Spectrometric determination of phosphorus soluble in sodium hydrogen carbonate solution.

Soyka, I. (1885): Untersuchungen zur Kanalisation. Unter Mitarbeit von Max von Pettenkofer. München, Leipzig: R. Oldenbourg. Online available at https://books.google.de/books?id=ZkosEAAAQBAJ&pg=PA23&lpg=PA23&dq=1880+kanalisation+wie+viele+einwohner&source=bl&ots=SBGk_frHT1&sig=ACfU3U1_kxz4UCcIkE4NTzN7TKQtc1513Q&hl=de&sa=X&ved=2ahUKEwiO4sub-MuFAxWk_7sIHYtHBXoQ6AF6BAguEAM#v=onepage&q=1880%20kanalisation%20wie%20viele%20einwohner&f=false [last access on 18.04.2024]

Stadtentwässerung Frankfurt am Main (SEF) (2024): Historie vor 1900. Online available at https://www.stadtentwaesserung-frankfurt.de/anlagen/historie/geschichte-der-alten-klaerbeckenanlage-vor-1900.html [last access on 12.04.2024]

Statistik Austria (2024): Gliederung Österreichs in Gemeinden. Vienna. Online available at https://www.data.gv.at/katalog/dataset/stat_gliederung-osterreichs-in-gemeinden14f53#resources [last access on 22.01.2024]

Statistisches Amt der Stadt Breslau (Ed.) (1889/91): Breslauer Statistik. im Auftr. d. Magistrats d. Königl. Haupt- und Residenzstadt Breslau. Stadt Breslau. Breslau: Morgenstern (13). Online available at https://www.difmoe.eu/periodical/uuid:129aa9cb-798d-470b-b3b6-006e3c95af84 [last access on 19.04.2024]

Stegert, C.; Lenhart, H.-J.; Blauw, A.; Friedland, R.; Leujak, W.; Kerimoglu, O. (2021): Evaluating Uncertainties in Reconstructing the Pre-eutrophic State of the North Sea. In: *Front. Mar. Sci.* 8, P. 3. Online available at https://doi.org/10.3389/fmars.2021.637483 [last access on 06.11.2024]

Stumpe, H. (1967): Die Wirkung verschieden gelagerter Stallmiste auf Pflanzenertrag und Bodeneigenschaften: 2. Mitteilung: Veränderung einiger wichtiger Bodeneigenschaften. In: *Archives of Agronomy and Soil Science* 11 (10), P. 963–982. Online available at https://doi.org/10.1080/03650346709413511 [last access on 30.10.2024]

Stumpe, H.; Garz, J.; Scharf, H. (1994): Wirkung der Phosphatdüngung in einem 40jährigen Dauerversuch auf einer Sandlöß-Braunschwarzerde in Halle. In: *J Plant Nutrition & Soil* 157 (2), P. 105–110. Online available at https://doi.org/10.1002/jpln.19941570208 [last access on 23.07.2024]

Topcu, D.; Behrendt, H.; Brockmann, U.; Claussen, U. (2011): Natural background concentrations of nutrients in the German Bight area (North Sea). In: *Environmental monitoring and assessment* (174), P. 361–388. Online available at https://doi.org/10.1007/s10661-010-1463-y [last access on 09.12.2024]

Umweltbundesamt (UBA) (Ed.) (1994): Stoffliche Belastung der Gewässer durch die Landwirtschaft und Maßnahmen zu ihrer Verringerung. Unter Mitarbeit von Almut Jering. Deutschland. Berlin: E. Schmidt (Berichte / Umweltbundesamt, 94,2). ISBN 3-503-03604-0.

Umweltbundesamt (UBA) (2024): Pollutant emissions into surface waters. Online available at https://www.umweltbundesamt.de/en/topics/water/rivers/pollutant-emissions-into-surface-waters [last access on 19.05.2025]

Venohr, M. (2006): Modellierung der Einflüsse von Temperatur, Abfluss und Hydromorphologie auf Stickstoffretention in Flusssystemen. Dissertation. Humboldt-Universität, Berlin. Mathematisch-Naturwissenschaftliche Fakultät II.

Venohr, M.; Hirt, U.; Hofmann, J.; Opitz, D.; Gericke, A.; Wetzig, A. et al. (2011): Modelling of Nutrient Emissions in River Systems - MONERIS - Methods and Background. In: *International Review of Hydrobiology* 96 (5), P. 435–483. Online available at https://doi.org/10.1002/iroh.201111331 [last access on 14.05.2025]

Weyl, T. (1893): Studien zur Strassenhygiene. Mit besonderer Berücksichtigung der Müllverbrennung: Reisebericht. Jena: Fischer. Online available at https://digital.zbmed.de/urn/urn:nbn:de:hbz:38m:1-70213 [last access on 02.05.2024]

Weyl, T. (Ed.) (1894): Die Städtereinigung. Einleitung, Abfuhrsysteme, Kanalisation. Unter Mitarbeit von Rudolf Blasius und F. W. Büsing. Jena: Verlag von Gustav Fischer (Handbuch der Hygiene, 2. Band, 1. Abteilung). Online available at https://leopard.tu-braunschweig.de/servlets/MCRFileNodeServlet/dbbs_derivate_00018104/X.C.267_II_1_1_.pdf [last access on 25.04.2024]

Wurbs, D.; Steininger, M. (2011): Wirkungen der Klimaänderungen auf die Böden. Untersuchungen zu den Auswirkungen des Klimawandels auf die Bodenerosion durch Wasser. Dessau-Roßlau (TEXTE, 16/2011). Online available at https://www.umweltbundesamt.de/publikationen/wirkungen-klimaaenderungen-auf-boeden [last access on 11.10.2023]

Zhang, J.; Beusen, A. H. W.; van Apeldoorn, D. F.; Mogollón, J. M.; Yu, C.; Bouwman, A. F. (2017): Spatiotemporal dynamics of soil phosphorus and crop uptake in global cropland during the 20th century. In: *Biogeosciences* 14 (8), P. 2055–2068. Online available at https://doi.org/10.5194/bg-14-2055-2017 [last access on 18.07.2024]

A Details on data sources for the 1880 scenario

A.1 Overview of general and substance-specific input data

Table 24: General input data and their references for modelling 1880.

Input data	Present Germany	Foreign territory
Land use	HANZE 2.0 (Paprotny & Mengel 2023) (chapter 3.1)	
Imperviousness of sealed surfaces	HANZE 2.0 (Paprotny & Mengel 2023) (chapter 3.2)	
Soil loss and sediment inputs	Adaptation of USLE factors based on Fuchs et al. (2022) (chapter 5.2)	ESDAC dataset on historical reconstruction of soil erosion (Fendrich et al. 2022) (chapter 5.2)
Digital elevation model[a]	DGM10 (BKG 2019) (chapter 5.2.1.5)	SRTM DEM (NASA 2005) (chapter 5.2.1.5)
Fine content (clay and silt) in topsoil[a]	Soil Map of Germany BUEK200 (BGR 2020) (chapter 5.2.2)	LUCAS database (Ballabio et al. 2016) (chapter 5.2.2)
Proportion of drained agricultural land	Adapted from current input data based on the approach of Gadegast & Venohr (2015) (chapter 5.5.1)	
Population	HANZE 2.0 (Paprotny & Mengel 2023) (chapter 3.3)	
Water consumption of inhabitants	55 L/(inh·d) for rural areas, 97 L/(inh·d) for urban areas based on Franzius et al. (1893) (chapter 4.2)	
Inhabitants connected to sewers	Based on population density using HANZE 2.0 (Paprotny & Mengel 2023) (chapter 5.3.1)	
Meteorological parameters for hydrological modelling	Input data for hydrological modelling with LARSIM-ME were derived using climate change vectors (ccv) and 20CRv3 re-analysis data (Slivinski et al. 2019) (chapter 4)	

[a] – Input data identical to current MoRE settings

Table 25: Substance-specific input data for modelling conditions in 1880.

Input data	Present Germany	Foreign territory
Atmospheric nitrogen deposition	input4MIPs dataset (Hegglin et al. in preparation) (chapter 5.1.1)	
Nitrogen surface load	4.49 kg/(ha·a) (chapter 5.3.4)	
Nitrogen inhabitant excretion	12.0 g/(inh·d) (chapter 5.3.2)	
Nitrogen concentration in interflow and base flow	Adapted based on current input data by Knoll et al. (2020) (chapter 5.6.1)	
Nitrogen topsoil content	Current input data as described in Morling et al. (2024) (chapter 5.2.3)	
Atmospheric phosphorus deposition	75 g/(ha·a) (chapter 5.1.2)	
Phosphorus surface load	1.64 kg/(ha·a) (chapter 5.3.4)	
Phosphorus inhabitant excretion	1.9 g/(inh·d) (chapter 5.3.2)	
Phosphorus concentration in groundwater	Current input data as described in Fuchs et al. (2022) (chapter 5.6.2)	
Phosphorus topsoil content	Current input data on naturally covered areas (Fuchs et al. 2022) were used for agricultural soils (chapter 5.2.3)	

A.2 Land use classification

HANZE 2.0 dataset (Paprotny & Mengel 2023) was used for deriving input data on land use in 1880 (refer to chapter 3.1). The land use in the dataset is coded with Corine land cover (CLC) classification (Kosztra et al. 2017). The translation table below lists the CLC codes and the assigned land use categories of the MoRE model.

Table 26: List of Corine land cover (CLC) classification and assigned land use categories used in the MoRE model.

CLC code	Description of CLC class[a]	MoRE land use class
211	Non-irrigated arable land	Arable land
221	Vineyards	Arable land
222	Fruit trees and berry plantations	Arable land
241	Annual crops associated with permanent crops	Arable land
242	Complex cultivation patterns	Arable land
243	Land principally occupied by agriculture, with significant areas of natural vegetation	Arable land
244	Agro-forestry areas	Arable land
323	Sclerophyllous vegetation	Naturally covered area
324	Transitional woodland/shrub	Naturally covered area
311	Broad-leaved forest	Naturally covered area
312	Coniferous forest	Naturally covered area
313	Mixed forest	Naturally covered area
321	Natural grassland	Naturally covered area
322	Moors and heathland	Naturally covered area
141	Green urban areas	Urban areas
111	Continuous urban fabric	Urban areas
112	Discontinuous urban fabric	Urban areas
142	Sport and leisure facilities	Urban areas
121	Industrial or commercial units	Urban areas
122	Road and rail networks and associated land	Urban areas
123	Port areas	Urban areas
124	Airports	Urban areas
231	Pastures	Pasture
131	Mineral extraction sites	Open pit mine

CLC code	Description of CLC class[a]	MoRE land use class
132	Dump sites	Open pit mine
133	Construction sites	Open pit mine
331	Beaches, dunes, sands	Open areas
332	Bare rock	Open areas
333	Sparsely vegetated areas	Open areas
334	Burnt areas	Open areas
335	Glaciers and perpetual snow	Open areas
411	Inland marshes	Wetland
412	Peatbogs	Wetland
421	Salt marshes	Wetland
423	Intertidal flats	Wetland
511	Water courses	Water surface
512	Water bodies	Water surface
521	Coastal lagoons	Water surface
522	Estuaries	Water surface
523	Sea and ocean	Water surface

[a] – The description was taken from the CLC nomenclature guidelines: https://land.copernicus.eu/content/corine-land-cover-nomenclature-guidelines/html/ (last access on 25.04.2025)

A.3 Input data based on population density

Schott (1912) collected statistical data on areas and inhabitants of urban agglomerations in the German Empire (1871 – 1910). For these data, the median population density of 37 cities accounted to 35.6 inh/ha in 1880 (Figure 35). The lowest population densities in this dataset range from 8 to 12 inh/ha. Based on this analysis, the HANZE 2.0 population raster of 1880 (Paprotny & Mengel 2023) was used to derive input data for modelling in MoRE. The integer raster has a spatial resolution of 1 ha and population density was attributed with water consumption and percentage of urban population connected to sewers according to Table 27. A population density of ≤ 9 inh/ha was considered to reflect rural conditions. This population is assumed to be not connected to any sewer, thus consumed water is expected to percolate into the ground. A range of 10 – 35 inh/ha was considered as less densely populated urban areas that did not yet all have a water supply and therefore typically had low connection rates to sewers. A population density of ≥ 36 inh/ha was assumed to represent well-developed urban areas with water supply and high connection to sewer systems. A maximum of 80 % connection was assumed as most urban areas were not likely to meet a complete sewer connection at that time. Water consumption was averaged for analytical units considering all raster cells located in an analytical unit. The population connected to sewers were obtained by multiplying the original population raster with the connection rate and adding up the number of connected inhabitants per analytical unit.

Figure 35: Population density in urban agglomerations of the German Empire in 1880 based on data by Schott (1912).

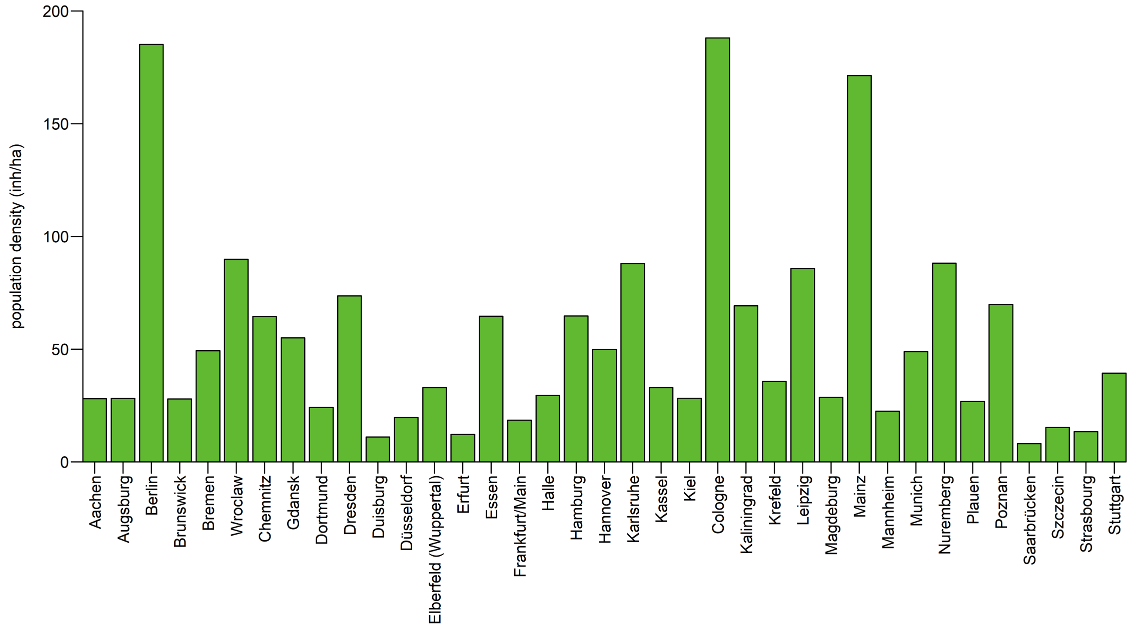

Source: own illustration, IWU-WG

Table 27: Population density classes and attributed water consumption as well as percentage of urban population connected to sewers.

Population density [inh/ha]	Water consumption[a] [L/(inh·d)]	Urban population connected to sewers[b] [%]
≤ 9	-	0
10 – 35	55	30
≥ 36	97	80

[a] – based on Franzius et al. (1893), refer to chapter 4.2

[b] – refer to chapter 5.3.1

A.4 Validation of climate change vectors based on 20CRv3

Figure 36: Mean yearly precipitation and mean air temperature for the area of present Germany derived from DWD (2023) and 20CRv3 (Slivinski et al. 2019).

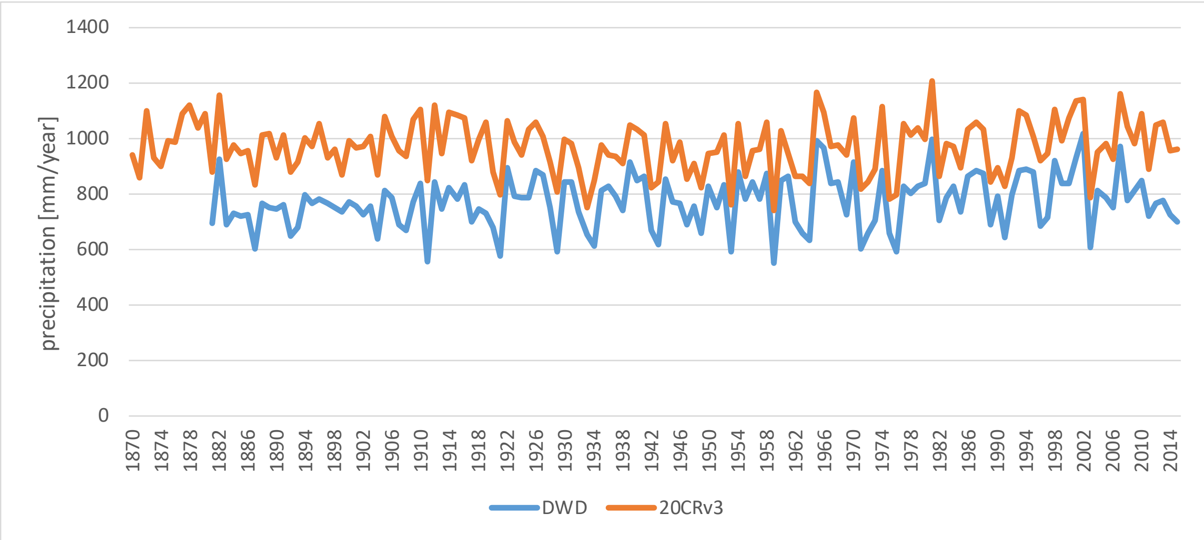

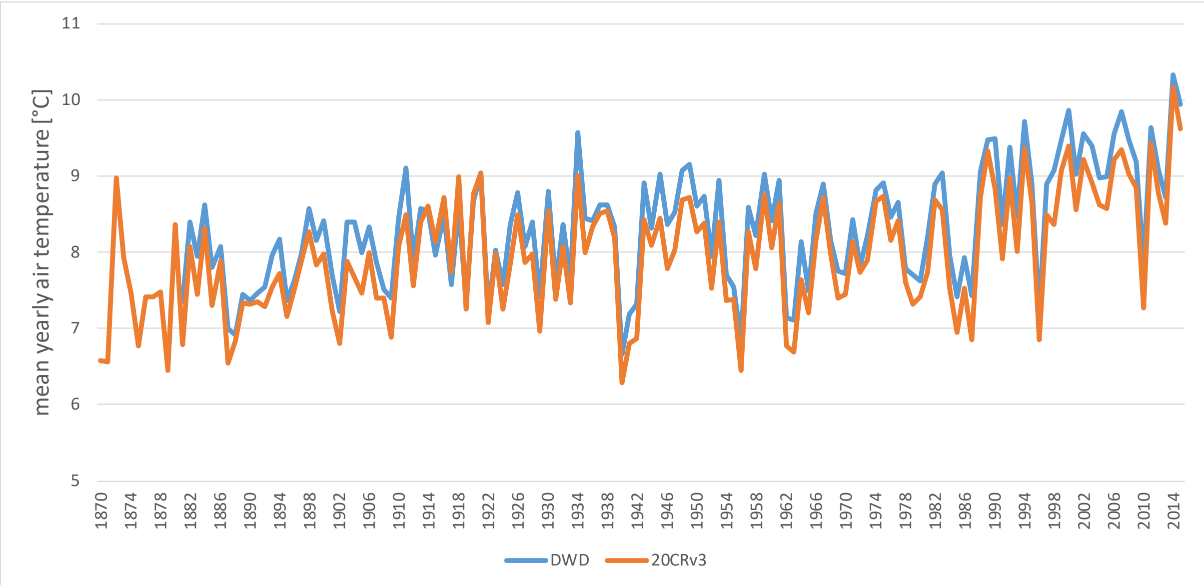

Source: own illustration, HYDRON

A.5 Urban water consumption and wastewater

A literature review was conducted to obtain daily water consumption and wastewater volumes (Table 28). The assumptions that population in larger cities used more water or that per capita water consumption increased over time due to improved water supply and on-going sewer constructions was not confirmed by the gathered literature data (Figure 37 and Figure 38). Thus, a simple approach was used for modelling based on daily water need separated for urban and rural population (chapter 4.2).

Note that some cities have different names nowadays or have been incorporated into others (e.g. Steglitz and Weißensee belong to Berlin today).

Table 28: Historical daily per capita water usage [L/(inh·d)] for different German cities as taken from literature.

No.	City	Water usage	value [L/(E·d]	year[b]	Reference
1	Berlin	Water supply	62	1880	Mohajeri (2005)
2	Berlin	Water supply	64	1887	Becker (1887)
3	Berlin	Water supply	88	1912	Dunbar (1998)
4	Berlin	Water supply	65	1888	Franzius et al. (1893)
5	Berlin	Water supply	49	1888	Franzius et al. (1893)
6	Berlin	Water supply	70	1889	Anonymus (1889a)
7	Bochum	Water supply	137	1888	Franzius et al. (1893)
8	Brunswick	Water supply	161[a]	1886	Lange (2002)
9	Brunswick	Water supply	73[a]	1886	Lange (2002)
10	Brunswick	Water supply	113	1894	Blasius (1894)
11	Bremen	Water supply	109	1912	Dunbar (1998)
12	Cologne	Water supply	119	1912	Dunbar (1998)
13	Cologne	Water supply	150	1888	Architekten- und Ingenieurverein für Niederrhein und Westfalen (1888)
14	Dortmund	Water supply	200	1888	Franzius et al. (1893)
15	Dresden	Water supply	99	1912	Dunbar (1998)
16	Dresden	Water supply	81	1889	Franzius et al. (1893)
17	Duisburg	Water supply	117	1888	Franzius et al. (1893)
18	Frankfurt/Main	Water supply	172	1912	Dunbar (1998)
19	Frankfurt/Main	Water supply	85	1885	Franzius et al. (1893)
20	Freiburg/Breisgau	Water supply	332	1912	Dunbar (1998)
21	Göttingen	Water supply	54	1912	Dunbar (1998)
22	Hamburg	Water supply	139	1912	Dunbar (1998)

No.	City	Water usage	value [L/(E·d]	year[b]	Reference
23	Hamburg	Water supply	204	1885	Franzius et al. (1893)
24	Hannover	Water supply	92	1912	Dunbar (1998)
25	Kaiserslautern	Water supply	120	1889	Frings (1889)
26	Strasbourg	Water supply	127[a]	1880	Krieger (1885)
27	Strasbourg	Water supply	73[a]	1885	Krieger (1885)
28	Wiesbaden	Water supply	71	1887	Becker (1887)
29	Worms	Water supply	150	1889	Frings (1889)
30	Wrocław	Water supply	74	1888	Statistisches Amt der Stadt Breslau (1889/91)
31	Wrocław	Water supply	100	1888	Statistisches Amt der Stadt Breslau (1889/91)
32	Wrocław	Water supply	70	1887	Becker (1887)
33	Wrocław	Water supply	72	1886	Franzius et al. (1893)
34	Würzburg	Water supply	130	1886	Hügel (1886)
35	Berlin	Wastewater	97	1885	Mohajeri (2005)
36	Berlin	Wastewater	114	1896	König (1899)
37	Berlin	Wastewater	103[a]	1888	König (1899)
38	Berlin	Wastewater	106	1899	König (1899)
39	Berlin	Wastewater	100	1887	Lubberger (1889)
40	Berlin	Wastewater	85[a]	1888	Anonymus (1889b)
41	Berlin	Wastewater	127	1890	Baumeister (1890)
42	Berlin	Wastewater	99	1890	Weyl (1894)
43	Brunswick	Wastewater	137[a]	1894	Blasius (1894)
44	Brunswick	Wastewater	49	1894	Weyl (1894)
45	Charlottenburg	Wastewater	136	1912	Dunbar (1998)
46	Charlottenburg	Wastewater	188	1903	Salomon (1907)
47	Chemnitz	Wastewater	100	1890	Baumeister (1890)
48	Cologne	Wastewater	140	1890	Baumeister (1890)
49	Dortmund	Wastewater	135	1890	Baumeister (1890)
50	Düsseldorf	Wastewater	127	1890	Baumeister (1890)
51	Elberfeld	Wastewater	200	1912	Dunbar (1998)
52	Emden	Wastewater	80	1890	Baumeister (1890)

No.	City	Water usage	value [L/(E·d]	year[b]	Reference
53	Frankfurt/Main	Wastewater	166	1899	König (1899)
54	Frankfurt/Main	Wastewater	200	1899	König (1899)
55	Frankfurt/Main	Wastewater	138	1900	Glasauer & Arndt (1995)
56	Frankfurt/Main	Wastewater	150	1890	Baumeister (1890)
57	Frankfurt/Main	Wastewater	120[a]	1886	Bauer (1998)
58	Freiburg/Breisgau	Wastewater	250	1899	König (1899)
59	Freiburg/Breisgau	Wastewater	380	1898	Korn (1898)
60	Guben	Wastewater	272	1912	Dunbar (1998)
61	Hamburg	Wastewater	140	1890	Baumeister (1890)
62	Hannover	Wastewater	107[a]	1913	Grohmann (2005)
63	Hannover	Wastewater	144	1891	Architekten- und Ingenieur-Verein zu Hannover (1891)
64	Karlsruhe	Wastewater	150	1890	Baumeister (1890)
65	Legnica	Wastewater	106[a]	1900	Salomon (1907)
66	Leipzig	Wastewater	216	1899	König (1899)
67	Leipzig	Wastewater	253	1899	König (1899)
68	Mannheim	Wastewater	160	1890	Baumeister (1890)
69	Mannheim	Wastewater	100	1890	Baumeister (1890)
70	Munich	Wastewater	93[a]	1880	Soyka (1885)
71	Munich	Wastewater	150	1890	Baumeister (1890)
72	Nuremburg	Wastewater	90	1890	Baumeister (1890)
73	Steglitz	Wastewater	49[a]	1896	Salomon (1907)
74	Stuttgart	Wastewater	150	1874	Gordon (1874)
75	Stuttgart	Wastewater	90	1874	Gordon (1874)
76	Szczecin	Wastewater	150	1868	Hobrecht 1868
77	Weißensee	Wastewater	42[a]	1902	Salomon (1907)
78	Wiesbaden	Wastewater	100	1890	Baumeister (1890)
79	Wiesbaden	Wastewater	116[a]	1886	Bauer (1998)
80	Witten	Wastewater	120	1873	Freudenberg (1873)
81	Wrocław	Wastewater	105	1887-1894	Frühwirth (1896)
82	Wrocław	Wastewater	132	1887-1894	Frühwirth (1896)
83	Wrocław	Wastewater	118	1896	König (1899)

No.	City	Water usage	value [L/(E·d]	year[b]	Reference
84	Wrocław	Wastewater	123	1888	Statistisches Amt der Stadt Breslau (1889/91)
85	Wrocław	Wastewater	126	1899	König (1899)
86	Wrocław	Wastewater	124	1890	Baumeister (1890)
87	Würzburg	Wastewater	110	1886	Hügel (1886)

[a] – value was calculated from information given within the reference (if no population was given, the number of inhabitants of the cities in 1880 was used as taken from Kaiserliches Statistisches Amt (1884)).
[b] – if no year was mentioned within the reference, the publication year was used

Figure 37: Historical daily per capita water usage [L/(inh·d)] for different German cities as taken from literature according to number of inhabitants in these cities in 1880 (Kaiserliches Statistisches Amt 1884).

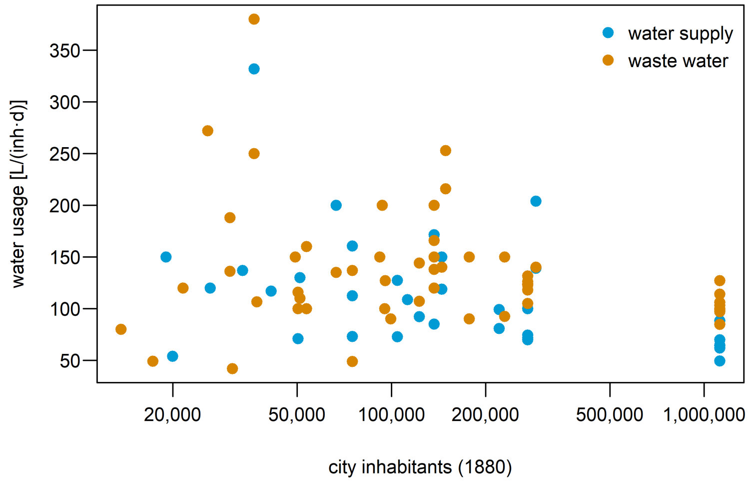

Source: own illustration, IWU-WG

Figure 38: Historical daily per capita water usage [L/(inh·d)] for different German cities as taken from literature according to the reference year (publication year of the reference in case no specific year was mentioned in the source).

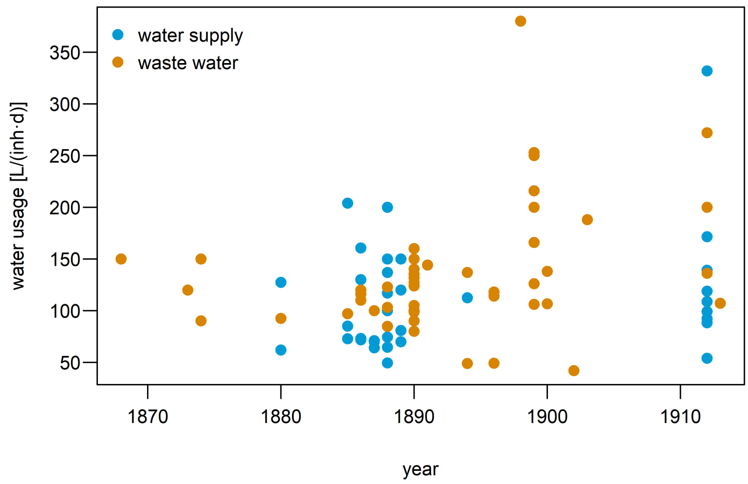

Source: own illustration, IWU-WG

A.6 Gauging stations for evaluation of historical water balance

Historical discharge measurements summarised in Table 29 were originally taken from the Global Runoff Data Centre (GRDC, BfG 2024). These data were used for Figure 13.

Table 29: Selected gauging stations from GRDC (BfG 2024) for evaluation of historical water balance (Figure 13).

Gauging station / river	Catchment size of gauge [km²]	Observed annual average runoff (1873 – 1887) [mm/a]	Modelled annual runoff 1800 [mm/a]
Basel, Rheinhalle / Rhine	35 897	883	777
Bodenwerder / Weser	15 924	303	315
Dresden / Elbe	53 096	175	179
Hannoversch Münden / Weser	12 442	279	312
Intschede / Weser	37 720	280	287
Cologne / Rhine	144 232	483	427
Neu Darchau / Elbe	131 950	172	172
Rees / Rhine	159 300	456	423
Schweinfurt Neuer Hafen / Main	12 715	276	302
Vlotho / Weser	17 618	323	323
Würzburg / Main	14 031	253	292

A.7 Daily inhabitant excretion rates

The tables below list the nitrogen (Table 30) and phosphorus (Table 31) values for daily inhabitant excretion rates obtained from literature. These data were used to produce Figure 20.

Table 30: Reported daily inhabitant excretion rates for nitrogen obtained from literature.

No.	Sample type	value [g/(inh·d)]	year[c]	reference
1	faeces	1.25[a]	1889	König 1899
2	faeces	1.75[b]	1889	König 1899
3	faeces	2.10	1882	König 1887
4	faeces	0.64	1882	König 1887
5	faeces	1.34	1894	Weyl 1894
6	faeces	1.10	1894	Weyl 1894
7	faeces	1.78	1894	Weyl 1894
8	faeces	1.87	1894	Weyl 1894
9	faeces	6.26	1894	Weyl 1894
10	faeces	1.10	1894	Weyl 1894
11	faeces	1.78	1894	Weyl 1894
12	faeces	1.34	1894	Weyl 1894
13	urine	6.30[a]	1889	König 1899
14	urine	12.90[b]	1889	König 1899
15	urine	12.10	1882	König 1887
16	urine	14.08	1882	König 1887
17	urine	9.54	1894	Weyl 1894
18	urine	13.70	1894	Weyl 1894
19	urine	16.44	1894	Weyl 1894
20	urine	18.74	1894	Weyl 1894
21	urine	13.70	1894	Weyl 1894
22	urine	16.44	1894	Weyl 1894
23	urine	10.57	1894	Weyl 1894
24	faeces and urine	7.55	1889	König 1899
25	faeces and urine	14.65	1889	König 189
26	faeces and urine	14.20	1882	König 1887
27	faeces and urine	14.72	1882	König 1887

No.	Sample type	value [g/(inh·d)]	year[c]	reference
28	faeces and urine	10.88	1894	Weyl 1894
29	faeces and urine	20.62	1894	Weyl 1894
30	faeces and urine	25.01	1894	Weyl 1894
31	faeces and urine	14.79	1894	Weyl 1894
32	faeces and urine	18.22	1894	Weyl 1894
33	faeces and urine	11.91	1894	Weyl 1894
34	faeces and urine	12	1890	Franzius et al. 1893
35	faeces and urine	16	1893	Franzius et al. 1893
36	faeces and urine	15	1893	Franzius et al. 1893
37	faeces and urine	11	1893	Franzius et al. 1893
38	faeces and urine	7	1893	Franzius et al. 1893
39	faeces and urine	12	1893	Franzius et al. 1893
40	faeces and urine	12.50	1893	Franzius et al. 1893
41	faeces and urine	10	1893	Franzius et al. 1893
42	faeces and urine	10	1853	Barles 2007
43	faeces and urine	13.67	1869	Barles & Lestel 2007
44	faeces and urine	9.90	1980	Garcier 2007
45	faeces and urine	9.04	1850	Gustafsson et al. 2012
46	faeces and urine	15	1900	Kopáček et al. 2013
47	faeces and urine	8.22	2002	Lange 2002
48	faeces and urine	10.96	1880	Naden et al. 2016

[a] – given as minimum value
[b] – given as maximum value
[c] – if no year was mentioned within the reference, the publication year was used

Table 31: Reported daily inhabitant excretion rates for phosphorus obtained from literature.

No.	Sample type	value [mg/(E·d]	year[c]	reference
1	faeces	0.43[a]	1889	König 1899
2	faeces	1.74[b]	1889	König 1899
3	faeces	0.51	1882	König 1887
4	faeces	0.16	1882	König 1887
5	faeces	0.61	1894	Weyl 1894
6	faeces	0.61	1894	Weyl 1894
7	urine	0.56[a]	1889	König 1899
8	urine	1.14[b]	1889	König 1899
9	urine	0.56	1882	König 1887
10	urine	0.84	1882	König 1887
11	urine	1.541	1894	Weyl 1894
12	urine	1.540	1894	Weyl 1894
13	faeces and urine	0.98	1889	König 1899
14	faeces and urine	1.74	1889	König 1899
15	faeces and urine	1.08	1882	König 1887
16	faeces and urine	1.01	1882	König 1887
17	faeces and urine	2.16	1894	Weyl 1894
18	faeces and urine	2.15	1894	Weyl 1894
19	faeces and urine	1.35	1893	Franzius et al. 1893
20	faeces and urine	0.94	1893	Franzius et al. 1893
21	faeces and urine	1.25	1893	Franzius et al. 1893
22	faeces and urine	3.50	1980	Garcier 2007
23	faeces and urine	1.10	1850	Gustafsson et al. 2012
24	faeces and urine	1.92	2002	Lange 2002
25	faeces and urine	1.44	1950	Naden et al. 2016

[a] – given as minimum value

[b] – given as maximum value

[c] – if no year was mentioned within the reference, the publication year was used

A.8 Nutrient concentrations in sewers

The tables below list nitrogen (Table 32) and phosphorus (Table 33) concentrations in sewers (untreated wastewaters) gathered from literature. These data were used to produce Figure 21.

Table 32: Reported nitrogen concentrations in sewers obtained from literature.

No.	City	Sample type	value [mg/L]	year[c]	reference
1	Ottensen	sewer water[a]	95.8	1887	König 1887
2	Wrocław	sewer water	40.5	1884	König 1887
3	Wrocław	sewer water	94.6	1885	König 1887
4	Berlin	sewer water	63	1894 – 1896	König 1899
5	Berlin	sewer water	74	1894 – 1896	König 1899
6	Berlin	sewer water	87	1894 – 1896	König 1899
7	Berlin	sewer water	87.3	1883	König 1899
8	Berlin	sewer water	98	1894 – 1896	König 1899
9	Berlin	sewers with WC	108.8	1889 – 1892	König 1899
10	Berlin	sewer water	127	1894 – 1896	König 1899
11	Berlin	sewer water	168	1894 – 1896	König 1899
12	Brunswick	sewers without WC	147	1899	König 1899
13	Dortmund	sewers without WC	73.5	1899	König 1899
14	Essen	sewers without WC	69.6	1899	König 1899
15	Frankfurt/Main	sewers with WC	119	1899	König 1899
16	Halle/Saale	sewers without WC	112.9	1899	König 1899
17	Halle/Saale	Sewers with WC	182.9	1899	König 1899
18	Kronenberg (Essen)	sewers without WC	90.4	1899	König 1899
19	Wrocław	sewers with WC	91.8	1890 – 1898	König 1899
20	Berlin	sewer water	70	1890	Baumeister 1890
21	Bremen	sewer water	60	1890	Baumeister 1890
22	Essen	sewer water	106	1890	Baumeister 1890
23	Frankfurt/Main	sewer water[b]	47	1890	Baumeister 1890
24	Frankfurt/Main	sewer water	67	1890	Baumeister 1890
25	Halle/Saale	sewer water	140	1890	Baumeister 1890
26	Wiesbaden	urban river used as sewer	23	1890	Baumeister 1890

[a] – dissolved fraction

[b] – dry weather conditions

[c] – if no year was mentioned within the reference, the publication year was used

Table 33: Reported phosphorus concentrations in sewers obtained from literature.

No.	City	Sample location	value [mg/L]	year[b]	reference
1	Essen	sewer water[a]	4.1	1885	König 1887
2	Essen	sewer water[a]	8.2	1886	König 1887
3	Essen	sewer water[a]	8.8	1886	König 1887
4	Essen	sewer water[a]	13.1	1885	König 1887
5	Halle/Saale	sewer water[a]	11.4	1886	König 1887
6	Ottensen	sewer water[a]	7.2	1885	König 1887
7	Ottensen	sewer water[a]	8.0	1887	König 1887
8	Berlin	sewer water	5.8	1883	König 1899
9	Berlin	sewer water	8.1	1873	König 1899
10	Berlin	sewers with WC	9.9	1889 – 1892	König 1899
11	Brunswik	sewers without WC	13.2	1899	König 1899
12	Dortmund	sewers without WC	4.1	1899	König 1899
13	Halle/Saale	sewers without WC	8.6	1899	König 1899
14	Halle/Saale	sewers with WC	13.6	1899	König 1899
15	Kronenberg (Essen)	sewers without WC	6.4	1899	König 1899
16	Wrocław	sewers with WC	6.1	1890 – 1898	König 1899
17	Wrocław	sewer water	7.2	1885	König 1899

[a] – dissolved fraction

[b] – if no year was mentioned within the reference, the publication year was used

B Model results on nutrient emissions per river basin

Table 34: Modelled total nitrogen emissions per river basin and emission pathway in 1880.

River basin	River basin area [km²]	Atmospheric deposition onto water surface [t N/a]	Erosion [t N/a]	Base flow [t N/a]	Interflow [t N/a]	Surface runoff [t N/a]	Tile drainage [t N/a]	Urban systems [t N/a]	Total emissions (sum of pathways) [t N/a]
Eider	5 862	15	108	1 258	1 157	40	606	1	3 184
Elbe	147 532	597	2 474	26 251	16 577	1 490	2 317	5 398	55 105
Ems	16 349	29	264	3 846	3 499	201	252	106	8 198
Meuse	32 561	89	706	10 136	5 989	806	33	1 199	18 959
Rhine	187 754	2 099	10 317	66 441	51 269	4 831	2 087	7 453	144 498
Weser	47 215	65	791	12 007	11 964	842	566	815	27 050
Oder	124 863	418	1 915	14 461	8 044	898	1 843	1 899	29 477
Schlei/Trave	6 104	51	84	1 458	1 033	92	221	143	3 083
Warnow/Peene	13 646	60	55	1 613	946	67	412	124	3 278
Sum	**581 886**	**3 423**	**16 714**	**137 472**	**100 479**	**9 267**	**8 338**	**17 139**	**292 832**

Table 35: Modelled total phosphorus emissions per river basin and emission pathway in 1880.

River basin	River basin area [km²]	Atmospheric deposition onto water surface [t P/a]	Erosion [t P/a]	Base flow [t P/a]	Interflow [t P/a]	Surface runoff [t P/a]	Tile drainage [t P/a]	Urban systems [t P/a]	Total emissions (sum of pathways) [t P/a]
Eider	5 862	< 1	15	10	10	1	5	< 1	42
Elbe	147 532	14	446	262	163	41	22	621	1 570
Ems	16 349	1	47	52	46	6	3	14	169
Meuse	32 561	2	88	76	45	23	< 1	137	372
Rhine	187 754	48	3 201	553	420	161	15	959	5 359
Weser	47 215	1	240	158	151	22	7	119	697
Oder	124 863	12	357	132	73	26	14	224	837
Schlei/Trave	6 104	1	31	18	13	3	2	21	90
Warnow/Peene	13 646	2	13	60	36	2	8	18	138
Sum	**581 886**	**81**	**4 438**	**1 322**	**956**	**285**	**77**	**2 114**	**9 273**

C Comparison to further historical modelling scenarios

C.1 Modelled nutrient emissions per river basin

This section compares the results for 1880 using the models MoRE (this study) and MONERIS (data kindly provided by M. Venohr, IGB Berlin). Table 36 summarizes total nutrient emissions. Information on individual emission pathways for nitrogen and phosphorus are summarized in Figure 39 and in Figure 40, respectively, in absolute (upper panel) and percent (lower panel) values. The left column for each river basins presents MoRE results from this study, while the right column for each basin shows MONERIS results. Note, that MONERIS did not differentiate between interflow and base flow and both emission pathways are displayed here by base the flow pathway.

Table 36: Total nutrient emission for river basins in 1880 modelled with MoRE (this study) and MONERIS.

	Total nitrogen [t N/a]		Total phosphorus [t P/a]	
River basin	**MoRE (this study)**	**MONERIS**	**MoRE (this study)**	**MONERIS**
Eider	3 184	4 964	42	55
Elbe	55 105	75 085	1 570	2 022
Ems	8 198	10 137	169	196
Meuse	18 959	21 867	372	555
Rhine	144 498	160 990	5 359	4 152
Weser	27 050	29 833	697	628
Oder	29 477	43 434	837	1 238
Schlei/Trave	3 083	3 877	90	73
Warnow/Peene	3 278	3 687	138	95
Total	**292 832**	**353 874**	**9 273**	**9 016**

Figure 39: Comparison of absolute (upper panel) and percent (lower panel) nitrogen emissions per pathway for individual river basins between MoRE (left columns) and MONERIS (right columns) modelling of 1880.

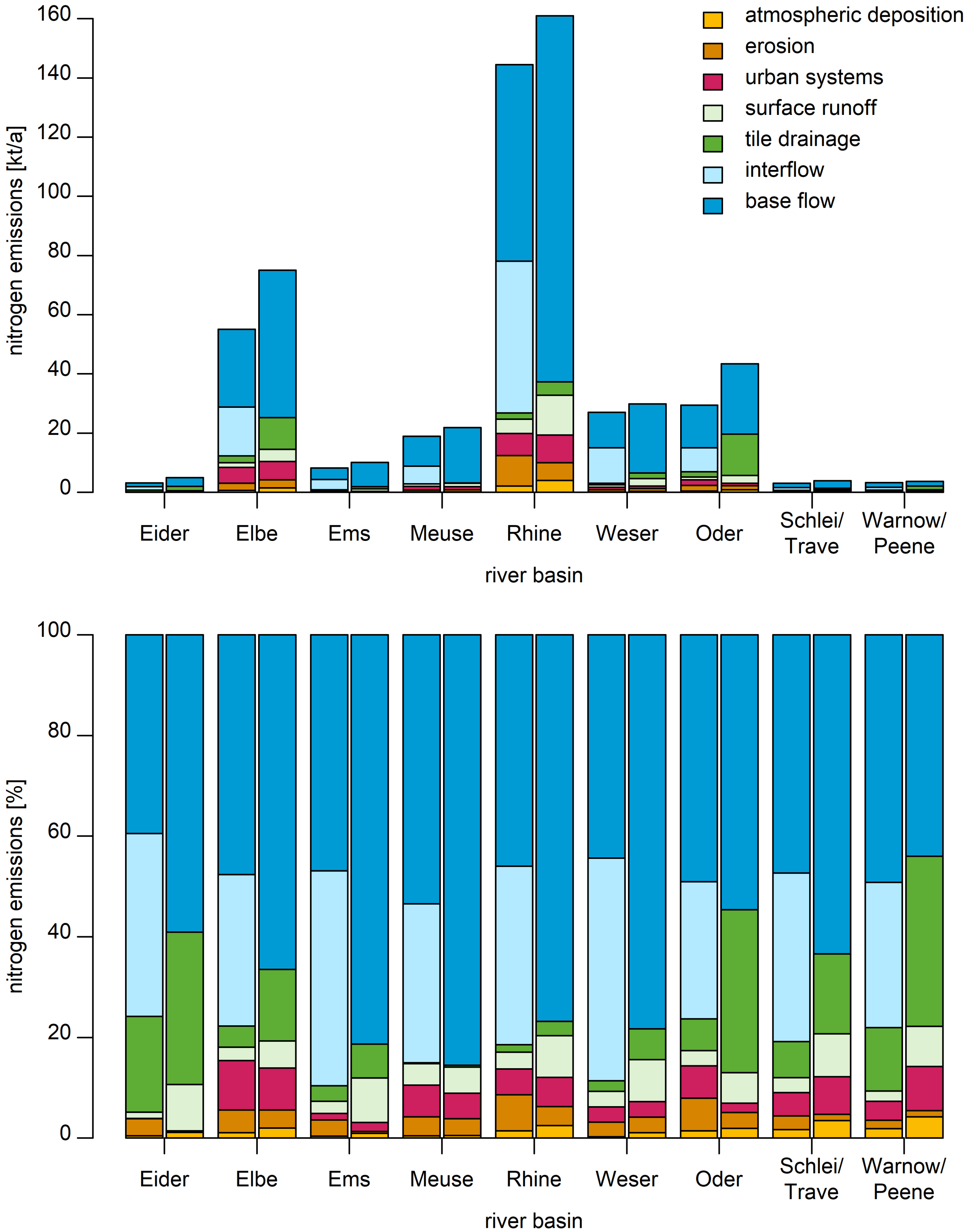

Source: own illustration, IWU-WG

Figure 40: Comparison of absolute (upper panel) and percent (lower panel) phosphorus emissions per pathway for individual river basins between MoRE (left columns) and MONERIS (right columns) modelling of 1880.

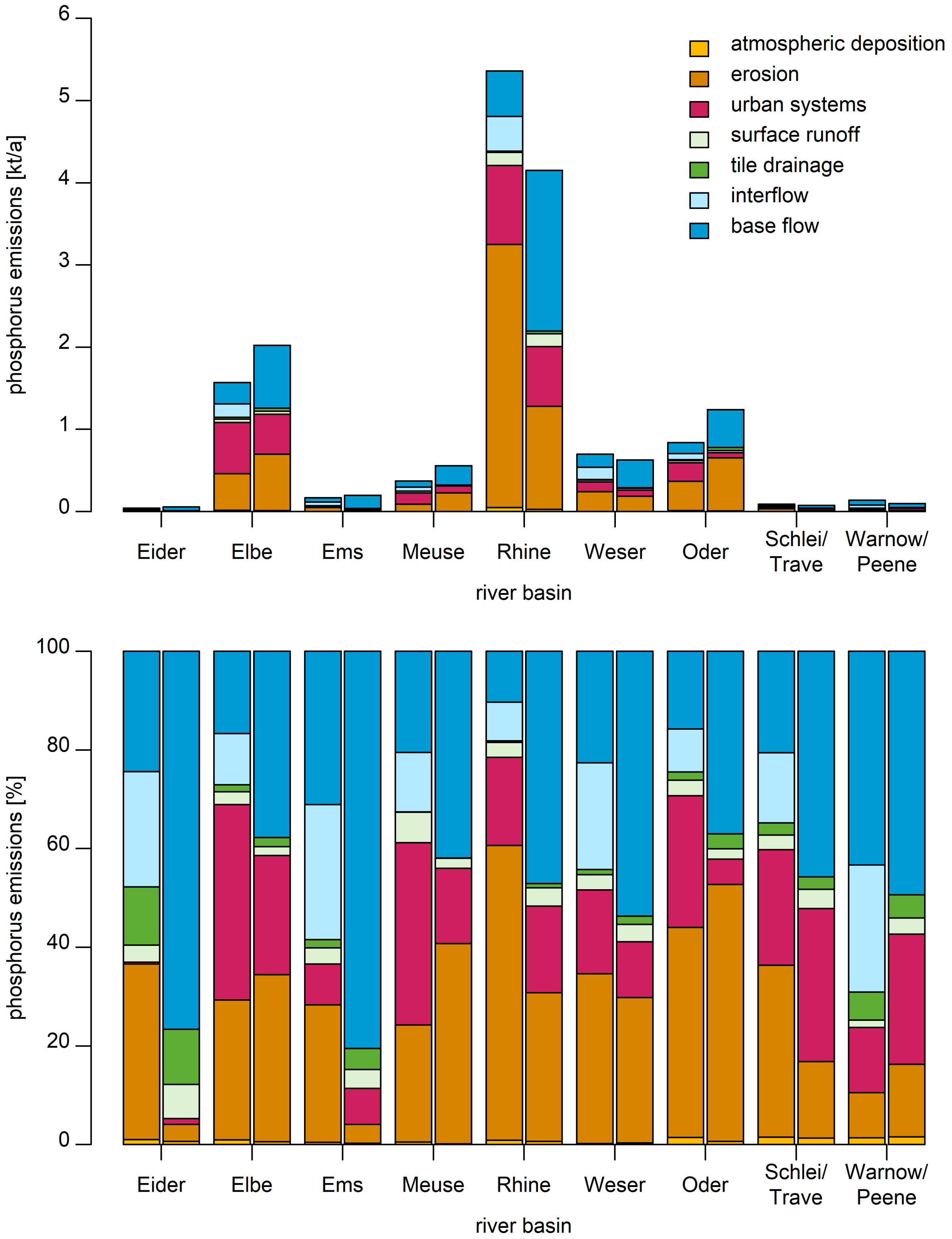

Source: own illustration, IWU-WG

C.2 Modelled surface water loads and concentrations

Table 37: Total nitrogen surface water loads and outlet concentrations for MoRE and MONERIS in 1880.

River basin[a]	MoRE			MONERIS		
	Total runoff [m³/s]	TN load [t N/a]	TN concentration [mg/L][b]	Total runoff [m³/s]	TN load [t N/a]	TN concentration [mg/L][b]
Eider	53	2 501	1.51	67	4 067	1.91
Elbe	841	37 339	1.41	768	46 671	1.93
Ems	133	6 421	1.54	143	8 362	1.85
Meuse	331	16 915	1.62	239	18 806	2.50
Rhine	2 4177	95 970	1.26	2 515	111 943	1.41
Weser	414	21 244	1.63	408	23 320	1.81
Oder	487	17 955	1.17	557	27 905	1.59
Schlei/Trave	60	2 000	1.05	55	2 399	1.39
Warnow/Peene	85	2 098	0.78	69	2 393	1.10
Total	**4 820**	**202 443**	**1.33**	**4 821**	**245 864**	**1.62**

[a] – the area of the river basins can be found in Table 34

[b] – average concentrations were calculated by dividing total surface water loads by total runoff for each river basin

Table 38: Total phosphorus surface water loads and outlet concentrations for MoRE and MONERIS in 1880.

River basin[a]	MoRE			MONERIS		
	Total runoff [m³/s]	TP load [t P/a]	TP concentration [mg/L][b]	Total runoff [m³/s]	TP load [t P/a]	TP concentration [mg/L][b]
Eider	53	23	0.014	67	37	0.017
Elbe	841	839	0.032	768	1 118	0.046
Ems	133	99	0.024	143	131	0.029
Meuse	331	272	0.026	239	403	0.054
Rhine	2 417	2 546	0.033	2 515	2 742	0.035
Weser	414	426	0.033	408	418	0.032
Oder	487	320	0.021	557	680	0.039
Schlei/Trave	60	56	0.029	55	39	0.023
Warnow/Peene	85	70	0.026	69	46	0.021
Total	**4 820**	**4 678**	**0.031**	**4 821**	**5 615**	**0.037**

[a] – the area of the river basins can be found in Table 35

[b] – average concentrations were calculated by dividing total surface water loads by total runoff for each river basin

C.3 Modelled discharge per river basin

Figure 41 compares the results for modelled historical runoff per river basin from this study (MoRE 1880), MONERIS model (Gadegast & Venohr 2015; Hirt et al. 2014), regional E-HYPE modelling (Blauw et al. 2019) and the global modelling of Beusen et al. (2016).

Figure 41: Comparison of total runoff for individual river basins from different historical modelling studies.

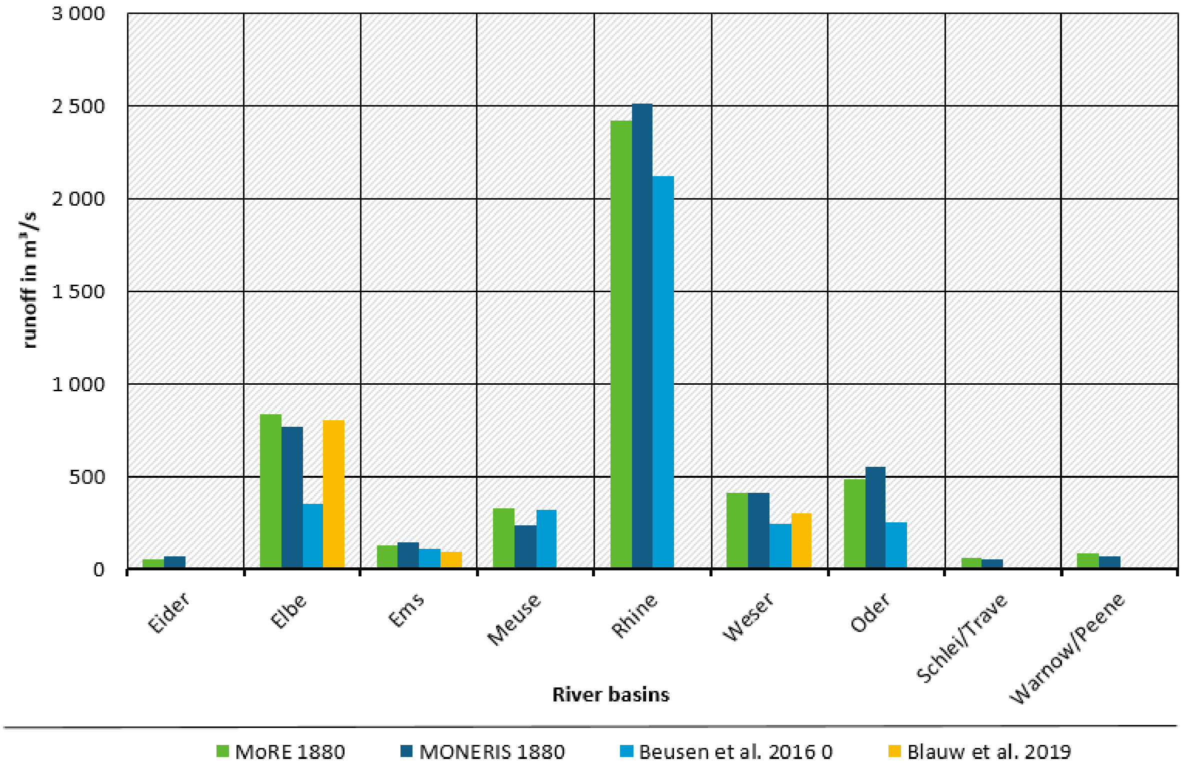

Source: own illustration, IWU-WG

D Historical modelling of the Upper Danube basin

The Upper Danube basin is part of both MoRE and LARSIM-ME models (Figure 4, Figure 5) and was included in the 1880 scenario even though it was not in the focus of this project. For the Danube basin, the same input data sets were prepared as described in the main text and in Appendix A. The following sections provide details on land use and population in 1880 for the Upper Danube basin as well as model results and a comparison to previous MONERIS results.

D.1 Land use and population

For the considered part of the Danube basin, most land was occupied by naturally covered areas (mostly forests, Table 39, Figure 42). Compared to the North Sea and Baltic Sea basins, a lower proportion of the area was dedicated to arable land (cf. Table 39 and Table 3). Further, there is a higher proportion of open (alpine) areas within the Danube basin (cf. Table 39 and Table 3, Figure 42). The impervious area accounted to approximately 390 km², which corresponds to an average sealing degree of 35 % for urban areas. A total of 3.96 million inhabitants were obtained for the Danube basin, of which 7 % (0.28 million inhabitants) were connected to a sewer system.

Figure 42: Land use in 1880 aggregated to land use classes of the MoRE model.

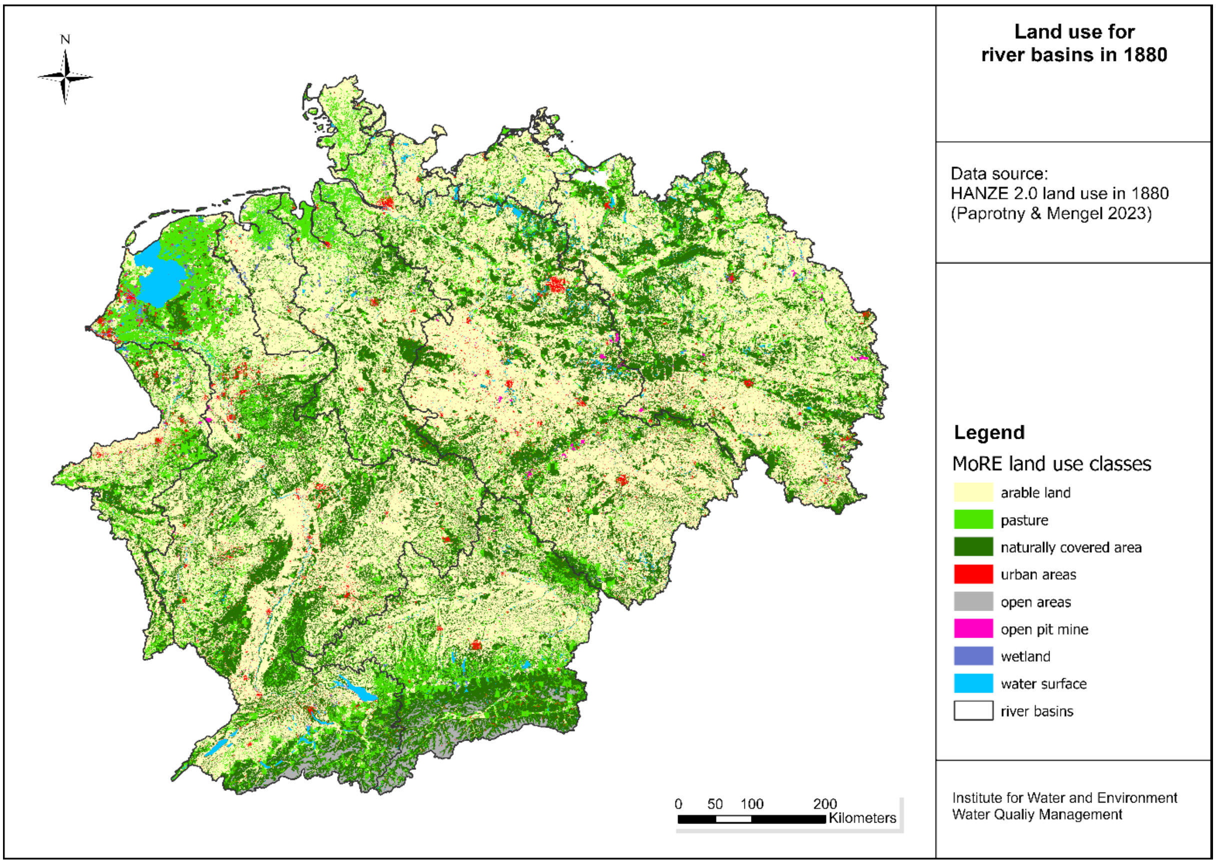

Source: own illustration, IWU-WG

Table 39: Land use in 1880 aggregated to MoRE land use classes for the Upper Danube basin, values rounded.

Land use category	Upper Danube basin [km²]	Upper Danube basin [%]
Arable land	28 900	37
Pastures	12 100	16
Naturally covered areas	29 800	39
Urban areas	1 100	1
Open areas	4 600	6
Open pit mining	100	< 1
Wetlands	200	< 1
Water surfaces	600	1
Total	**77 400**	**100**

D.2 Model results

D.2.1 Total emissions into surface waters

Total nitrogen emissions amount to roughly 78 kt N/a (Table 40). Base flow and interflow are the most important emission pathways, together making up 90 % of the total emissions. Compared to North Sea and Baltic Sea basins, many other emission pathways are accordingly less important (especially tile drainage and urban systems, cf. Table 21 and Table 40). The highest area-specific nitrogen emissions occur in the mountainous areas (Figure 43).

Total phosphorus emissions amount to 3.3 kt P/a for the Danube basin (Table 40). Emissions via erosion deliver 80 % of the total phosphorus emissions, making this pathway proportionally even more important than for North Sea and Baltic Sea basins (cf. Table 22 and Table 40). This can be also seen by the higher area-specific emissions in the mountainous areas of the Danube basin (Figure 44). In contrast, urban systems are proportionally less important for the total phosphorus emissions (cf. Table 22 and Table 40), which can be attributed to smaller cities located in this basin and a lower percentage of population connected to sewers.

Table 40: Nutrient emissions for the Upper Danube basin in 1880.

Emission pathway	Nitrogen [t N/a]	Nitrogen [%]	Phosphorus [t P/a]	Phosphorus [%]
Atmospheric deposition onto water surfaces	194	<1	5	<1
Erosion	2 609	3	2 654	80
Urban systems	800	1	115	3
Surface runoff	1 985	3	97	3
Tile drainage	836	1	4	<1
Interflow	30 677	39	178	5
Base flow	40 710	52	250	8
Total	**77 812**	**100**	**3 303**	**100**

Figure 43: Total area-specific nitrogen emissions into surface waters in 1880.

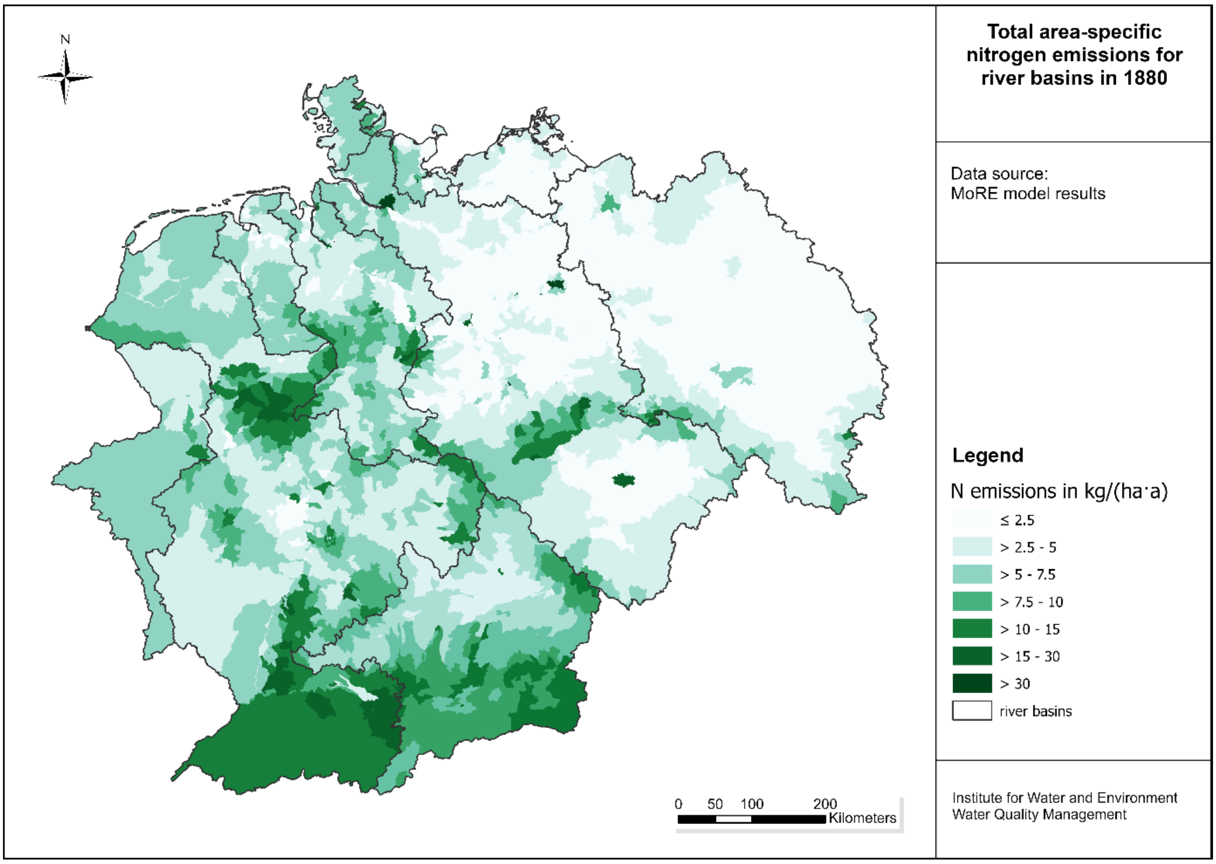

Source: own illustration, IWU-WG

Figure 44: Total area-specific phosphorus emissions into surface waters in 1880.

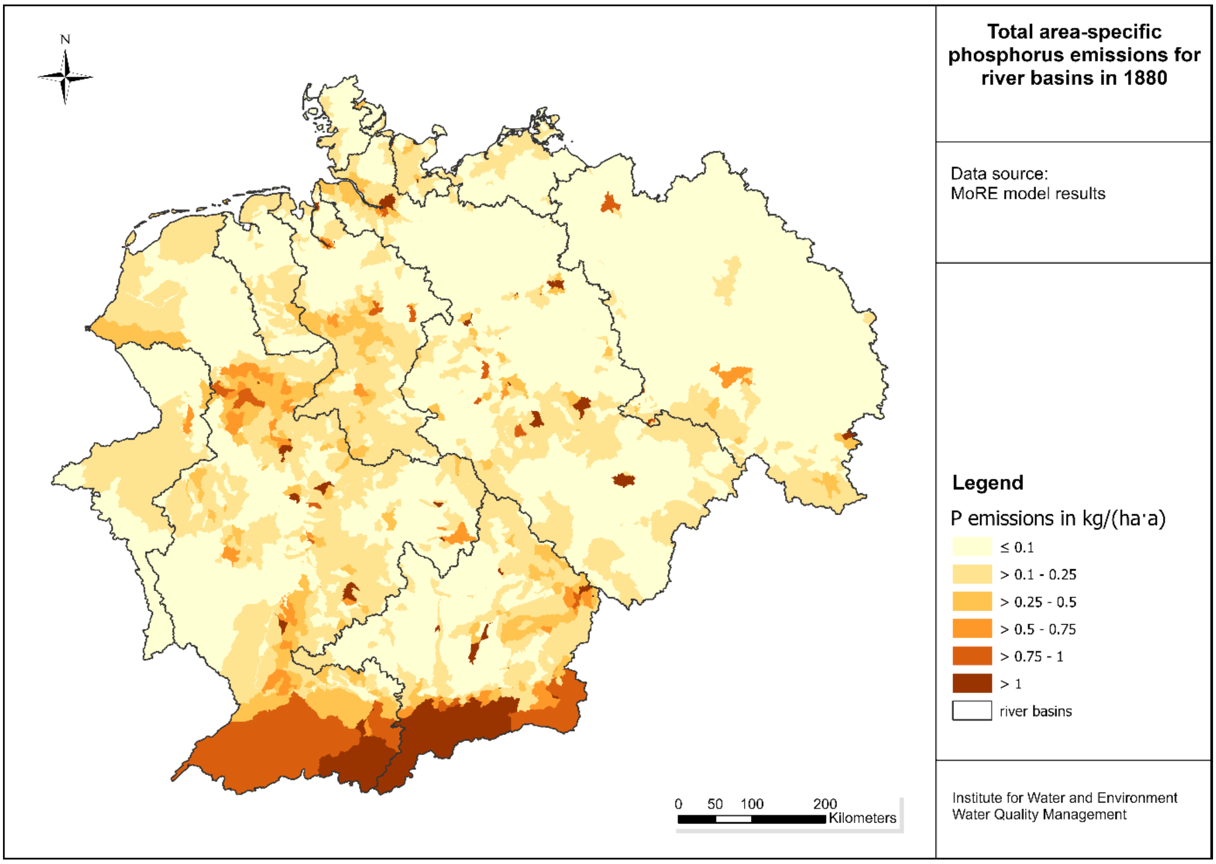

Source: own illustration, IWU-WG

D.2.2 Surface water loads and concentrations

Approximately 66 kt N/a and 2.4 kt P/a of nutrient loads (Table 41) were transported to the outlet of the considered part of the Danube basin. This corresponds to a retention of total emissions of 15 % and 28 % for nitrogen and phosphorus, respectively. The nutrient retention is lower compared to North Sea and Baltic Sea basins (refer to chapter 6.2), which is caused by higher runoff (i.e. higher hydraulic load in the retention modelling) in the mountainous areas of the Danube basin.

Table 41: Nutrient surface water loads and outlet concentrations for the Upper Danube basin in 1880.

River basin	Total runoff [m³/s]	Nitrogen [t N/a]	Nitrogen [mg/L]	Phosphorus [t P/a]	Phosphorus [mg/L]
Danube	1 408	66 061	1.49[a]	2 371	0.053[a]

[a] – average concentrations were calculated by dividing surface water loads by total runoff

Nitrogen concentrations in surface waters of the Danube basin ranged from 0.42 mg/L to 2.40 mg/L, thus being in a similar range to the other river basins (Figure 45). Phosphorus concentrations ranged from roughly 0.01 mg/L up to 0.40 mg/L. The highest phosphorus concentrations can be found in the alpine areas of the Danube basin which show higher emissions via erosion. This can be also observed for the alpine parts of the Rhine basin (Figure 46).

Figure 45: Total nitrogen concentrations in surface waters in 1880.

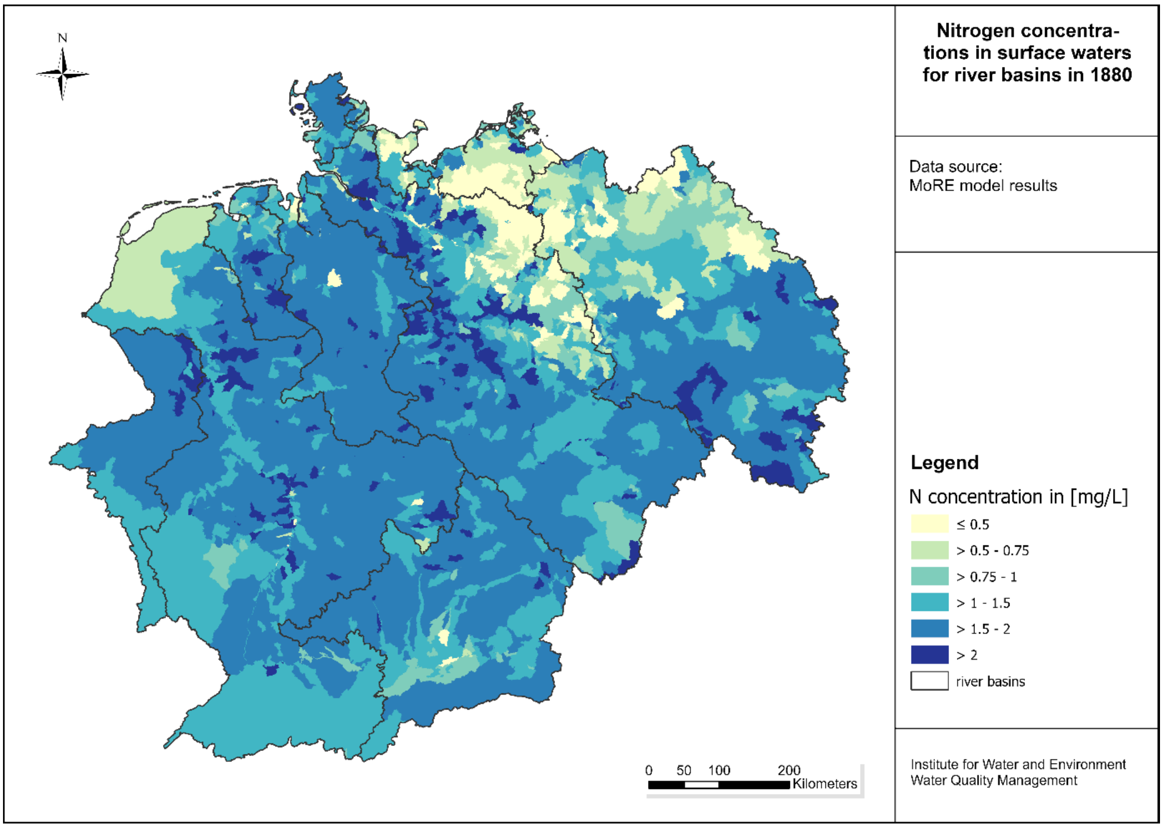

Source: own illustration, IWU-WG

Figure 46: Total phosphorus concentrations in surface waters in 1880.

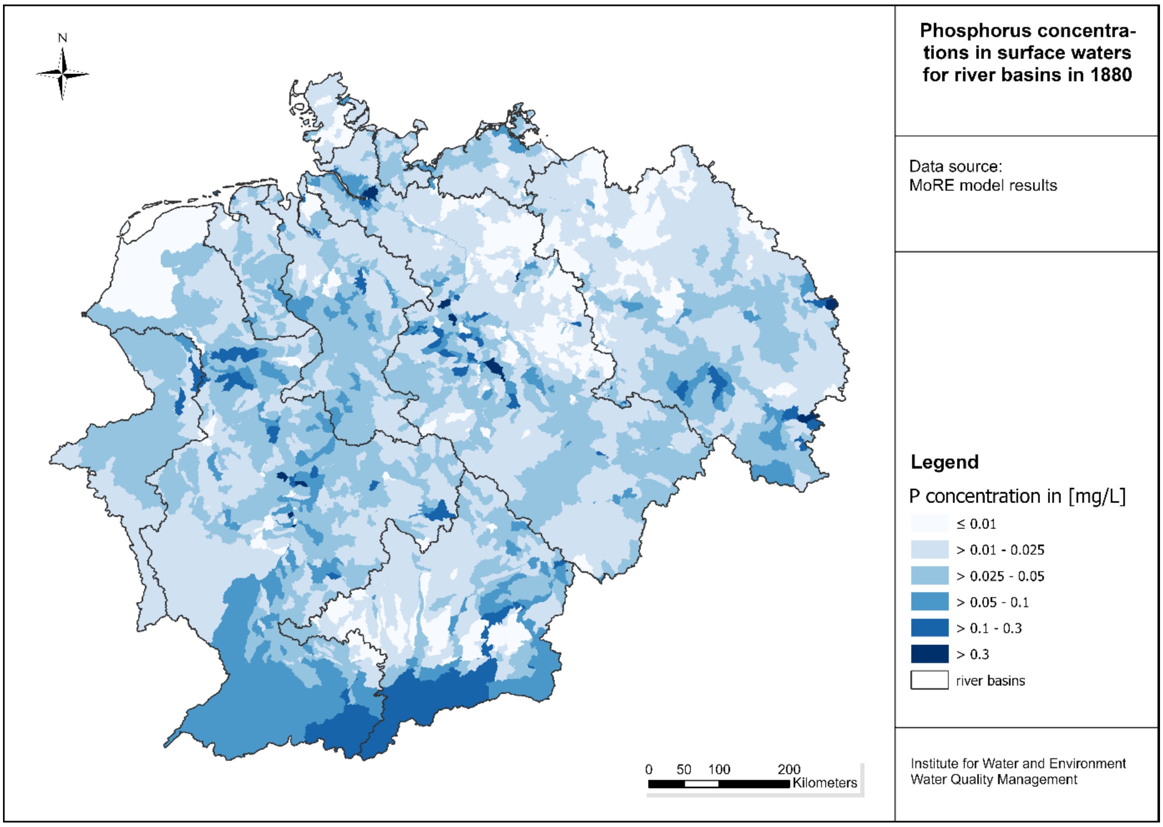

Source: own illustration, IWU-WG

D.3 Comparison to historical MONERIS modelling

Results of the previous MONERIS modelling of 1880 were kindly provided by M. Venohr (IGB Berlin) and contained also information on the Danube basin. They agree well with our results regarding total runoff and nutrient retention (Table 42). However, total emissions and transported loads in the MoRE modelling are higher compared to MONERIS results for both nitrogen and phosphorus, respectively. Consequently, also the obtained average nutrient concentrations were higher in this study compared to the previous MONERIS results (Table 42).

Table 42: Comparison of nutrients modelled with MoRE (this study) and MONERIS for the Upper Danube basin in 1880.

Parameter	Unit	MoRE (this study)	MONERIS
Total runoff	[m^3/s]	1 408	1 408
Total nitrogen emission	[t N/a]	77 812	60 467
Transported total nitrogen load	[t N/a]	66 061	48 920
Nitrogen retention	[%]	15	19
Average nitrogen concentration[a]	[mg/L]	1.49	1.10
Total phosphorus emission	[t N/a]	3 303	1 594
Transported total phosphorus load	[t N/a]	2 371	1 168
Phosphorus retention	[%]	28	27
Average phosphorus concentration[a]	[mg/L]	0.053	0.026

[a] – average concentrations were calculated by dividing surface water loads by total runoff

E Recent water quality measurements

Data on recent water quality were compared to modelled concentrations of different historical scenarios (refer to chapter 7). Water quality measurements from riverine monitoring stations in Germany are routinely stored with beginning of 2006 in the MoRE database for model validation. Single measurements for total nitrogen and total phosphorus for the period 2006 – 2020 were selected. In case, at least 10 measurements were available for a monitoring station per year, a yearly average concentration (arithmetic mean) was calculated. Data are shown for the following monitoring stations:

- Hohenwutzen, Oder River (ID BB09) at river kilometer 661
- Seemanshöft, Elbe River (ID HH011) at river kilometer 628.9 (downstream the German-Czech border)
- Kleve-Bimmen, Rhine River (ID NW02) at river kilometer 865

Figure 47: Total nitrogen measurements (above) and calculated yearly average concentrations (below) at monitoring station Hohenwutzen in Oder River (ID BB09).

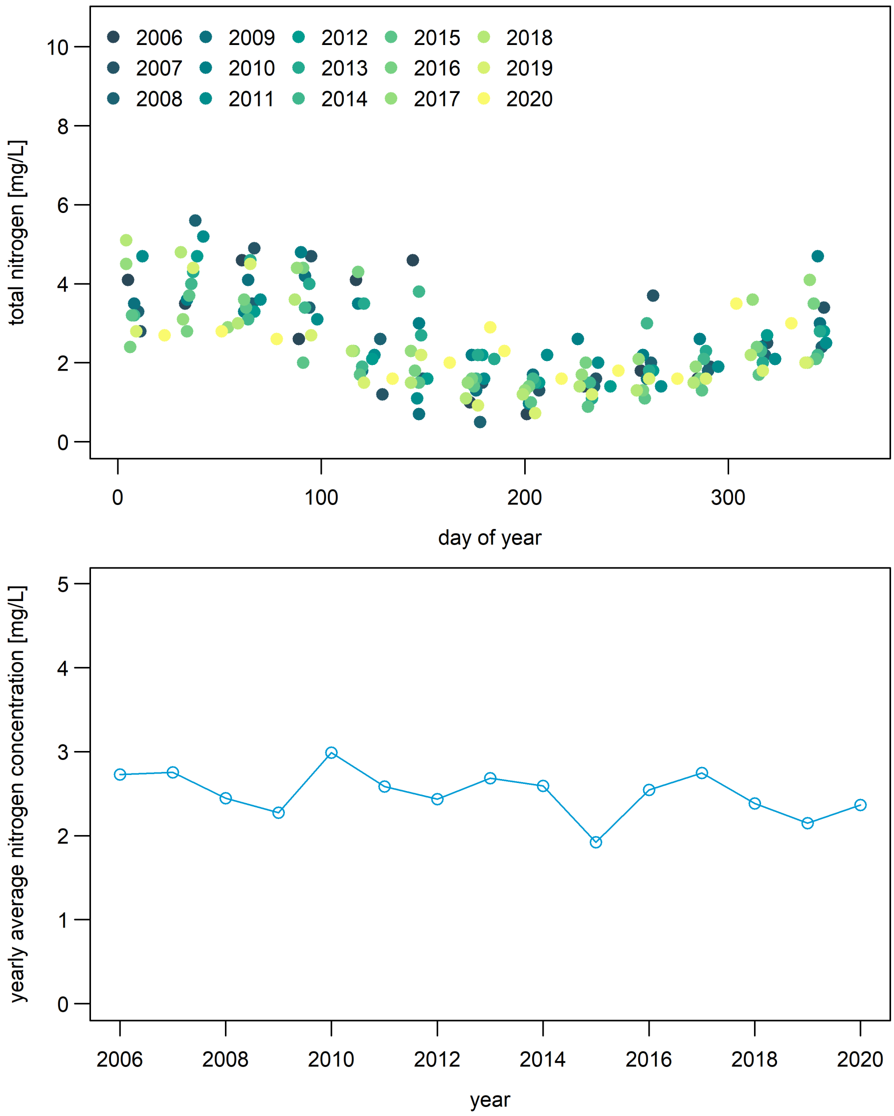

Source: own illustration, IWU-WG

Figure 48: Total nitrogen measurements (above) and calculated yearly average concentrations (below) at monitoring station Seemannshöft in Elbe River (ID HH011).

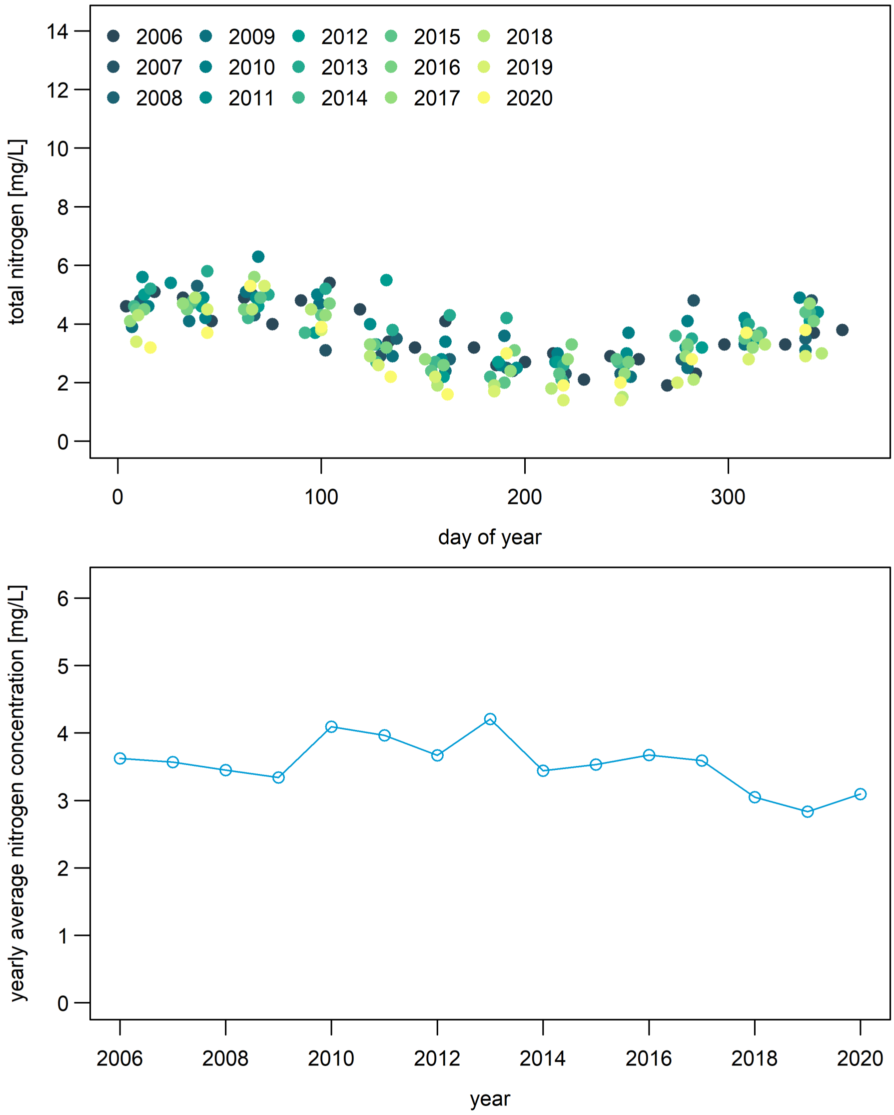

Source: own illustration, IWU-WG

Figure 49: Total nitrogen measurements (above) and calculated yearly average concentrations (below) at monitoring station Kleve-Bimmen in Rhine River (ID NW02).

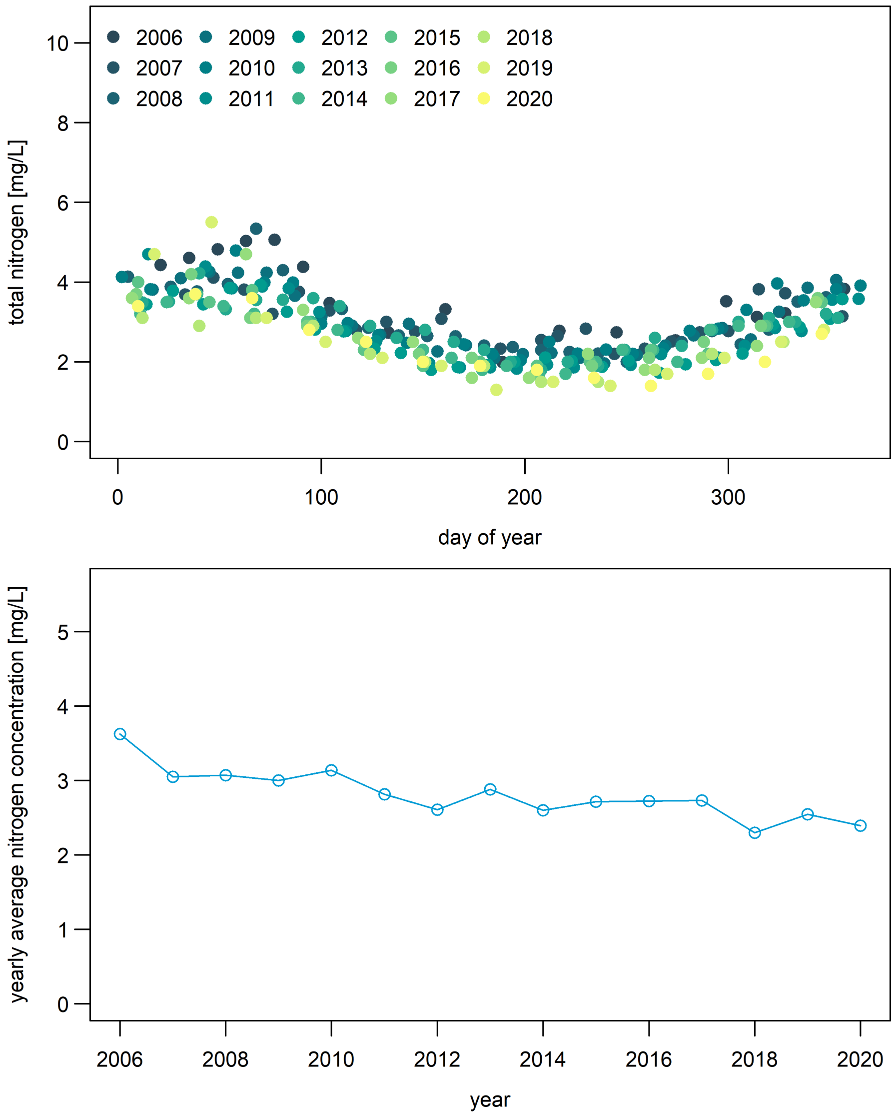

Source: own illustration, IWU-WG

Figure 50: Total phosphorus measurements (above) and calculated yearly average concentrations (below) at monitoring station Hohenwutzen in Oder River (ID BB09).

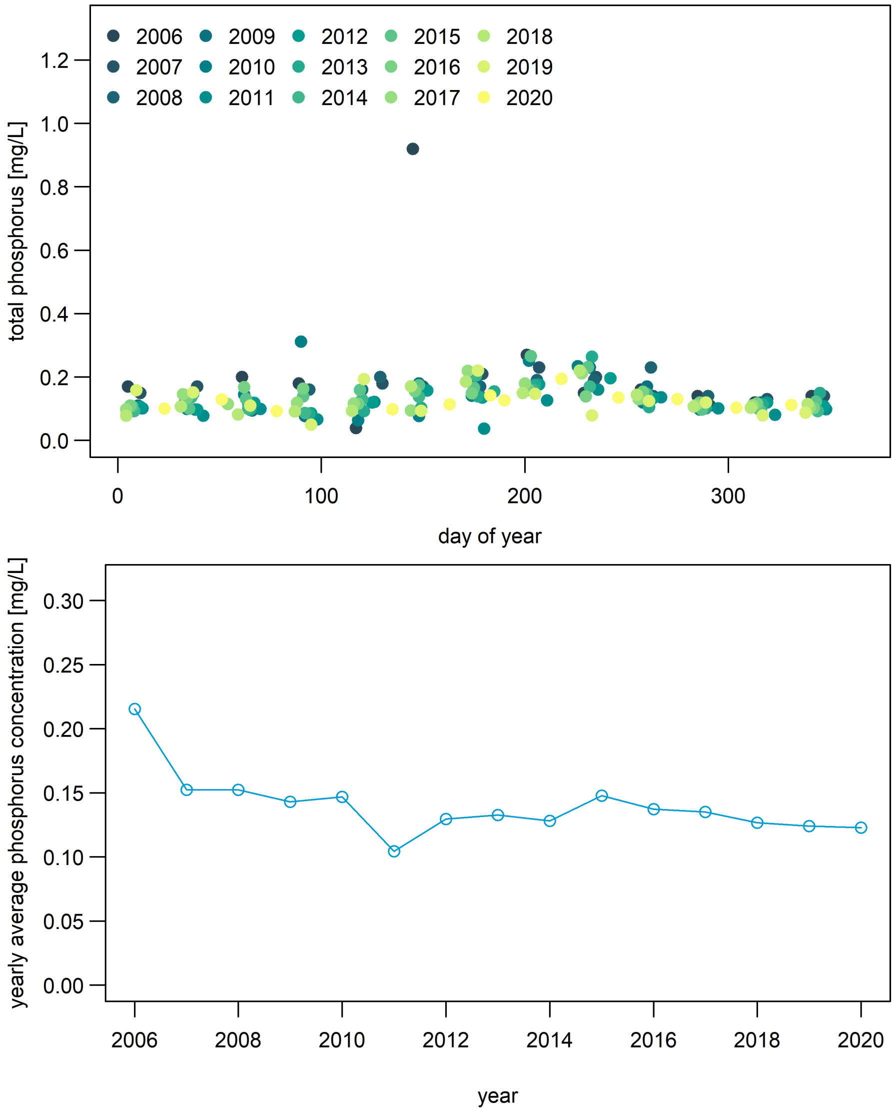

Source: own illustration, IWU-WG

Figure 51: Total phosphorus measurements (above) and calculated yearly average concentrations (below) at monitoring station Seemannshöft in Elbe River (ID BB09).

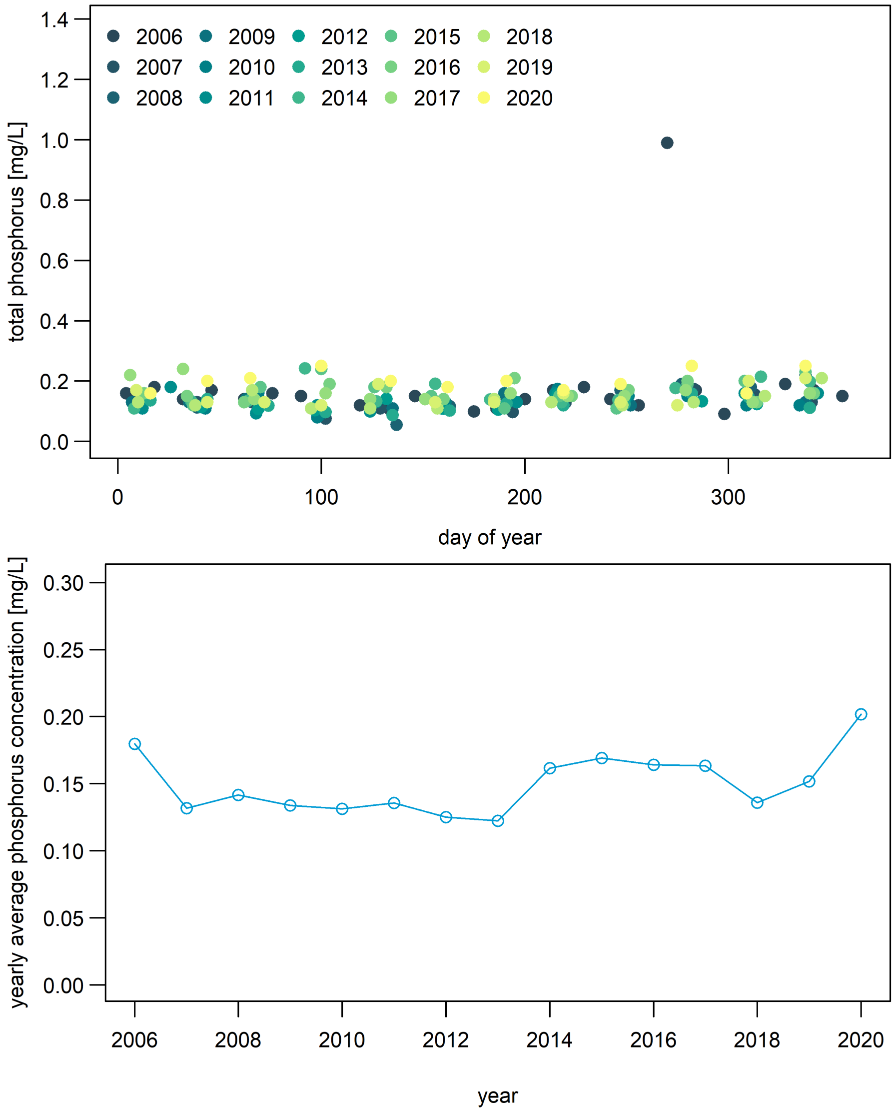

Source: own illustration, IWU-WG

Figure 52: Total phosphorus measurements (above) and calculated yearly average concentrations (below) at monitoring station Kleve-Bimmen in Rhine River (ID NW02).

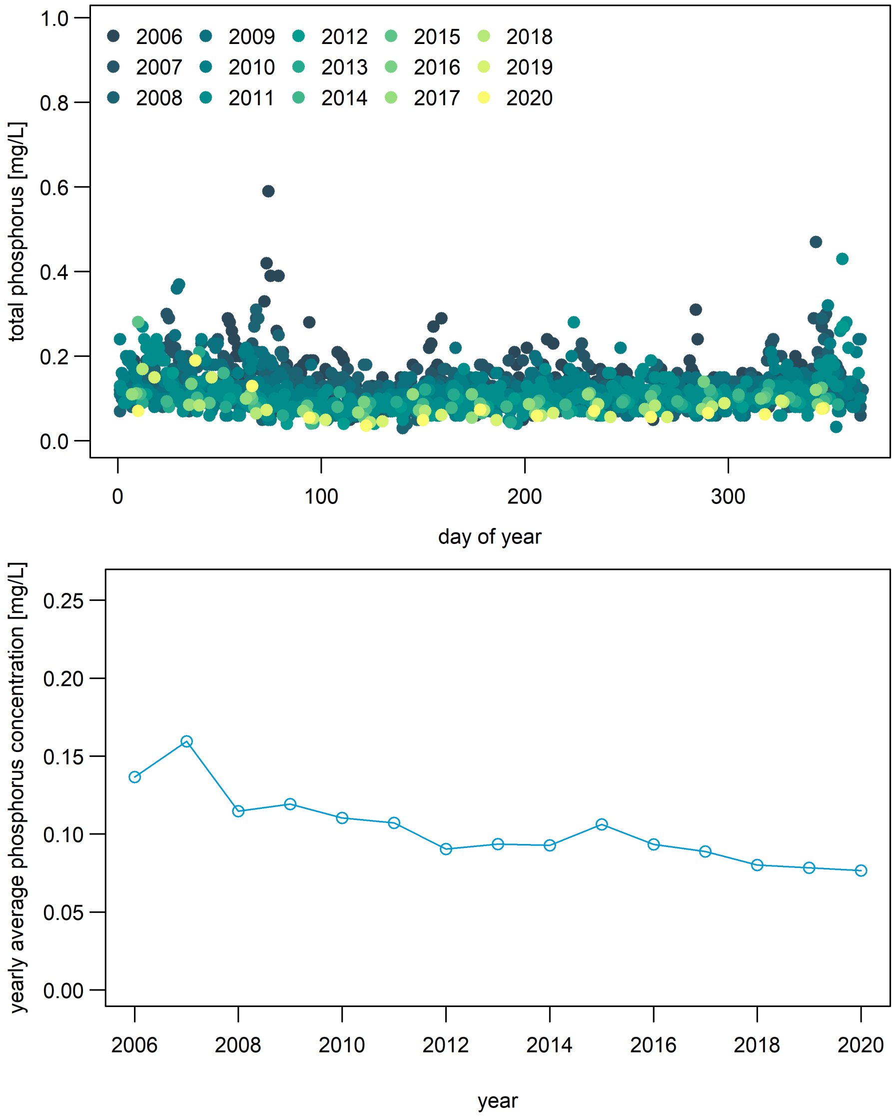

Source: own illustration, IWU-WG